

**Pyridine carboxamide and pyrazole palladium(II) complexes as catalyst precursors
for phenylacetylene polymerization.**

By

Poslet Morgan Shumbula



Submitted in partial fulfillment of the requirements for the degree of

Master of Science in the Faculty of Science

Department of Chemistry

University of the Western Cape

Private Bag X 17

Bellville

7535

Supervisor: Professor James Darkwa

November 2005

DECLARATION

I declare that “*pyridine carboxamide and pyrazole palladium(II) complexes as catalyst precursors for phenylacetylene polymerization*” is my own work, and it has not been submitted for any degree or examination in any other university, and all the sources I have used or quoted have been indicated and acknowledged by means of complete reference.

Name: Poslet Morgan Shumbula (Mr)

Date: November 2005

Signature: _____



DEDICATION

To the Shumbula family, may the Omnipresent, Omniscient and Omnipotent God bless you for the support you have given me.

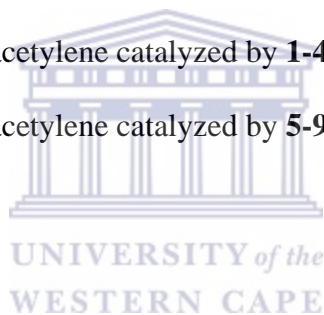


TABLE OF CONTENTS

	PAGE
ABSTRACT	vii
LIST OF TABLES	ix
LIST OF FIGURES	x
ABBREVIATIONS	xii
ACKNOWLEDGEMENTS	xiii
CHAPTER 1	1
PHENYLACETYLENE POLYMERIZATION AND CATALYSIS	
1.1 Polymerization of acetylene	1
1.2 Polymerization of substituted acetylenes	3
1.3 Polymerization of phenylacetylene by early and late transition metal catalysts	4
1.3.1 Polymerization of phenylacetylene by Ziegler catalysts	6
1.3.2 Polymerization of phenylacetylene by group 6 transition metal catalysts	6
1.3.3 Polymerization of phenylacetylene by group 9 transition metal catalysts	7
1.3.4 Polymerization of phenylacetylene by group 10 transition metal catalysts	9
1.4 Mechanistic pathways for polymerization of phenylacetylene	10
1.5 Stereochemistry of poly(phenylacetylene) (PPA)	12
1.6 Isomerization of poly(phenylacetylene)	17
1.7 Objectives of the project	21
1.8 References	22

CHAPTER 2	27
SYNTHESIS AND CHARACTERIZATION OF PYRIDINE CARBOXAMIDE PALLADIUM(II) COMPLEXES	
2.1 Introduction	28
2.1.1 Asymmetric catalysis	29
2.1.2 Molecular receptors	32
2.1.3 Dendrimer synthesis	33
2.1.4 Metal complexes syntheses	38
2.2 Experimental	38
2.2.1 Materials and instrumentation	38
2.3 Synthesis and characterization of the ligands	39
2.4 Synthesis and characterization of palladium complexes	42
2.5 Results and discussion	44
2.5.1 Synthesis and characterization of pyridine carboxamide ligands	44
2.5.2 Synthesis and characterization of pyridine carboxamide palladium(II) complexes	57
2.6 Conclusions	64
2.7 References	65
CHAPTER 3	68
POLYMERIZATION AND OLIGOMERIZATION OF PHENYLACETYLENE CATALYZED BY NITROGEN DONOR LIGANDS PALLADIUM COMPLEXES	
3.1 Introduction	68

3.2 Materials and instrumentation	70
3.3 Synthesis and characterization of $[\text{Pd}\{3,5\text{-(CF}_3)_2\text{pz}\}_2\text{Cl}_2]$ (8)	71
3.3.1 Crystallographic experimental section	71
3.3.2 X-ray analysis of complex 8	73
3.4 Polymerization procedure for phenylacetylene	76
3.5 Results and discussion	77
3.5.1 Conversion of catalyst precursors to active catalysts and phenylacetylene polymerization	77
3.5.2 Characterization of polymers and oligomers by NMR spectroscopy, IR spectroscopy and GPC	80
3.5.3 Polymerization of phenylacetylene catalyzed by 1-4	87
3.5.4 Polymerization of phenylacetylene catalyzed by 5-9	90
3.6 Conclusions	99
3.7 References	99
CHAPTER 4	102
4.1 Conclusions	102



ABSTRACT

This thesis reports the synthesis of pyridine carboxamide ligands and their palladium complexes, which were used as catalyst precursors to generate active catalysts for phenylacetylene oligomers and polymerization reactions. Pyridine carboxamide ligands 2-(N-phenylcarbamoyl)pyridine (**L1**), 2-{N-(4-methylphenylcarbamoyl)}pyridine (**L2**), 2-{N-(3,5-dimethylphenylcarbamoyl)}pyridine (**L3**) and 2-{N-(3,5-dimethylphenylcarbamoyl)}6-methylpyridine (**L4**) were prepared by reacting pyridine-2-carboxylic acid or 6-methylpyridine-2-carboxylic acid and an equimolar quantity of the appropriate aniline. Compounds **L1-L4** were characterized by ^1H and ^{13}C NMR, IR spectroscopy, mass spectrometry and elemental analysis.

The pyridine carboxamide palladium complexes dichloro{2-(N-phenylcarbamoyl)}pyridinepalladium(II) (**1**), dichloro{2-(N-4-methylphenylcarbamoyl)}pyridinepalladium(II) (**2**), dichloro{2-(N-(3,5-dimethylphenylcarbamoyl)}pyridinepalladium(II) (**3**) and dichloro{2-(N-(3,5-dimethylphenylcarbamoyl)}6-methylpyridinepalladium(II) (**4**) were prepared from the reaction of $\text{PdCl}_2(\text{NCCH}_3)_2$ with the appropriate pyridine carboxamide ligands. These complexes, which were insoluble in most organic solvents, were also characterized by ^1H and ^{13}C NMR, IR spectroscopy and elemental analysis. IR spectroscopy was used to determine the structural mode of bonding of the carboxamide ligands in the complexes.

Complexes **1-4** were further used as catalyst precursors for phenylacetylene polymerization. The active catalysts from these precursors were generated *in situ* by

reacting dichloro{2-(N-phenylcarbamoyl)}pyridinepalladium(II) (**1**), dichloro{2-(N-4-methylphenylcarbamoyl)}pyridinepalladium(II) (**2**), dichloro{2-(N-(3,5-dimethylphenylcarbamoyl)}pyridinepalladium(II) (**3**) and dichloro{2-(N-(3,5-dimethylphenylcarbamoyl)}6-methylpyridinepalladium(II) (**4**) with 2 mole equivalents of silver triflate (AgOTf) in the presence of acetonitrile. The catalysts reacted with phenylacetylene to produce poly(phenylacetylene) with molecular weight as high as 17 000 Da.

Other catalyst precursors that were investigated for phenylacetylene polymerization are [Pd(3,5-Rpz)₂Cl₂] (R = H (**5**), Me (**6**), ^tBu (**7**), CF₃ (**8**) and [Pd(3,5-^tBu₂pz)₂ClMe] (**9**). The active catalysts (**5-8**) were also generated by reacting the precursors with 2 mole equivalents of silver triflate while catalyst **9**, was generated by reacting the precursor with 1 mole equivalent of silver triflate. These catalysts gave molecular weights as high as 20 000 Da. Comparison is made between the pyridine carboxamide palladium(II) catalysts (**1-4**) and the simple pyrazole palladium(II) catalysts (**5-9**). Catalysts **1-4** were found to be more active than catalysts **5-9** at room temperature. The resulting poly(phenylacetylenes) were characterized by ¹H and ¹³C NMR, IR spectroscopy and GPC. ¹H and ¹³C NMR spectra of the polymers obtained showed that polymers were mainly ca. 86% *cis-transoidal* poly(phenylacetylene).

LIST OF TABLES

TABLES	PAGE
2.1 Selected IR frequencies (cm^{-1}) of the ligands	48
2.2 Selected IR frequencies (cm^{-1}) of the complexes	61
3.1 Crystal data and structure refinement for 8	74
3.2 Selected bond lengths and bond angles for 8	75
3.3 Polymerization of phenylacetylene catalyzed by 1-4	88
3.4 Polymerization of phenylacetylene catalyzed by 5-9	91
3.5 Polymerization of phenylacetylene catalyzed by 9	97



LIST OF FIGURES

FIGURES	PAGE
1.1 Stereoisomers of poly(phenylacetylene)	13
1.2 IR spectrum of <i>cis-transoidal</i> poly(phenylacetylene) (KBr pellets)	15
1.3 (a) ^1H and (b) $^{13}\text{C}\{^1\text{H}\}$ NMR spectra of a <i>cis-transoidal</i> polyphenylacetylene) in CDCl_3 at room temperature	17
1.4 ^1H NMR spectra (a) <i>cis-transoidal</i> PPA (CCl_4 , TMS) and (b) <i>trans-cisoidal</i> PPA obtained by thermal isomerization of <i>cis-transoidal</i> PPA (CCl_4 , TMS)	19
2.1 ^1H NMR spectrum of 2-[N-(4-methylphenylcarbamoyl)]pyridine (L2)	49
2.2 $^{13}\text{C}\{^1\text{H}\}$ NMR spectrum of 2-[N-(4-methylphenylcarbamoyl)]pyridine (L2)	50
2.3 Infrared spectrum of 2-[N-(4-methylphenylcarbamoyl)]pyridine (L2)	51
2.4 Mass spectrum of 2-[N-(4-methylphenylcarbamoyl)]pyridine (L2)	55
2.5 Mass spectrum of 2-[N-(3,5-dimethylphenylcarbamoyl)]pyridine (L3)	56
2.6 ^1H NMR spectrum of dichloro[2-(N-4-methylphenylcarbamoyl)]pyridine- palladium(II) (2)	59
2.7 $^{13}\text{C}\{^1\text{H}\}$ NMR spectrum of dichloro{2-(N-4-methylphenylcarbamoyl)}pyri- dinepalladium(II) (2)	60
2.8 Infrared spectrum of dichloro{2-(N-4-methylphenylcarbamoyl)}pyridine- palladium(II) (2)	62
3.1 Molecular structure of complex 8	75
3.2 (a) ^1H and (b) $^{13}\text{C}\{^1\text{H}\}$ NMR spectra of <i>cis-transoidal</i> poly(phenylacetylene)	81
3.3 Structure of <i>cis-transoidal</i> poly(phenylacetylene)	81
3.4 ^1H NMR spectrum showing poly(phenylacetylene) degradation in chloroform	83

3.5 ^1H NMR spectrum of <i>trans-cisoidal</i> poly(phenylacetylene)	84
3.6 Structure of <i>trans-cisoidal</i> poly(phenylacetylene)	84
3.7 ^1H NMR spectrum of a <i>trans-cisoidal</i> oligomer	85
3.8 Infrared spectrum of a polymer isolated from a reaction run in a mixture of $\text{CH}_2\text{Cl}_2:\text{CH}_3\text{CN}$	86
3.9 Effect of solvent ratio on percentage monomer conversion using catalyst 5	92
3.10 Influence of catalysts on percentage monomer conversion using AgOTf as an activator	96
3.11 Influence of catalysts on percentage monomer conversion using AgNO_3 as an activator	96
3.12 Effect of time on TON using catalyst 9	98
2.13 Effect of time on percentage monomer conversion using catalyst 9	98



ABBREVIATIONS

PPA = poly(phenylacetylene)

GPC = Gel Permeation Chromatography

VPO = Vapour Phase Osmometry

IR = Infrared

M_n = Number average molecular weight

M_w = Weight average molecular weight

Da = Daltons

M_w/M_n = Polydispersity index

NMR = Nuclear Magnetic Resonance

Pz = pyrazole

TON = Turn over number



ACKNOWLEDGEMENTS

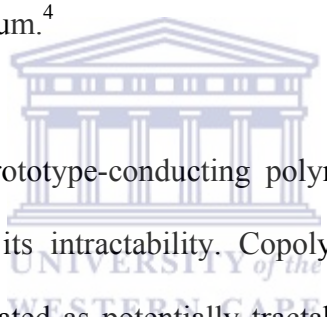
I would like to say thanks to my supervisor, Professor James Darkwa, who kept on advising me in this research. His words of encouragement ushered me to achieve part of my dream and may God bless him so very much. I also want to extend my word of gratitude to Ms. Valerie Grummel (University of Stellenbosch) for GPC analysis of poly(phenylacetylene), Mr. Pierro Bincassa (University of Cape Town) for elemental analysis of samples, Dr Ilia Guzei (University of Wisconsin-Madison) for X-ray structural analysis of the complex reported in this thesis. I am also grateful to the National Research Foundation (NRF) and Eskom for the funding of this project. To Professor Selwyn F. Mapolie and my co-researchers from the Organometallics group, thank you so much for the contribution you made during the course of my project. Special thanks to the Department of Chemistry, University of the Western Cape, where this research was carried, its staff members and fellow post-graduates for making me feel at home. Finally I thank the Almighty God for His word that kept me going when I met challenges along the way. It was not easy, but it was worthy.

CHAPTER 1

PHENYLACETYLENE POLYMERIZATION AND CATALYSIS

1.1 Polymerization of acetylenes

Polyacetylenes have been extensively studied for the past four decades. They may be conceptually defined as the linear polymers having a π -conjugated system in the main chain.¹ Their chemistry and physical properties have recently been the subject of intensive research.² This polymer, however, has certain drawbacks viz., instability to air and insolubility in organic solvents. According to literature, polyacetylene readily takes up oxygen in air at room temperature leading to decomposition,³ while it retains its weight below 320 °C under helium.⁴

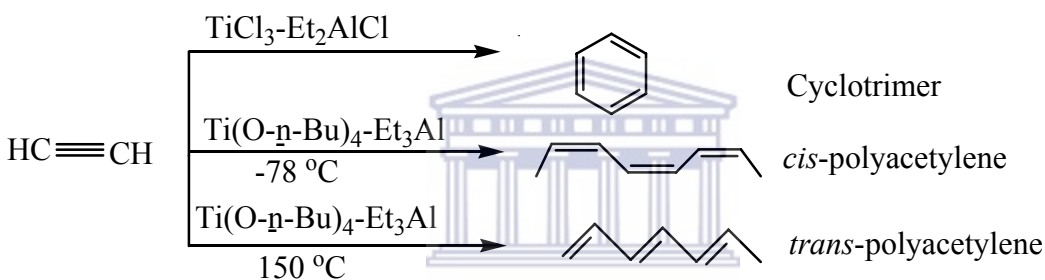


Polyacetylene serves as the prototype-conducting polymer, and there has been much synthetic effort to ameliorate its intractability. Copolymers, blends, graft and block copolymers have been investigated as potentially tractable forms of polyacetylene, but each approach has had severe limitations.⁵ Various vinyl polymers are manufactured on a large scale, whereas practically no polyacetylenes are produced by industry. One of the reasons is that it is difficult to synthesize high molecular weight polyacetylenes in good yields. However, the synthesis of high molecular weight polyacetylenes is currently becoming feasible.

Polyacetylenes which have alternating double bonds along the main chain often show the following unique properties: (i) electrical conductivity (semiconductivity), (ii) paramagnetism, (iii) chain stiffness, (iv) geometrical isomerism, and (v) colour.

However, the addition of small amounts of various dopants (both acceptors and donors) dramatically changes its electrical, optical, and magnetic behaviour.

Acetylene is selectively polymerized in the presence of Ziegler catalysts whose components have low Lewis acidity such as $\text{Ti}(\text{O-n-Bu})_4\text{-Et}_3\text{Al}(1:4)$, with *cis*-polyacetylene being formed at low temperature and *trans*-polyacetylene at high temperature, while cyclotrimers are formed with $\text{TiCl}_3\text{-Et}_2\text{AlCl}$ when employed at room temperature (Scheme 1.1).⁶



Scheme 1.1 Schematic representation showing polymerization of acetylenes using Ziegler catalysts

Acetylene was first polymerized to a linear π -conjugated polymer by Natta *et al.*⁷ using $\text{Ti}(\text{O-Pr})_4/\text{Et}_3\text{Al}$ in 1958. However, it was Watson *et al.*⁸ who studied the polymerization of acetylene with various Ziegler-type catalysts and gave the first report for the preparation of *cis*-polyacetylene.

Although a number of publications dealing with chemical, physical, and electrical properties of polyacetylene have appeared in the past four decades,⁹ the characterization

of polyacetylene has not been fully investigated mainly due to its insolubility and infusibility, and the applications of polyacetylene have been restricted due to poor functionality peculiar to its simple chemical structure. However, to increase the processability and provide various functionalities of polyacetylenes, synthesis and characterization of substituted polyacetylenes has been the subject of extensive investigations.

1.2 Polymerization of substituted acetylenes

Synthesis of substituted polyacetylenes has attracted much interest among polymer scientists because polyacetylenes with suitable substituents not only will have better processability and stability, but also may possess novel properties such as magnetism and liquid crystallinity that are not found in the parent form.¹⁰ Substituted polyacetylene polymers prepared from the following monomers e.g. aromatic acetylene, $\text{PhC}\equiv\text{CR}$ ($\text{R} = \text{CH}_3, \text{C}_2\text{H}_5$); aliphatic acetylenes, $\text{HC}\equiv\text{CC}(\text{CH}_3)_3$; chloro-containing acetylenes, $\text{ClC}\equiv\text{CPh}$; silicon-containing acetylenes, $\text{CH}_3\text{C}\equiv\text{CSi}(\text{CH}_3)_2\text{CH}_3$ are stable in air but display low conductivity (ca. 10^{-15} to 10^{-18} S. cm^{-1}). No doubt their stability is due to the fact that the olefinic bonds are trisubstituted compared to the corresponding disubstituted olefinic bonds.

The presence of substituents along the chain leads to steric hindrance and this determines deviations from a planar structure that decrease π -electron delocalization. The loss of such delocalization has many consequences, such as a variation in the colour, e.g. polyacetylene is dark gray and poly-*t*-butylacetylene is white, and also a change in

electrical conductivity, e.g. 10^{-4} S.cm⁻¹ for polyacetylene and 10^{-15} S.cm⁻¹ for poly-*t*-butylacetylene.¹¹ These substituted polyacetylenes have good gas permeability, photoconductivity and radiodegradability and may therefore become new speciality polymers.¹²

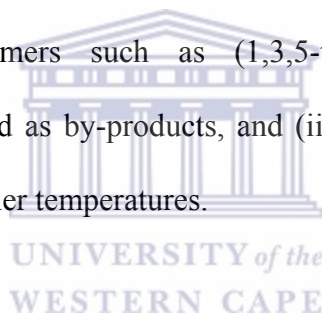
Polymerization of substituted acetylenes has been carried out with a wide range of catalysts and conditions,¹³ such as, homogeneous and heterogeneous Ziegler-Natta catalysts, with early and late transition metal complexes e.g Pd, Pt, Ru, W, Mo, Ni and others, with free radical initiators such as 2,2'-azobis(isobutyronitrile) (AIBN), benzoyl peroxide (BPO), and di-*tert*-butylperoxide, by thermal polymerization, γ -irradiation, cationic initiation with BF₃, and anionic initiation by butyllithium, triethylamine, and sodium amide.¹⁴ So far, various polyacetylenes with aromatic and related pendant groups with early and late transition metal catalysts have been prepared and studied.¹⁵ In general, the high solubility and high stability of substituted polyacetylenes are two most important properties which are not seen with polyacetylene.

1.3 Polymerization of phenylacetylene by early and late transition metal catalysts

The monosubstituted acetylene that has most often been employed to study polymerization is probably phenylacetylene.¹⁶ The chemical and physical properties of poly(phenylacetylene) are quite remarkable when compared with polyacetylene and other substituted polyacetylenes. Its colour varies from red-brown to yellow, it is soluble in common organic solvents such as toluene, dichloromethane and chloroform, it is stable in air and displays high semi-conductor properties (10^{-10} S. cm⁻¹), which is ca. 10^8 fold more

conducting than polystyrenes; which is the corresponding non-conjugated structure.¹⁷ Phenylacetylene has been reported to polymerize by coordination, radical or cationic mechanism. However, only oligomers with molecular weights of ca. 1 000 Da are formed by radical or cationic mechanism. In coordination polymerizations, not only polymers with a molecular weight of several thousand Da but also benzene-insoluble polymers and methanol-soluble oligomers, including a cyclic trimer, are usually formed.¹⁸

In summary, previous polymerization reactions of phenylacetylene catalyzed by late transition metal complexes have often been accompanied by the following problems: (i) the molecular weight of the poly(phenylacetylene) formed were low (usually less than 3 000 Da), (ii) a cyclic trimers such as (1,3,5-triphenylbenzene) and (1,2,4-triphenylbenzenes) were formed as by-products, and (iii) the reactions were performed over longer periods and /or higher temperatures.



The low molecular weight of the polymer produced from phenylacetylene by a cationic mechanism has been explained in terms of either a low reactivity of phenylacetylene for electrophiles¹⁹ or a high stability of the propagating end due to the conjugation of double bonds.²⁰ Thus it is rather difficult to synthesize selectively polymers whose molecular weights are higher than 10 000 Da. The subsequent sections describe various catalysts that have been used in the polymerization of phenylacetylene, such as Ziegler-Natta catalysts, group 6 transition metal catalysts, group 9 transition metal catalysts and group 10 transition metal catalysts.

1.3.1 Polymerization of phenylacetylene by Ziegler catalysts

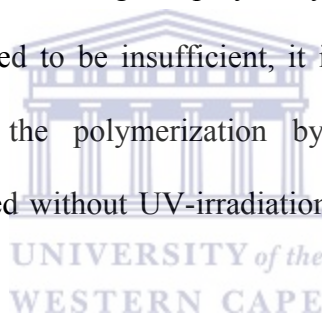
Ziegler catalysts were the most versatile catalysts for the polymerization of phenylacetylene before group 5 and 6 transition metal catalysts were found.²¹ However, they were reported to produce relatively high molecular weight of phenylacetylene, and a large fraction of the products was insoluble. For example, VO(sal)₂-Et₃Al polymerized phenylacetylene to give molecular weights of 7 500 Da.²²

1.3.2 Polymerization of phenylacetylene by group 6 transition metal catalysts

In 1974, Masuda and Higashimura found that phenylacetylene could be polymerized with WCl₆ and MoCl₅ to give polymers with molecular weights ranging between 5 000 and 15 000 Da in good yields.²³ The polymers produced were found to be soluble in benzene. Since then, there have been many studies on the polymerization of phenylacetylene and disubstituted acetylene compounds using tungsten and molybdenum-based catalyst systems.²⁴ For example, dinitrosylalkylidene complexes of molybdenum and tungsten,²⁵ which had been used for the olefin metathesis reactions and the metathesis polymerization of cycloolefins,²⁶ were found to be very active catalysts for polymerization of phenylacetylene. Spectroscopic studies of materials from these catalysts showed that *cis*-rich or *trans*-rich polymer can be formed by varying conditions such as temperature.

Living and stereospecific polymerization are also attained using molybdenum-based catalysts. Polymerization of phenylacetylene with group 6 transition metal catalysts is believed to proceed via metathesis polymerization mechanism like ring-opening

polymerization of cycloolefin.²⁷ Polymerization with WCl_6 is significantly accelerated in the presence of tetraphenyltin (Ph_4Sn) as a cocatalyst.²⁸ Poly(phenylacetylenes) having high molecular weight ($M_n \approx 100\ 000$ Da) were also prepared using solvents that contain active hydrogens such as 1,4-dioxane, cyclohexenes, and tetralin with a WCl_6 - Ph_4Sn catalyst system.²⁹ The active hydrogen of solvents seems to prevent polymer degradation reactions via a radical mechanism and/or modify the nature of the active species. Enhancing of molecular weights is also achieved using a catalyst system obtained by UV-irradiation of $W(CO)_6$ in carbon tetrachloride.³⁰ It is therefore clear that halogen-containing solvents play an essential role in the formation of the active species. Among them, carbon tetrachloride allows the highest polymer yield. Since catalytic amounts of carbon tetrachloride have proved to be insufficient, it is most favorable to use carbon tetrachloride as solvent for the polymerization by metal hexacarbonyls.³¹ This polymerization does not proceed without UV-irradiation or in a hydrocarbon solvent in place of carbon tetrachloride.

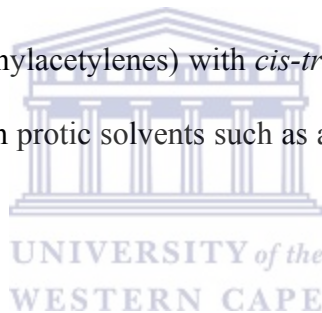


1.3.3 Polymerization of phenylacetylene by group 9 transition metal catalysts

Although polymerization of phenylacetylene can be obtained by cationic³² and radical³³ polymerization as well as by Ziegler-Natta systems³⁴ or typical metathesis catalysts like WCl_6 or $MoCl_5$,³⁵ the most widely studied catalysts are rhodium(I) complexes.³⁶ They have been of intense interest because of their potentially high reactivity toward alkynes and capability of inducing stereocontrolled living polymerization. Rhodium catalysts are known to be effective in polymerizing only monosubstituted acetylenes, especially phenylacetylene.³⁷

Among the most recently used catalysts are precursor complexes of formula $\text{Rh}(\text{C}\equiv\text{CPh})(\text{nbd})(\text{PPh}_3)_2$,³⁸ $[\text{Rh}(\text{diene})\text{Cl}]_2$ and $\text{Rh}(\text{diene})(\text{tosylate})(\text{H}_2\text{O})$,³⁹ *in situ* catalytic systems $[\text{RhCl}(\text{nbd})]_2/\text{Ph}_2\text{C}=\text{C}(\text{Ph})\text{Li}/\text{PPh}_3$,⁴⁰ or $[\text{Rh}(\text{cod})\text{Cl}]_2/[2,6-(\text{PPh}_2\text{CH}_2)_2\text{-C}_6\text{H}_4]$ (diene: 2,5-norbornadiene (nbd) or 1,5-cyclooctadiene (cod)).⁴¹ $[\text{RhCl}(\text{diene})_2]$ also initiates cyclopolymerization of 1,5-hexadiyne to give a highly conjugated polymer.⁴² These initiators often require an appropriate additive such as NaOH, NaOC_2H_5 , or triethylamine to attain high activity. However, these rhodium complexes are not effective for polymerization of simple monoalkylated acetylenes.⁴³

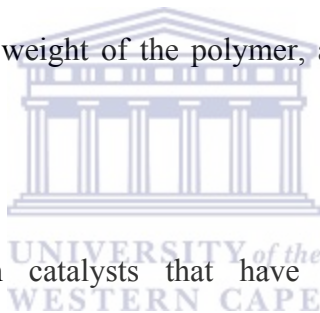
There are two major features observed with the rhodium catalysts: first, they selectively produce stereoregular poly(phenylacetylenes) with *cis-transoidal* structure.⁴⁴ Second, the polymerization readily occurs in protic solvents such as amine,⁴⁵ alcohols,^{44(b),46} and even water.⁴⁷



Following studies on rhodium catalysts for alkyne polymerization,⁴⁸ Farnetti *et al.*⁴⁹ investigated the properties of iridium compounds, $[\text{Ir}(\text{cod})\text{Cl}]_2$ and $[\text{Ir}(\text{Cod})(\text{OMe})_2]$ which were found to be effective in promoting phenylacetylene polymerization with negligible formation of oligomeric products, with the highest molecular weight being 7 180 Da. Polymerization reactions proceed in various solvents such as tetrahydrofuran (THF), chloroform and benzene, but polymerization is most favored when triethylamine is used as a reaction medium. The polymers obtained have moderate percentage conversions in the range of 10-51% and the ^1H NMR spectra confirmed both *cis* and *trans* structures.

1.3.4 Polymerization of phenylacetylene by group 10 transition metal catalysts

Few group 10 transition metal catalysts have been reported to polymerize phenylacetylene. Tsuchihara has reported that the nickel catalyst system, $\text{Ni}(\text{COD})_2\text{CF}_3\text{COO}(\text{allyl})$, polymerize phenylacetylene to produce yellowish-red polymers in good yield with a molecular weight of 12 000 Da. The polymers were found to be soluble in various organic solvents such as toluene and chloroform.⁵⁰ Other examples of nickel catalysts that were reported to polymerize phenylacetylene are, $\text{Ni}(\text{MeCN})_6(\text{BF}_4)_2/\text{AlEt}_2\text{Cl}$ which afforded PPA with a molecular weight of 5 000 Da⁵¹ and nickelocene, which has been reported by Douglas *et al.*⁵² to polymerize phenylacetylene at 115 °C, in the absence of solvent, with 92 % conversion of monomer to polymer. But the molecular weight of the polymer, as determined by Vapour Phase Osmometry was 1 600 Da.



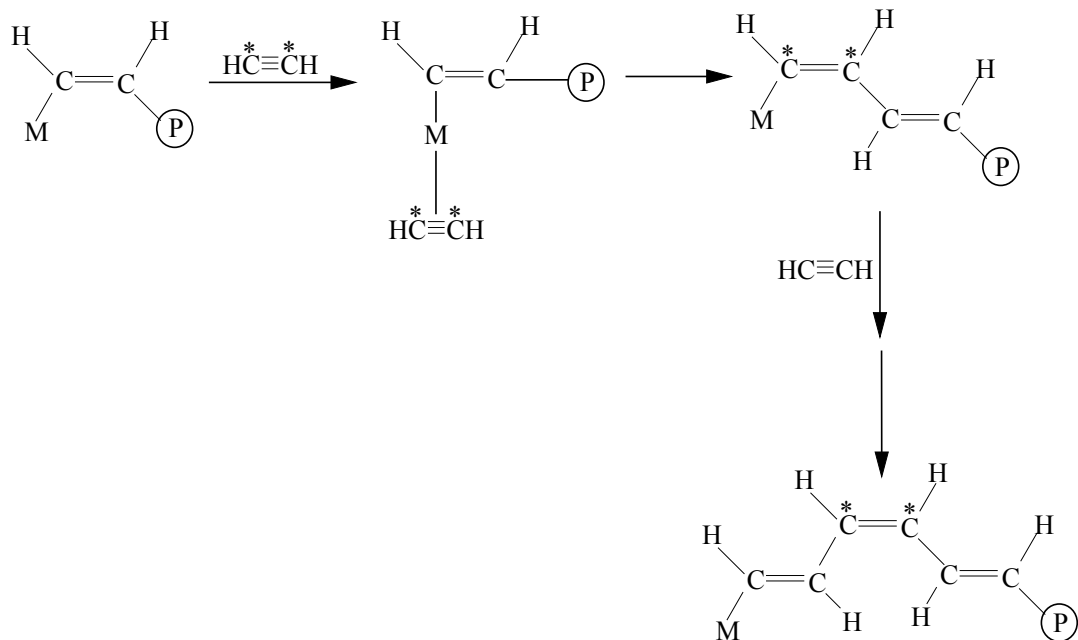
There are various palladium catalysts that have been reported to polymerize phenylacetylene. Sen *et al.*⁵³ have reported that catalyst $[\text{Pd}(\text{CH}_3\text{CN})_4][\text{BF}_4]_2$ polymerize phenylacetylene to give PPA with molecular weight of 9 000 Da. Polymerization reactions performed in acetonitrile solvent gave polymers that were highly coloured. Li *et al.*⁵⁴ reported that the cationic [bis(diphenylphosphino)ferrocene]palladium catalyst formed poly(phenylacetylene) with molecular weights as high as 17 707 Da. This polymerization reaction was also performed in the presence of acetonitrile, implying that the coordinating solvent is crucial in stabilizing cationic active catalysts.

Recently, palladium(II) complexes of the type $[\text{Pd}(\text{NN}'\text{O})\text{Cl}]$ ($\text{NN}'\text{O}$ = 2-acetylpyridine

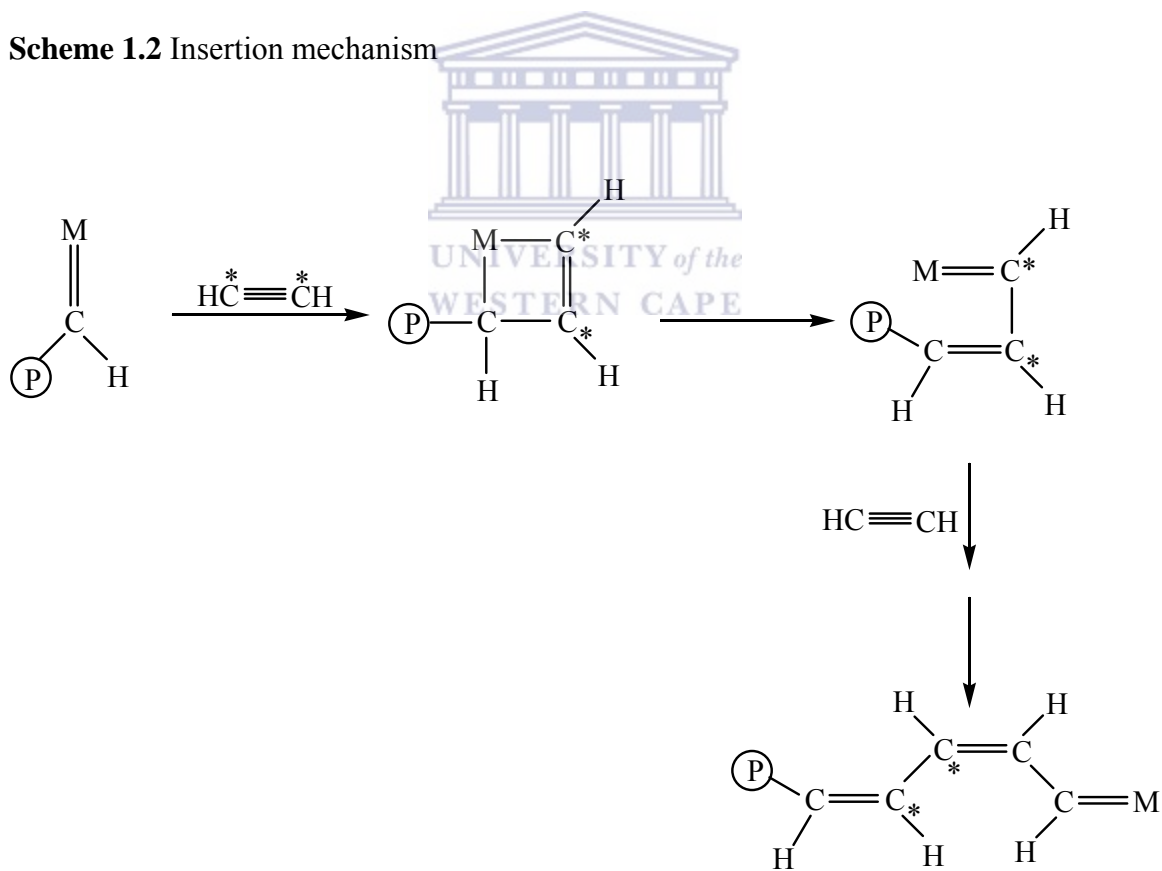
or 2-formylpyridine benzoylhydrazones) were reported to polymerize phenylacetylene in water at room temperature, leading to poly(phenylacetylene) with a high molecular weight of 23 495 Da.⁵⁵ So far, this is the only palladium nitrogen ligand complexes reported to polymerize phenylacetylene prior to the work reported in this thesis. Like group 9 transition metal catalysts, polymerization of phenylacetylene with group 10 transition metal catalysts is also believed to proceed via insertion mechanism.

1.4 Mechanistic pathways for the polymerization of phenylacetylene

The two most common mechanisms for polymerization of acetylenes by transition metal catalysts are insertion of acetylene into a metal-carbon single bond (insertion mechanism)⁵⁶ and addition of acetylene to a metal-carbon double bond to give a metallacyclobutene complex, which opens to give a complex with a new metal-carbon double bond (metathesis mechanism).⁵⁷ Evidence for the “insertion” mechanism has been accumulating for many years, but evidence for the “metathesis” mechanism is still relatively scarce. Currently available data do not distinguish between the more traditional four-center olefin insertion mechanism of Cossee and Arlman⁵⁸ and the recent metallacycle proposal of Green and co-workers.⁵⁹ The direct four-center acetylene insertion mechanism is illustrated in Scheme 1.2,⁶⁰ while the metallacycle mechanism suggested by Katz is shown in Scheme 1.3.⁵⁷



Scheme 1.2 Insertion mechanism



Scheme 1.3 Metathesis mechanism

In contrast to the olefin case, however, a clear-cut distinction can be drawn between these two mechanisms. Scheme 1.2 predicts that the two carbons of a given monomer unit will end up doubly bonded to one another in the resulting polymer, according to Scheme 1.3 these carbons will be connected by a single bond.⁶¹ It is however generally believed that acetylene polymerization catalyzed by group 10 metal catalysts proceed via an insertion mechanism, leading to stereoregular polymers.

1.6 Stereochemistry of poly(phenylacetylene) (PPA)

With regard to the structures of stereoregular poly(phenylacetylenes), four stereoisomers are possible in terms of the configuration of the C=C bond and the configuration of the C–C single bond of the polymer main chain as shown in Figure 1.1.

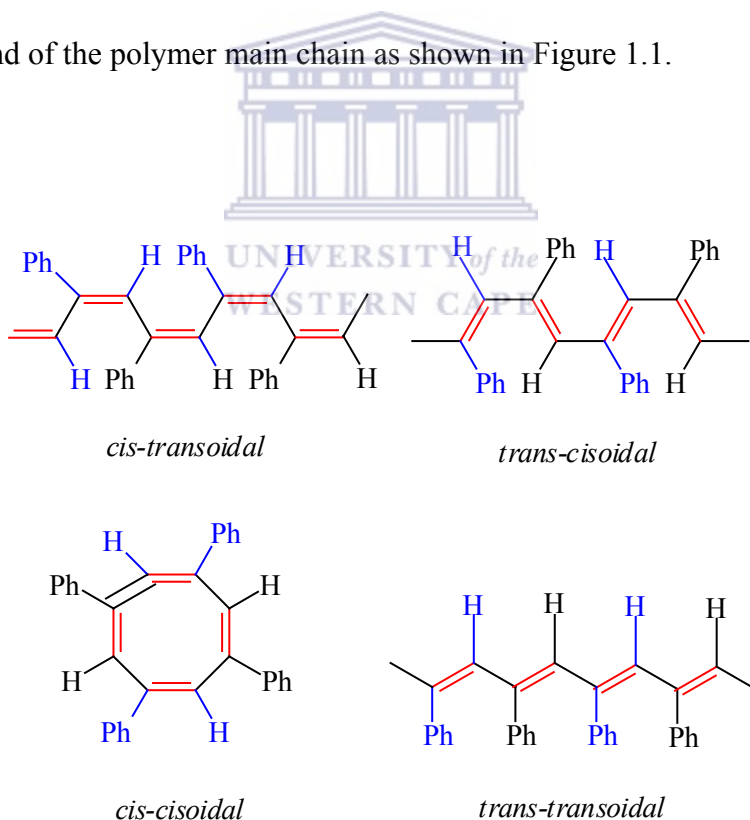


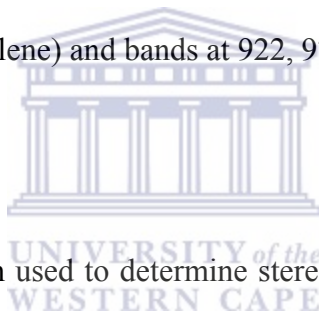
Figure 1.1 Stereoisomers of poly(phenylacetylene)

Although the first *trans*-polyacetylene was synthesized by Natta *et al.*⁶² in 1958, *cis* and *trans* configurations of polyacetylene were reported by Watson *et al.*⁶³ and by Kleist *et al.*⁶⁴ in 1961 and 1969, respectively. Berlin *et al.*⁶⁵ and Simionescu *et al.*⁶⁶ then reported the isomerization of poly(phenylacetylene).

It was established that the benzene soluble fractions of poly(phenylacetylene) obtained with $\text{AlH}(\text{i-Bu})_2/\text{Fe}(\text{acac})_3$ (where *acac* = acetylacetonate), $\text{AlEt}_3/\text{TiCl}_3$, or $\text{AlEt}_3/\text{Fe}(\text{dmg})_2 \cdot 2\text{Py}$ (where *dmg* = dimethylglyoxime) as catalysts have mainly a *cis-transoidal* configurations and that the benzene insoluble crystalline fractions obtained with the last two catalysts have *cis-transoidal* structure. Using other Ziegler-Natta catalysts, i.e; $\text{AlEt}_3/\text{TiCl}_4$ and $\text{AlEt}_3/\text{M}(\text{acac})_n$, Berlin *et al.*⁶⁷ and Simionescu *et al.*⁶⁸ synthesized *trans*-PPA.

IR spectroscopy and ¹H NMR spectroscopy have been used to identify the stereoregularity of the poly(phenylacetylene). It has been found that in the polymerization of phenylacetylene with Ziegler-Natta catalysts, the benzene insoluble but methanol soluble fraction has a *cis-cisoidal* structure whilst the benzene soluble but methanol insoluble fraction has a *cis-transoidal* structure.⁶⁹ Polymers obtained thermally with $(\text{PPh}_3)_2\text{PdCl}_2$ gave only methanol insoluble fraction, which is *trans-cisoidal*. However, the *trans-cisoidal* structure could also be obtained by polymerization with Ziegler-Natta catalysts, but it appears only by isomerization of one of the *cis* structures as will be shown later.⁷⁰

Infrared spectroscopy is a useful tool to identify stereoisomers of PPA. The infrared spectra of *cis-cisoidal* and *cis-transoidal* (Figure 1.2) show a band at 740 cm⁻¹, but not the band at 1265 cm⁻¹, which is found in *trans*-isomers. The absorption at 740 cm⁻¹, is thus a function of the *cis* content in a polymer.⁶⁶ Bands at 922, 895, and 855 cm⁻¹, are also characteristic of PPA. The strongest band is located at 895 cm⁻¹ in the case of *cis-cisoidal* and *cis-transoidal* structures and at 922 cm⁻¹ in the case of *trans-cisoidal* structure.⁷¹ The *trans-cisoidal* structure shows a very weak band at 970 cm⁻¹, which has been assigned by other authors to *trans* C-H out-of-plane deformation vibration.⁷² The very weak band at 1380 cm⁻¹ present in *cis-cisoidal* and *cis-transoidal* structures may also be assigned to *cis* polymers. In general, the bands at 740, 895, and 1380 cm⁻¹ are specific to *cis*-poly(phenylacetylene) and bands at 922, 970 and 1265 cm⁻¹ are specific for *trans*-poly(phenylacetylene).



¹H NMR analysis has also been used to determine stereoregularity through the equation below:

$$\% \text{ cis.} = [A_{5.82} / (A_{\text{total}} / 6)] \times 100 \quad \text{OR} \quad \% \text{ cis} = A_{5.82} \cdot 10^4 / A_{\text{total}} \cdot 16.66 \quad (1.1)$$

where $A_{5.82}$ is the area of the vinyl proton in the *cis*-isomer and A_{total} the total area of the polymer spectrum. However, *cis* content lower than 70% cannot be determined from the NMR spectrum, due to the superimposition of the 5.82 ppm signal with the resonance of aromatic protons.⁷⁰ *Cis-transoidal* PPA is characterized by ¹H NMR spectrum with three peaks (Figure 1.3a), whilst according to theoretical calculations, the ¹H NMR spectrum of the *cis-cisoidal* poly(phenylacetylene) must be different.

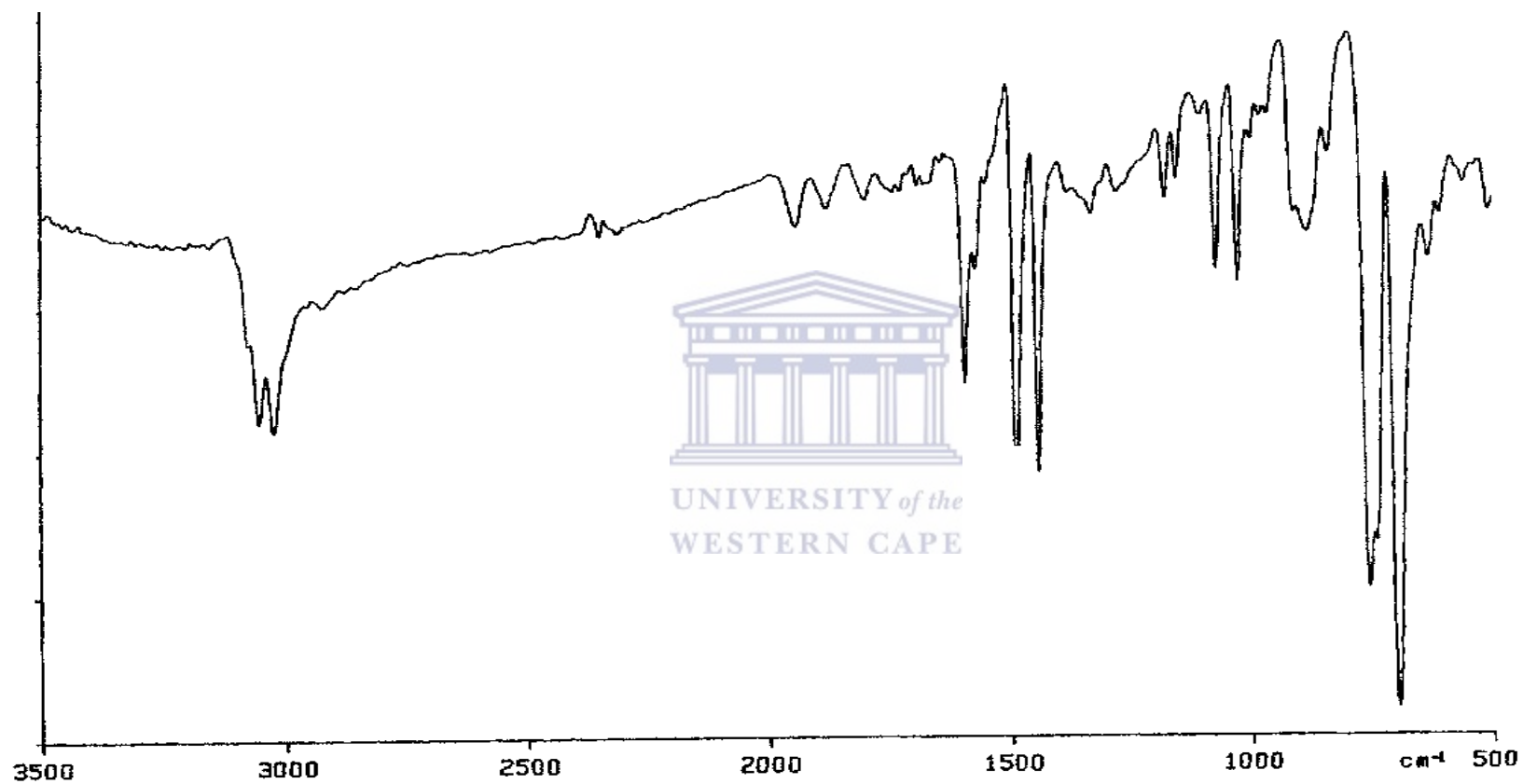


Figure 1.2 IR spectrum of *cis-transoidal* poly(phenylacetylene) (KBr pellets)

The stereoregularity of *cis-transoidal* poly(phenylacetylene) is supported by ^{13}C NMR spectrum (Figure 1.3b) with signals at 142.90 ppm (quarternary C of the main chain), and 139.30 ppm (*ipso*-carbon of Ph), 131.80 ppm (vinylic carbon), 127.80 ppm (*o*-C of Ph), 127.50 ppm (*m*-C of Ph), 126.70 ppm (*p*-C of Ph).⁷³

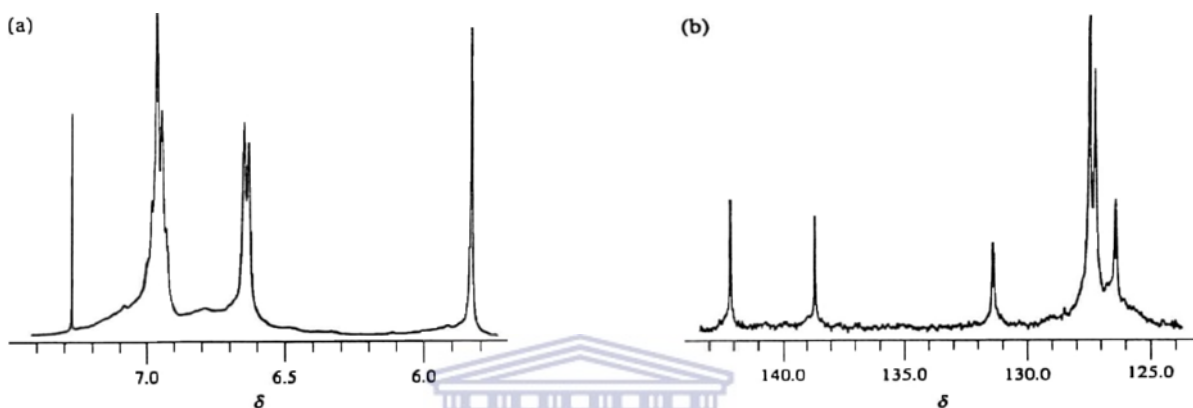


Figure 1.3 (a) ^1H and (b) $^{13}\text{C}\{^1\text{H}\}$ NMR spectra of a *cis-transoidal* poly(phenylacetylene) in CDCl_3 at room temperature.⁷³

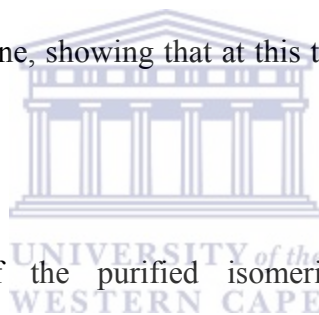
The ^1H NMR spectrum of *trans-cisoidal* poly(phenylacetylene) has one broad peak as will be seen under the discussion of PPA isomerization. Its ^{13}C NMR also displays one broad peak centered at 128.25 ppm.⁴⁹

1.7 Isomerization of poly(phenylacetylene)

The thermal isomerization of the polyene chain is of interest because the change from the *cis* form to the *trans* form affects molecular properties such as conductivity, second harmonic generation, and magnetism.⁷⁴ All of these physical properties are closely related to the electronic states of the polyacetylene backbone. There have been many X-

ray, IR, and ^1H NMR spectroscopic reports on the chain structure and the *cis-trans* isomerization of substituted polyacetylene polymerized using the various catalysts.⁷⁵ In the case of ^1H NMR measurements, the thermal isomerization give rise to anomalous spectra in which the ^1H and ^{13}C NMR signals of the main chain become broader.

Simionescu *et al.*⁷⁰ reported that the ^1H NMR spectrum of the *cis-transoidal* structure of PPA gives the best resolution at about 70 °C, and has three proton resonances centered at 5.82 ppm (one *cis* polyenic proton), 6.70 ppm (one aromatic proton), and 6.85 ppm (four aromatic protons). At higher temperatures the peak area at 5.82 ppm and 6.70 ppm start to decrease. A new signal appears at 7.60 ppm above 120 °C and was assigned to 2,4,6 protons of 1,3,5-triphenylbenzene, showing that at this temperature cyclization begins to occur.



The ^1H NMR spectrum of the purified isomerized polymer at 190 °C in hexachlorobutadiene solution is presented in Figure 1.4b, together with the ^1H NMR spectrum of *cis-transoidal* PPA (Figure 1.4a), which has one *cis* polyenic proton at 5.82 ppm, and the remaining *cis*-PPA protons are at 6.70 and 6.92 ppm. Initial signs of isomerization to the *trans*-PPA are apparent due to the broadening of the peaks.

Comparative study of ^1H NMR spectrum of *trans-cisoidal* PPA (Figure 1.4b) allowed the following assignments; the peak between 2.0 and 4.5 ppm represents the methinic protons resonances of 1,3- or 1,4-cyclohexadiene structure and the peak between 4.6 and 6.2 ppm represents the resonances of *cis* olefinic protons from cyclohexadiene structures, and

between 6.2 and 7.6 ppm the resonances of the monosubstituted benzene protons and the *trans* polyenic protons appear, while the proton resonances of polyphenylene structure appear between 7.6 and 8.2 ppm.⁷⁶

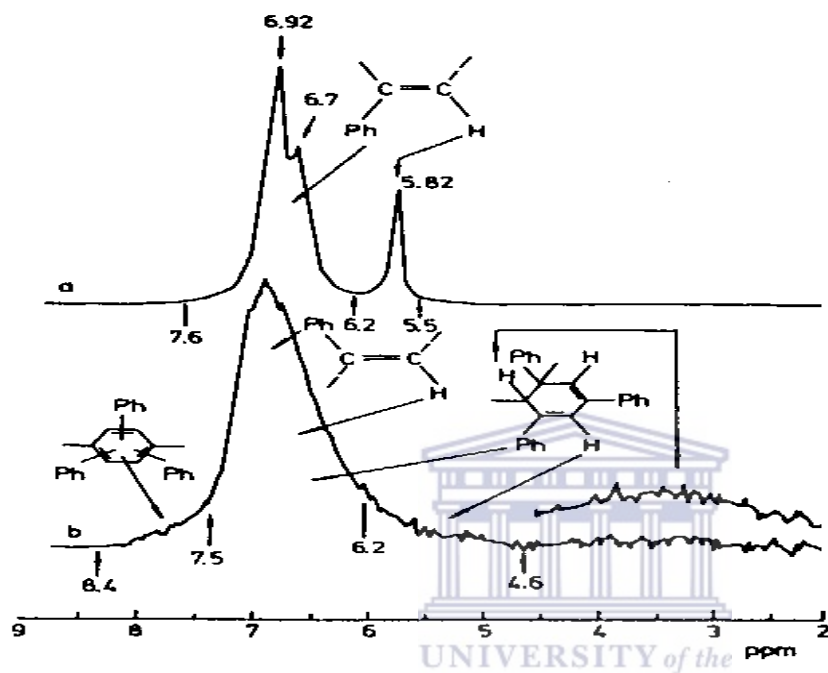
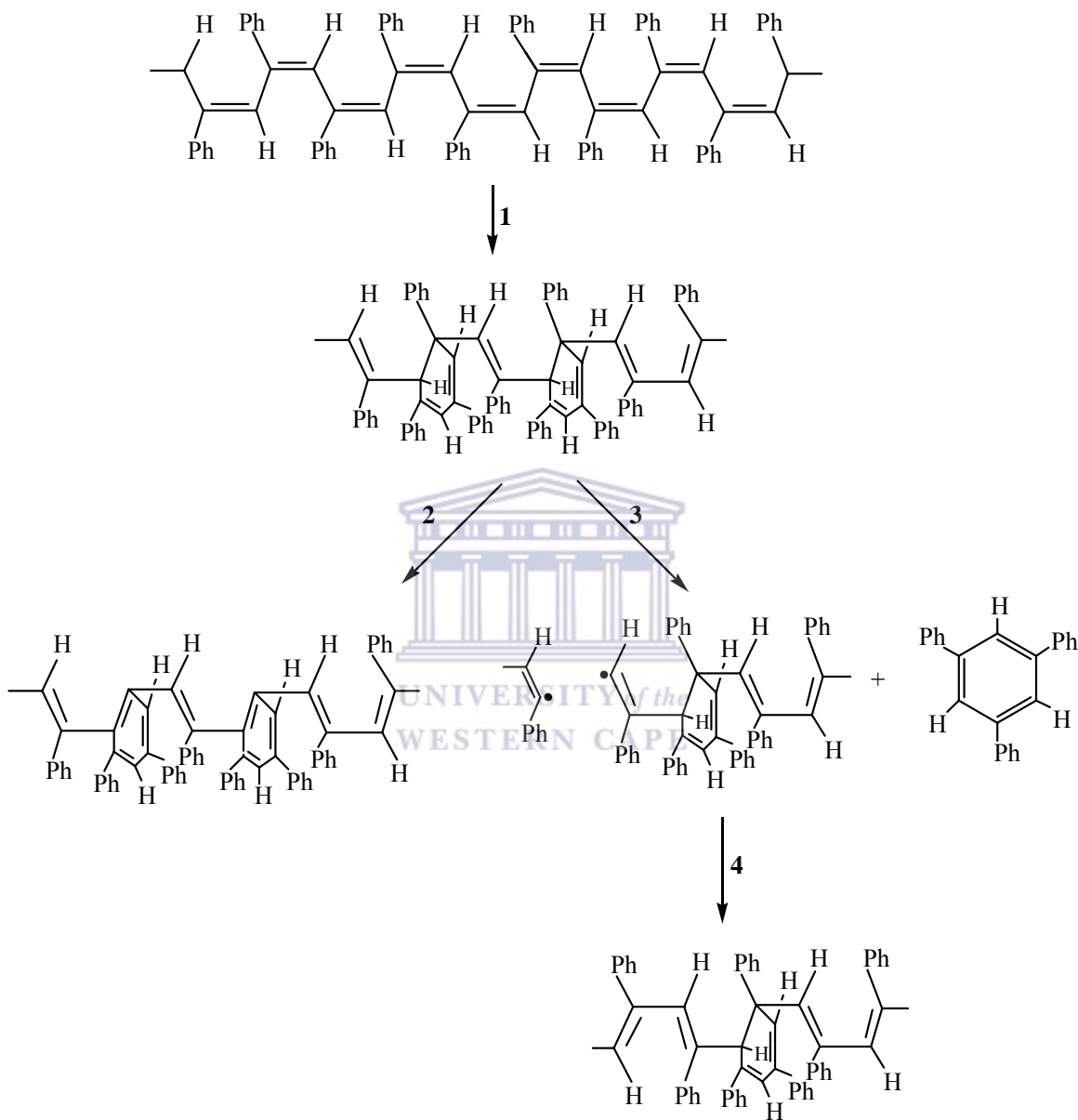


Figure 1.4 ^1H NMR spectra of (a) *cis-transoidal* PPA (CCl_4 , TMS) and (b) *trans-cisoidal* PPA obtained by thermal isomerization of *cis-transoidal* PPA (CCl_4 , TMS)

The simplest scheme representing the reactions of the *cis-trans* thermal isomerization of poly(phenylacetylene) is shown below (Scheme 1.4). In the first step, (1) the thermal isomerization is accompanied by cyclization reactions, leading to a polymer chain containing 1,3-cyclohexadiene structures. This cyclization reaction induces the migration of at least one *cis*-double bond and changes its configuration from *cis* to *trans* without the breaking of the π bond. Two ways are possible after that: (i) the aromatization of cyclohexadiene structures (2) and (ii) the scission of the polymer chain with release of

trisubstituted benzenes (**3**). The macroradical recombination is one of the possible reactions that follow (**4**).⁷⁶

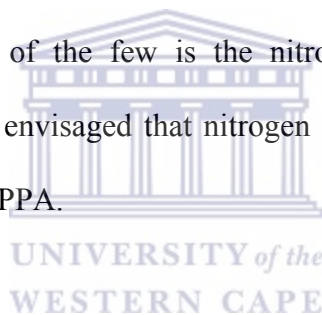


Scheme 1.4 Possible reactions occurring during *cis-trans* thermal isomerization of *cis-transoidal* poly(phenylacetylene).

In short, stereoisomers of polyacetylenes are either formed directly from the reaction or the subsequent isomerization of the polyacetylene in solution. In this project both processes to stereoisomers were observed.

1.9 Objectives of the project

This chapter reviews work done on the polymerization of phenylacetylene using early and late transition metal catalysts. It describes some of the vital points such as (i) mechanisms through which polymerization occurs, (ii) molecular weights of the polymers obtained and (iii) the possible stereoisomers that can be formed. It is important to note that very few group 10 metal catalysts produce polymers with molecular weight higher than 10 000 Da. One of the few is the nitrogen ligand containing catalyst [Pd(NN'OCl)], therefore it was envisaged that nitrogen ligand containing catalyst could produce high molecular weight PPA.



The objectives of this project therefore were to (i) synthesize and characterize pyridine carboxamide ligands and their palladium complexes, and (ii) investigate their catalytic activity in the polymerization process of phenylacetylene. Another objective was to compare the catalytic activity of the pyridine carboxamide palladium(II) catalysts with σ -donor pyrazole palladium(II) catalysts whose synthesis was already reported in literature.⁷⁷ The rest of the thesis describes how we achieved our objectives.

1.10 References

1. Roncali, J. *Chem. Rev.* 1997, **97**, 173; (b) Gal, Y. S.; Choi, S. K. *J. Appl. Polym. Sci.* 1993, **50**, 601.
2. Chien, J. C. W. "Polyacetylene"; Academic Press: New York, 1984.
3. Will, F. G.; Mckee, D. W. *J. Polym. Sci., Polym. Chem. Ed.* 1983, **21**, 3479.
4. Chien, J. C. W.; Uden, P. C.; Fan, J.-L. *J. Polym. Chem. Ed.* 1982, **20**, 2159.
5. John A. Shelburne, III, and Baker, G. L. *Macromolecules* 1987, **20**, 1212.
6. Wegner, G. *Angew. Chem. Int. Ed. Engl.* 198, **120**, 361.
7. Natta, G.; Mazzanti, G.; Corradini, P. *Atti Accad. Naz. Lincei, Cl. Sci. Fis., Mat. Nat., Rend* 1958, **25**, 3.
8. Watson, W. H., Jr.; McMordie, W. D., Jr.; Lands, L. G. *J. Polym. Sci.* 1961, **55**, 137.
9. (a) Bleier, H.; Roth, S.; Shen, Y. Q.; Schafer-Siebert, D.; Leising, G. *Phys. Rev. B.* 1988, **38**, 6031; (b) Coustel, N.; Foxonet, N.; Ribet, J. L.; Bernier, P.; Fischer, J. E. *Macromolecules* 1991, **24**, 5867; (c) Matnishyan, A. A.; Kobryanskii, V. M. *Russ. Chem. Rev.* 1983, **52**, 751.
10. Tang, B. Z.; Kong, X.; Wan, X. *Macromolecules* 1997, **30**, 5620.
11. Gruber, A. S.; Boiteux, G.; de Souza, R. F.; de Souza, M. O. *Polym. Bull.* 2002, **47**, 529.
12. Masuda, T.; Tang, B. Z.; Tanaka, A.; Higashimura, T. *Macromolecules* 1986, **19**, 1459.
13. (a) Simionescu, C. I.; Percec, V. *Prog. Polym. Sci.* 1982, **8**, 133; (b) Masuda, T. *Polymeric Materials Encyclopedia*; CRC Press: New York, 1996; **1**, 32.

14. Yue'eva, L. P. *Russ. Chem. Rev.* 1974, **43**, 48.
15. Tlenkopachev, M.; Korshak, M. E.; Ogawa, T. *Polym. Bull.* 1995, **34**, 405.
16. Chauser, M. G.; Rodionov, Yu. M.; Misin, V. M.; Cherkashin, M. I. *Russ. Chem. Rev.* 1976, **45**, 348.
17. Chiang, A. C.; Waters, P. F.; Aldridge, M. H. *J. Polym. Sci., Chem.* 1982, **20**, 1807.
18. Masuda, T.; Sasaki, N.; Higashimura, T. *Macromolecules* 1975, **8**, 717.
19. Fahey, R. C. *Top. Stereochem* 1968, **2**, 273.
20. Manassen, J, Rein, R. *J. Polym. Sci., Part A-1*: 1970, **8**, 1403.
21. Gibson, H. W.; Porchan, J. M., *Encyclopedia of Polymer Science and Engineering*. 2nd ed. 1984, **1**, 87.
22. Masuda, T.; Higashimura, T. *Adv. Polym. Sci.* 1987, **81**, 122.
23. Masuda, T.; Hasegawa K.; Higashimura, T. *Macromolecules* 1974, **7**, 728.
24. Shrock, R. R.; Luo, S.; Zanetti, N.; Fox, H. H. *Organometallics* 1994, **13**, 3396.
25. Keller, A.; Sterenberg, L. *J. Mol. Catal.* 1992, **57**, 207.
26. Gibson, V. C. *Adv. Mater.* 1994, **6**, 37.
27. Minaki, N.; Hayano, S.; Masuda, T. *Polymer* 2002, **43**, 3579.
28. Masuda, T.; Thieu, K. Q.; Sasaki, N.; Higashimura, T. *Macromolecules* 1976, **9**, 661.
29. Masuda, T.; Takahashi, T.; Yamamoto, K.; Higashimura, T. *J. Polym. Sci., Polym. Chem. Ed.* 1982, **20**, 2603.
30. Masuda, T.; Yamamoto, K.; Higashimura, T. *Polymer* 1982, **23**, 1663.
31. Masuda, T.; Higashimura, T. *Adv. Polym. Sci.* 1987, **81**, 122.

32. Kambara, S.; Noguchi, H. *Macromol. Chem.* 1964, **79**, 244.
33. Natansohn, A.; Percec, V.; Simionescu, C. I. *J. Macromol. Sci. Chem. A* 1981, **15**, 643.
34. Natta, G.; Pino, P.; Mazzanti, G. *Italian Patent 530735 C. A.* 1958, **52**, 151286.
35. Masuda, T.; Hamano, T.; Higashimura, T.; Ueda, T.; Muramatsu, H. *Macromolecules* 1988, **21**, 281.
36. Furlani, A.; Napoletano, C.; Russo, M. V.; Camus, A.; Marsich, N. *J. Polym. Sci. A* 1989, **27**, 75.
37. Kishimoto, Y.; Itou, M.; Miyatake, T.; Ikariya, T.; Noyori, R. *Macromolecules* 1995, **28**, 6662.
38. Kishimoto, Y.; Miyatake, T.; Ikariya, T.; Noyori, R. *Macromolecules* 1996, **29**, 5054.
39. Tabata, M.; Sone, T.; Sadahiro, Y. *Macromol. Chem. Phys.* 1999, **200**, 265.
40. Misumi, Y.; Masuda, T. *Macromolecules* 1998, **31**, 7572.
41. Yao, J.; Wong, W. T.; Jia, G. *J. Organomet. Chem.* 2000, **598**, 228.
42. Cataldo, F. *Polym. Int.* 1993, **30**, 375.
43. Zhou, J.-Q.; Alpher, H. J. *Chem. Soc., Chem. Commun.* 1991, 233.
44. (a) Furlani, A.; Napoletano, C.; Russo, M. V.; Feast, W. *J. Polym. Bull.* 1986, **16**, 311; (b) Furlani, A.; Napoletano, C.; Russo, M. V.; Camus, A.; Marsich, N. *J. Polym. Sci. Part A: Polym. Chem.* 1989, **27**, 75.
45. Tabata, M.; Yang, W.; Yokota, K. *Polym. J.* 1990, **22**, 1105.
46. Tabata, M.; Yang, W.; Yokota, K. *J. Polym. Sci., Part A: Polym. Chem.* 1994, **32**, 1113.

47. Tang, B. Z.; Poon, W. H.; Leung, S. M.; Leung, W. H.; Peng, H. *Macromolecules* 1997, **30**, 2209.
48. Falcon, M.; Farnetti, E.; Marsich, N. *J. Organomet. Chem.* 2001, **629**, 187.
49. Marigo, M.; Marsich, N.; Farnetti, E. *J. Mol. Catal. A: Chem.* 2002, **187**, 169.
50. Tsuchihara, K. *Polymer Comm.* 2000, **41**, 2621.
51. Gruber, A. S.; Boiteux, G.; de Souza, R. F.; de Souza, M. O. *Polym. Bull.* 2002, **47**, 529.
52. Douglas, W. E.; Overend, A. S. *J. Organomet. Chem.* 1993, **444**, C62.
53. Sen, A.; Lai, T. W. *Organometallics* 1982, **1**, 415.
54. Li, K.; Wei, G. Darkwa, J. Pollack, S. K. *Macromolecules* 2002, **35**, 4573.
55. Pelagatti, P.; Carcelli, M.; Pelizzi, C.; Costa, M. *Inorg. Chim. Acta* 2003, **342**, 323.
56. (a) Shelburne, III, J. A.; Baker, G. L. *Macromolecules* 1987, **20**, 1212; (b) Shirakawa, S.; Ikeda, S. *J. Polym. Sci., Polym. Chem. Ed.* 1974, **12**, 929.
57. Masuda, T.; Higashimura, T. *Adv. Polym. Sci.* 1986, **81**, 121; (b) Han, C.-C.; Katz, T. J. *Organometallics* 1985, **4**, 2186.
58. (a) Cosse, J. *J. Catal.* 1964, **3**, 80; (b) Arlman, E. J.; Cossee, P. *Ibid.* 1964, **3**, 99.
59. Irvin, K. J.; Rooney, J. J.; Stewart, C. D.; Green, M. L. H.; Mahtab, R. J. *J. Chem. Soc., Chem. Commun.* 1978, 604.
60. (a) Cf: Shirakawa, S.; Ikeda, S. *J. Polym. Sci., Polym. Chem. Ed.* 1974, **12**, 929
(b) Wegner, G. *Angew. Chem. Int. Ed. Engl.* 1981, **20**, 361.
61. Yannoni, C. S.; Kendrick, R. D. *J. Chem. Phys.* 1981, **74**, 747.
62. Natta, G.; Mazzanti, G.; Corradini, P. *Rend. Nazl. Lincei Rend. Classe Sci. Fis.*

- Mat. Nat.* 1958, **25**, 3.
63. Watson, Jr., W. H.; McMordie, Jr., W. C.; Lands, L. G. *J. Polym. Sci.* 1961, **55**, 137.
64. Kleist, F. D.; Bryd, N. R. *J. Polym. Sci. A-1*. 1969, **7**, 3419.
65. Berlin, A.A.; Cerkushin, M. I. *Vysokomol. Soedin.* 1971, **A13**, 2298.
66. Simionescu, C. I.; Dumitrescu, S.; Negulescu, I.; Grigoras, M.; Diaconu, I.; Leanca, M.; Goras, L. *Vysokomol. Soedin.* 1974, **A16**, 790.
67. Berlin, A. A.; Cerkushin, M. I.; Cernisheva, I. P.; Aseev, E. I.; Borkan, E. I.; Kisilitzo, P. P. *Vysokomol. Soedin.* 1967, **A9**, 1840.
68. Simionescu, C. I.; Dumitrescu, S. *Eur. Polym. J.* 1970, **6**, 635.
69. Bellamy, L. J. *The infrared Spectra of Complex Molecules*, Wiley, New York 1954.
70. Simionescu, C. I.; Percec, V.; Dumitrescu, S. *J. Polym. Sci. Polym. Chem. Ed.* 1977, **15**, 2497.
71. Kern, R. J. *J. Polym. Sci. A-1*. 1969, **7**, 621.
72. Furlani, A.; Collati, I.; Sartori, G. *J. Organomet. Chem.* 1969, **17**, 463.
73. Furlani, A.; Napoletan, C.; Russo, M. V.; Feast, W. J. *J. Polym. Bull.* 1986, **16**, 311.
74. (a) Fujii, A.; Ishida, T.; Koga, N.; Iwamura, H. *Macromolecules* 1991, **24**, 1077;
(b) Miura, Y.; Matsumoto, M.; Ushiotani, Y.; Teki, Y.; Takui, T.; Itoh, K. *Macromolecules* 1993, **26**, 6673.
75. Matsunami, S.; Watanabe, T.; Kamimura, H.; Ishii, F.; Tsuda, K. *Polymer* 1996, **37**, 4853.
76. Simionescu, C. I.; Percec, V. *J. Polym. Sci. Polym. Chem. Ed.* 1980, **18**, 147.

77. Li, K.; Darkwa, J.; Guzei, I. A.; Mapolie, S. F. *J. Organomet. Chem.* 2002, **660**,
108.



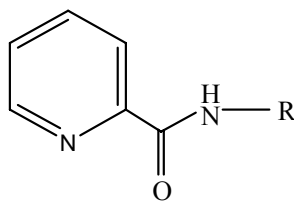
CHAPTER 2

SYNTHESIS AND CHARACTERIZATION OF PYRIDINE CARBOXAMIDE

PALLADIUM(II) COMPLEXES.

2.1 Introduction

The carboxamide [-C(O)NH-] group, which seems to be everywhere throughout nature in the primary structure of proteins, is an important ligand construction unit for coordination chemists. Pyridine carboxamides (**I**) (Scheme 2.1), a flourishing class of multidentate ligands containing this linkage, are available from condensation reactions between pyridyl-bearing amine or carboxylic acid precursors, promoted by coupling agents such as 1,1-carbonyldiimidazole, diphenoxyphosphoryl azide or triphenylphosphite.¹ Pyridine carboxamide ligands are inexpensive and easy to prepare. Their chemical reactivity can easily be tuned through modification of substituent groups at the pyridine ring or amide bridge.²



R = Ph, CH₃, Py

I

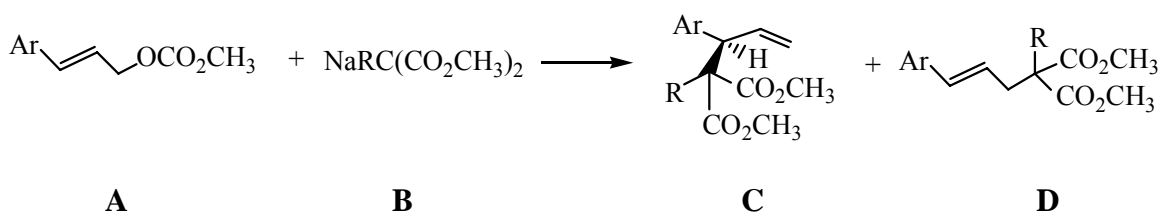
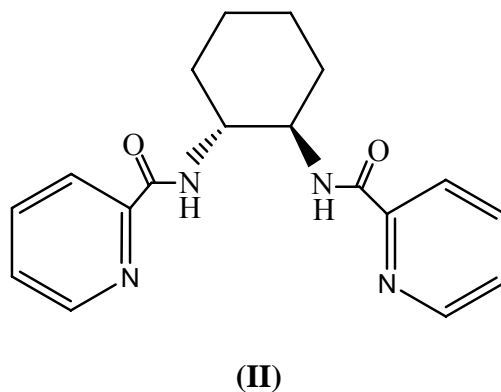
Scheme 2.1

Upon deprotonation of the carboxamide nitrogen atom, this centre and the pyridyl ring(s) of the anion chelate to metal ions. Pyridine carboxamide ligands have found use in

asymmetric catalysis,³ molecular receptors,⁴ dendrimer synthesis⁵ and in the synthesis of metal complexes.⁶ The next sections highlight these applications of pyridine carboxamide ligands.

2.1.1 Asymmetric catalysis

The field of asymmetric catalysis is continuously growing and the number of sophisticated methods and reactions used to achieve high stereoselectivity is infinitely increasing.⁷ One of the numerous catalysts used for this reaction is a tungsten pyridine carboxamide complex used by Trost *et al.*³ The pyridine carboxamide that was employed is N,N'-bis(2-pyridinecarboxamide)-1,2-cyclohexane (**II**). Trost *et al.*³ reported that the catalyst was generated by stirring 1:1.5 mole mixture of $(C_2H_5CN)_3W(CO)_3$:ligand in THF at 60 °C.⁸ The test reaction employed the cinnamate (**A**) (Ar = Ph) with dimethyl sodium malonate (**B**) (R = H) in THF at reflux (Scheme 2.2). However, a low yield of a 19:1 ratio of **C:D** with **C** having an enantiomeric excess (ee) of 98% was obtained when 5 mol % of catalyst was used. Increasing the catalyst concentration to 15 mol % increased the yield to 55% and the **C:D** ratio to 49:1 with **C** still having 98% ee.



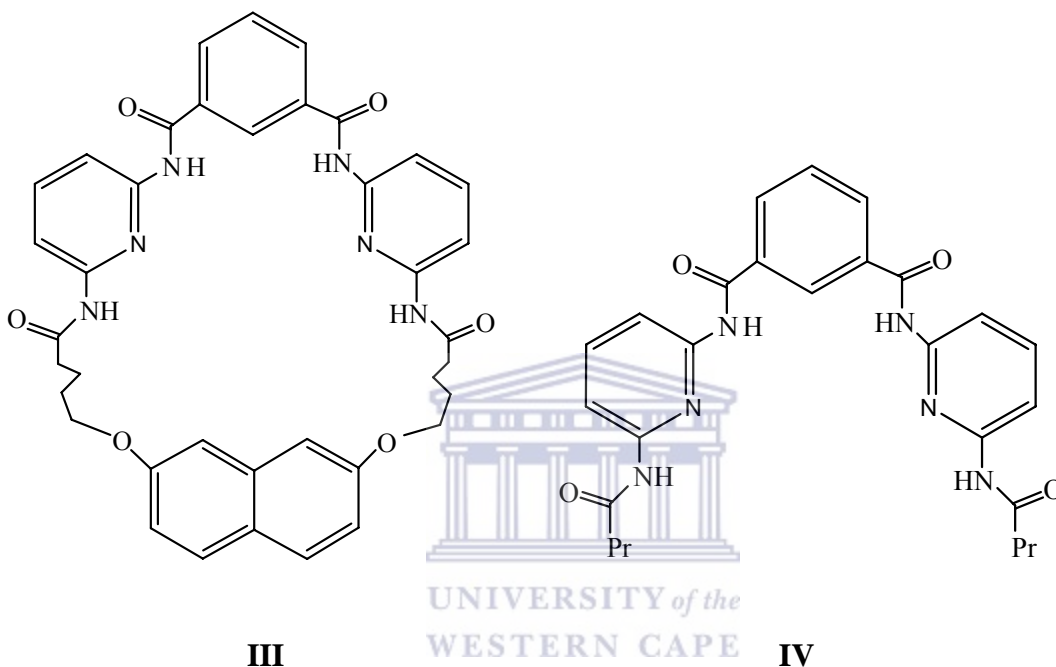
Scheme 2.2

Attempt to repeat the above but replacing the tungsten complex by $(\text{C}_2\text{H}_5\text{CN})_3\text{Mo}(\text{CO})_3$ gave 88% yield of a 97:3 ratio of **C:D** with **C** having an ee of 99%. Lowering the temperature to room temperature still provided a good yield and somewhat improved regioselectivity while maintaining a high ee.³ These two catalysts are examples of the usefulness of pyridine carboxamide in asymmetric catalysis.

2.1.2 Molecular receptors

Interest in the development of functional receptors for organic molecules such as barbiturates arises due to their importance as sedatives and anticonvulsants, whilst the detection of ureas is important with regard to possible applications in dialysis. However, previous studies concerning the binding of barbiturates and ureas have largely focused on

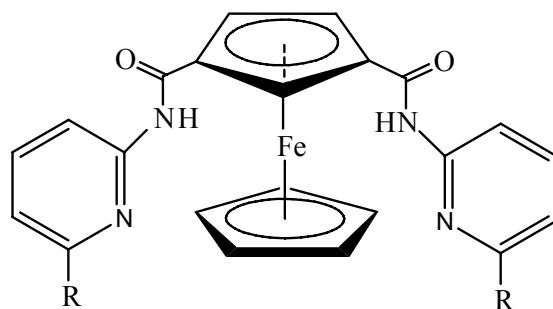
organic receptors that bind the neutral guest through hydrogen bonds.⁹ Hamilton *et al.*¹⁰ have reported the complexation of barbiturates by macrocyclic and acyclic receptors (e.g. **III** and **IV**) (Scheme 2.3) containing two 2,6-diaminopyridine units linked via an isophthaloyl group.



Scheme 2.3

However, instead of using receptors **III** and **IV**, Tucker *et al.*¹¹ have reported that a similar binding motif can be constructed through the incorporation of a redox-active ferrocene unit into the receptor framework. This synthetic strategy involved the synthesis of ferrocene-1,3-dicarbonylchloride,¹² which was then reacted in the presence of triethylamine, with either two equivalents of 2-amino-6-methylpyridine or with an excess of 2,6-diaminopyridine, to yield compound **V** and **VI** (Scheme 2.4) respectively. Further

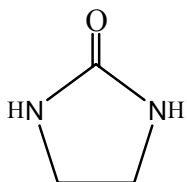
reaction of **VI** with propionyl chloride, again in the presence of triethylamine, yielded compound **VII** (Scheme 2.4).



V R = CH₃

VI R = NH₂

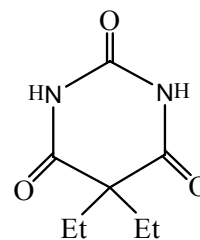
VII R = HNCOEt



Ethylene urea



Trimethylene urea



Barbital

Scheme 2.4

All the reactions produced a series of ferrocene receptors containing either two hydrogen bond donor groups with two hydrogen bond acceptor groups (receptor **V**) or four hydrogen bond donor groups with two hydrogen bond acceptor groups (receptor **VI** and **VII**)

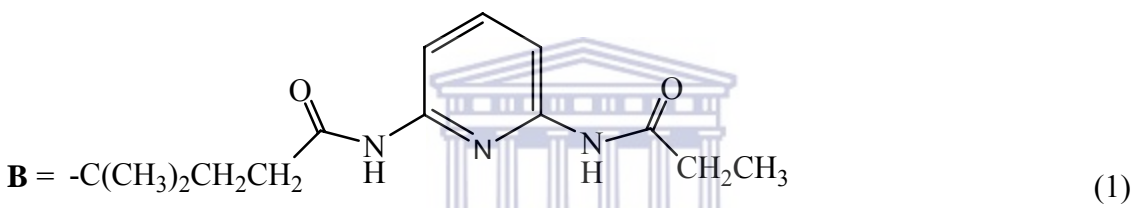
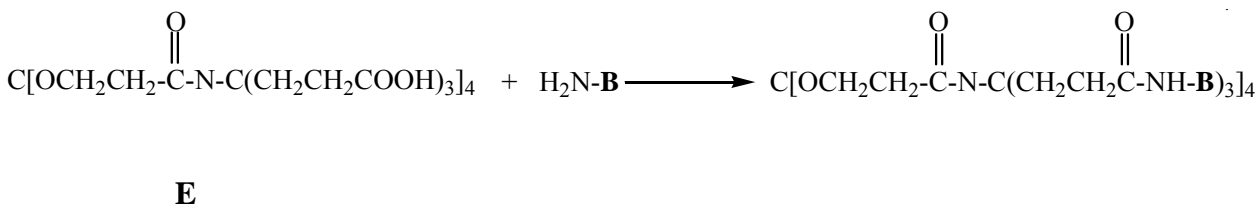
Receptor **V** forms the most stable complex via four hydrogen bonds with trimethylene urea, suggesting that ethylene urea is too small for the cavity formed by these receptors. Interesting, **V** only forms a weak complex with barbital, which is similar in size to trimethylene urea. This reflects the fact that there are two carbonyl groups on the barbital guest, which are not involved directly in hydrogen bonding but nevertheless are adjacent to a hydrogen bond, leading to unfavorable diagonal secondary electrostatic interactions.¹³

In a related manner, trimethylene urea forms weaker complexes with **VI** and **VII** compared to receptor **V**. As expected, the highest binding constants, via the formation of six hydrogen bonds, are observed between barbital and receptors **VI** and **VII**. In point of fact, **VI** binds more strongly than **VII**, where the difference between these two receptors arises at the hydrogen bond donor groups with the R substituent, being amines or amides respectively.¹⁴ It is clear from these binding sites that the pyridine carboxamide motif is crucial in the binding capacities of these receptors and demonstrate another usefulness of pyridine carboxamides as ligands.

2.1.3 Dendrimer synthesis

Dendrimers are highly branched macromolecules possessing “tree-like” structures and are synthesized by repetitively linking molecular blocks AB_n (n usually 2 or 3) to a central core.¹⁵ Since both the internal and external chemical functionalities of dendrimers can be “tailored” to alter their physical and chemical properties,¹⁶ several potential applications have been found for these polymers including catalysis, self-assembly,

molecular recognition and encapsulation. Newkome *et al.*¹⁷ have successfully synthesized dendrimers with internal pyridine carboxamide binding sites by coupling the alkylamine building block **B**-NH₂ to the terminal carboxylic acids of polyamido dendrimer (**E**) (eq 1) (Scheme 2.5) using standard peptide coupling conditions.



Scheme 2.5
UNIVERSITY of the
WESTERN CAPE

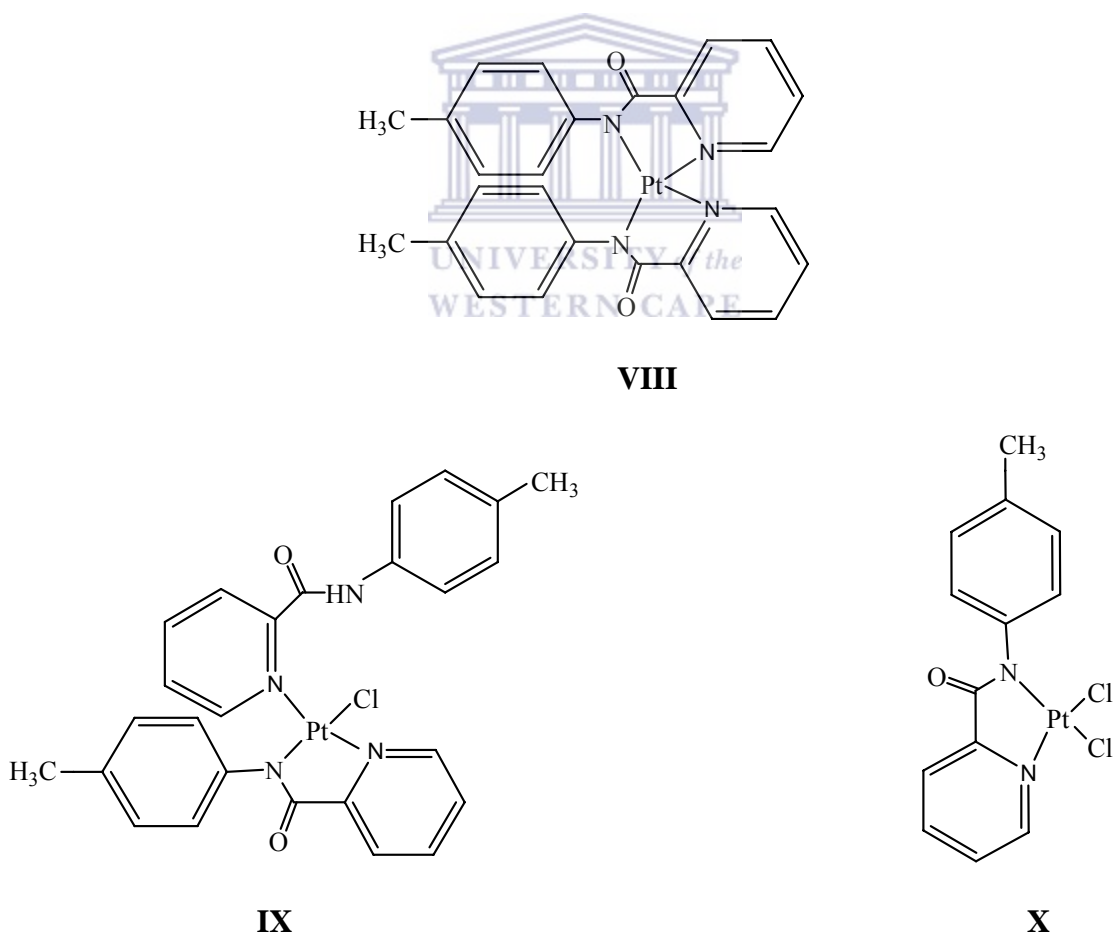
These diamidopyridino dendrimers can be readily synthesized and have been previously examined for specific H-bonding to glutarimide and barbituric acid.

2.1.4 Metal complexes synthesis

Complexes containing pyridine carboxamide ligands have been much less studied than those containing amido or amine ligands. However, both early and more recent studies have shown that pyridine carboxamide ligands can readily form very stable complexes with a wide range of metals such as platinum, copper, cobalt, ruthenium.⁶ Below are examples of complexes these metals form with pyridine carboxamide and some of the

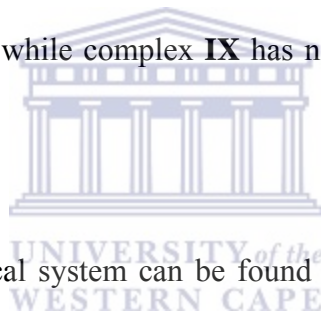
uses of the metal complexes formed. Attention is also drawn to structural types as these contrast the proposed structures of analogous palladium complexes prepared in my project.

Guo *et al.*¹⁸ have synthesized three novel platinum(II) complexes using pyridine carboxamide ligands, which were found to have antitumour properties. The formation of complex **VIII**, **IX** or **X** (Scheme 2.6) is dependent on the absence or presence of chloride. In the absence of chloride containing precursors **VIII** is the product obtained, whilst precursors containing chlorides produced **IX** or **X** depending on the reaction conditions.



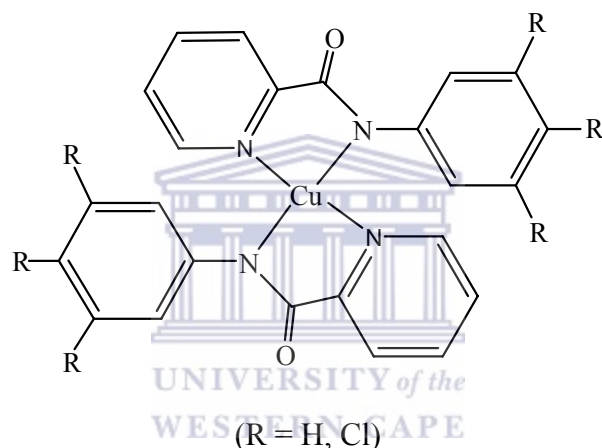
Scheme 2.6

Complexes **VIII** and **IX** were structurally characterized. The platinum in complex **VIII** adopted a distorted square-planar geometry coordinated by two equivalent pyridine nitrogen atoms and two amide nitrogen atoms from two ligands that are arranged in a *cis* configuration. The approximately square-planar coordination of the platinum atom generates two five-membered rings. However, the platinum in complex **IX** is coordinated in a square planar geometry which is composed of two pyridyl nitrogen atoms, one amide nitrogen atom and a chloride anion. The two pyridyl nitrogen atoms in the ligands are *trans* to each other. According to Guo *et al.*,¹⁸ complexes **VIII** and **IX** have different antitumour activity *in vitro*. For example, complex **VIII** is inactive against human leukemia HL-60, human liver cancer BEL-7402, murine leukemia P388 and human lung cancer A-549 tumor cell lines, while complex **IX** has notable activity against these cell lines.



Another application in biological system can be found in a report by Olmstead *et al.*¹⁹ who investigated the behaviour of pyridine carboxamide ligands towards the biologically relevant d-block metal copper as model compounds in biological systems. Copper is integral to the active site of numerous electron transfer and oxygenase metalloproteins, moreover these biosites often contain several copper ions in very close proximity to one another, e.g. ascorbate oxidase and lactase have four copper atoms in the active site. Using pyridine dicarboxamides, e.g. N,N'-bis(2-(2-pyridyl)ethyl)pyridine-2,6-dicarboxamide, Olmstead *et al.*¹⁹ isolated copper complexes with the copper(II) ion coordinated to five nitrogen atoms.

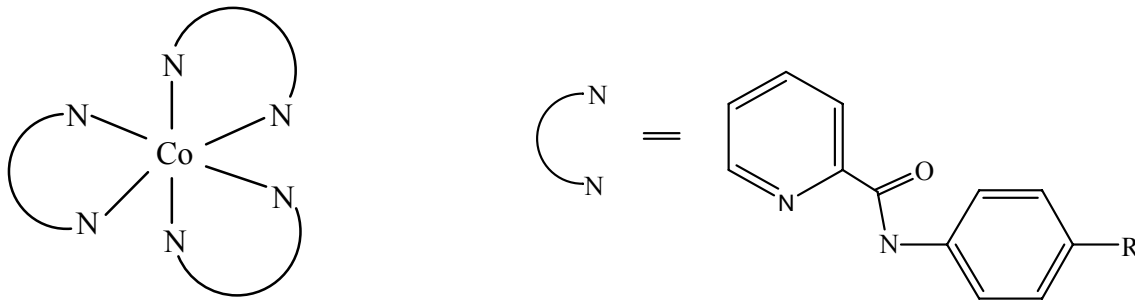
However, work done by Mukherjee *et al.*,²⁰ which concentrated on the control of the stereochemistry of four-coordinate copper(II) complexes by pyridine carboxamide ligands, showed that the copper(II) centre is generally coordinated to four nitrogen donor atoms (**XII**) (Scheme 2.7), with the two pyridyl nitrogen atoms in *trans* position and the two amide nitrogen atoms in *trans* position too. This mode of coordination of the pyridine carboxamide is in line with our proposed coordination for palladium complexes reported in this thesis.



XII

Scheme 2.7

Chan *et al.* have reported the synthesis and characterization of trivalent cobalt complexes (**XI**) (Scheme 2.8) containing pyridine carboxamide ligands.²¹ The complexes were found to be highly active and remarkably selective in the oxidation of ethylbenzene to acetophenone using dioxygen as the oxidant and demonstrated the usefulness of pyridine carboxamide metal complexes in oxidation catalysis.



(R = H, Me, OMe, Cl)

XI

Scheme 2.8

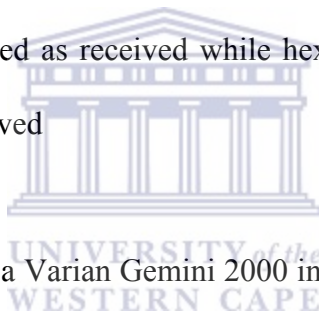
The chemistry of ruthenium complexes with pyridine carboxamide ligands is well explored. Dutta *et al.*²² reported the synthesis and characterization of pyridine carboxamide ligands and their complexes with ruthenium. They claimed that the presence of the pyridyl nitrogen at the adjacent position of the amide linkage helps the ligand to bind to a metal ion in a bidentate fashion forming a five-membered chelate ring either through N-bonding or through O-bonding. The techniques that were used to detect whether the pyridine carboxamide ligands coordinate to the ruthenium metal through the pyridyl nitrogen atom and the amide nitrogen or carbonyl oxygen atom are IR and X-ray. The IR spectra showed that the carbonyl frequency of the coordinated amide ligands appear at a lower frequency (1635 cm^{-1}) compared to that of the free ligands (1677 cm^{-1}). Dutta *et al.*²² then inferred from the IR data that coordination to the ruthenium is through the pyridyl nitrogen atom and the amide nitrogen atom. This was supported by X-ray crystal structure, which confirmed the amide nitrogen coordination and not carbonyl

oxygen.²² It is thus clear that IR data can be used in identifying binding modes of pyridine carboxamide ligands. This approach is used in characterizing the type of complexes formed by pyridine carboxamide and palladium reported in this thesis.

2.2 Experimental

2.2.1 Materials and instrumentation

All reactions were performed under dry, deoxygenated nitrogen atmosphere using standard Schlenk techniques. Dichloromethane was dried with P₂O₅ and diethyl ether with sodium/benzophenone, distilled and stored over molecular sieves. Pyridine-2-carboxylic acid, 6-methylnicotinic acid, 3,5-dimethylaniline, and acetonitrile were purchased from Aldrich and used as received while hexane was obtained from B & M Scientific and also used as received



NMR spectra were recorded on a Varian Gemini 2000 instrument (¹H at 200 MHz, ¹³C at 50 MHz) at room temperature. The chemical shifts are reported in δ (ppm) and referenced to residual proton and ¹³C signals of deuterated chloroform or DMSO as internal standards. IR spectra were recorded as nujol mulls on a Perkin Elmer, paragon 1000PC FT-IR spectrometer. Elemental analyses were performed using a Carlo Erba EA1108 elemental analyzer in the microanalytical laboratory of the University of Cape Town. GC-MS analysis was performed using a Finnigan-Matt GCQ-Gas chromatography equipped with an electron impact ionization source at 70eV, a 30 m HP-MS capillary column with a stationary phase based on 5% phenyl-methylpolysiloxane.

2.3. Synthesis and characterization of the ligands

Ligands **L1** and **L2** were prepared by a literature procedure reported by Bhattacharya *et al.*,²³ but in our hands we did not obtain their reported high yields and thus describe exactly how we isolated these compounds. We also report the full characterization to show that only pure ligands were used in the synthesis of the palladium complexes. Ligands **L3** and **L4** are, however, new compounds that were synthesized for the first time.

2.3.1 2-(*N*-phenylcarbamoyl)pyridine (**L1**)

To a solution of pyridine-2-carboxylic acid (2.00 g, 16.20 mmol) in pyridine (10 ml), was added aniline (1.51 ml, 16.20 mmol) and warmed with stirring for 15 min. To the resulting solution was added triphenylphosphite (5.03 g, 16.20 mmol) and the mixture was stirred at 110 °C for 4 h. After cooling to room temperature, the reaction mixture was washed with distilled water (100 ml) and the resulting yellow paste was dissolved in dichloromethane (40 ml) and extracted with 5.25 M aqueous hydrochloric acid. The acidic aqueous extract was neutralized with solid sodium bicarbonate. The resulting white solid formed was filtered and washed thoroughly with distilled water to remove unreacted aniline. The solid was then extracted with dichloromethane (20 ml), filtered and the filtrate evaporated to dryness. Recrystallization of the ligand was done from dichloromethane and hexane to give a white solid. Yield: 1.85 g (58%). Anal. Calcd. for C₁₂H₁₀N₂O: C, 72.71; H, 5.08; N, 14.13% Found C, 73.11; H, 5.23; N, 14.17%. ¹H NMR (CDCl₃): δ 7.21 (1H, t, H⁹, ³J_{HH} = 7.0 Hz), 7.40 (2H, t, H⁸, ³J_{HH} = 7.4 Hz), 7.52 (1H, dd, H⁵, ⁴J_{HH} = 1.8 Hz, ³J_{HH} = 7.8 Hz), 7.69 (2H, d, H⁷, ³J_{HH} = 7.6 Hz), 8.24

(1H, br s, H⁴), 8.31 (1H, d, H³, ³J_{HH} = 8.2 Hz), 8.78(1H, d, H⁶, ³J_{HH} = 7.4 Hz), 9.24 (1H, s, NH). ¹³C{¹H} NMR (CDCl₃): δ 164.5, 153.2, 148.5, 138.1, 135.9, 131.5, 129.8, 125.7, 124.3, 121.1. IR (nujol mull, cm⁻¹): ν(C=O) 1654, ν(N-H) 3334. EIMS (70 eV): m/z (%) = 197 (100) [M⁺]; 106 (85) [M⁺-C₆H₆N]; 78 (55) [M⁺-C₇H₆NO].

2.3.2. 2-[N-(4-methylphenylcarbamoyl)]pyridine (L2)

Compound **L2** was prepared in a similar way to **L1** by reacting pyridine-2-carboxylic acid (3.08 g, 25.00 mmol) and 4-methylaniline (2.68 g, 25.00 mmol) in the presence of triphenylphosphite (7.76 g, 6.60 ml, 25 mmol) to give a white solid. Yield: 3.46 g (65%). Anal. Calcd. for C₁₃H₁₂N₂O: C, 73.56; H, 5.70; N, 13.20% Found C, 73.67; H, 5.89; N, 13.09%. ¹H NMR (CDCl₃): δ 2.35 (3H, s, CH₃-phenyl), 7.18 (2H, d, H⁸, ³J_{HH} = 8.0 Hz), 7.54 - 7.40 (3H, m, H⁷ and H⁵), 7.95 (1H, br s, H⁴), 8.21(1H, d, H³, ³J_{HH} = 7.6 Hz), 8.76 (1H, d, H⁶, ³J_{HH} = 4.8 Hz), 9.08 (1H, s, NH). ¹³C{¹H} NMR (CDCl₃): δ 163.7, 151.9, 148.5, 136.2, 135.3, 132.9, 130.6, 129.0, 123.4, 120.3, 20.4. IR (nujol mull, cm⁻¹): ν(C=O) 1677, ν(N-H) 3309. EIMS (70 eV): m/z (%) = 212 (100) [M⁺]; 197 (10) [M⁺-CH₃]; 106 (95) [M⁺-C₇H₉N], 78 (55) [C₈H₉NO].

2.3.3 2-[N-(3,5-dimethylphenylcarbamoyl)]pyridine (L3)

Compound **L3** was prepared in a similar way to **L1** by reacting pyridine-2-carboxylic acid (2.00 g, 16.20 mmol) and 3,5-dimethylaniline (1.96 g, 2.00 ml, 16.20 mmol) in the presence of triphenylphosphite (5.01 g, 4.23 ml, 16.20 mmol) to give a white solid. Yield: 2.31 g (63%). Anal. Calcd. for C₁₄H₁₄N₂O: C, 74.31; H, 6.24; N, 12.38% Found C, 74.23; H, 6.63; N, 12.22%. ¹H NMR (CDCl₃): δ 2.31 (6H, s, CH₃- phenyl), 6.81 (1H, s,

H⁹), 7.25 (2H, s, H⁷), 7.41(1H, dd, H⁵, ⁴J_{HH} = 2.6 Hz, ³J_{HH} = 7.0 Hz), 8.03 (1H, br s, H⁴), 8.18 (1H, d, H³, ³J_{HH} = 7.0 Hz), 8.73(1H, d, H⁶, ³J_{HH} = 6.6 Hz), 9.06 (1H, s, NH). ¹³C{¹H} NMR (CDCl₃): δ 163.7, 152.2, 147.8, 138.8, 137.2, 135.3, 130.9, 126.8, 123.6, 118.2, 21.3. IR (nujol mull, cm⁻¹): ν(C=O) 1649, ν(N-H) 3225. EIMS (70 eV): m/z (%): 226 (20) [M⁺], 120 (20) [M⁺-C₆H₄NO], 106 (68) [M⁺-C₇H₆NO], 91 (50) [M⁺-C₇H₇N₂O], 78 (100) [M⁺-C₈H₈N₂O].

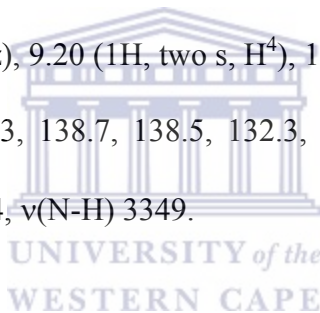
2.3.4 2-[N-(3,5-dimethylphenylcarbamoyl)]6-methylpyridine (L4).

Compound **L4** was prepared in a similar way to **L1** by reacting 6-methylpyridine carboxylic acid (2.00 g, 14.60 mmol) and 3,5-dimethylaniline (1.77 g, 1.82 ml, 14.60 mmol) in the presence of triphenylphosphite (4.53 g, 3.83 ml, 14.60 mmol) to give a white solid. Yield: 1.96 g (56%). Anal. Calcd. for C₁₅H₁₆N₂O: C, 74.97; H, 6.71; N, 11.66%. Found C, 74.30; H, 7.24; N, 11.34%. ¹H NMR (CDCl₃): δ 2.32 (6H, s, CH₃-phenyl), 2.64 (3H, s, CH₃-pyridine), 6.82 (1H, s, H⁹), 7.30-7.27 (3H, s, H⁷ and H⁵), 7.78 (1H, br s, H⁴), 8.09 (1H, d, H³, ³J_{HH} = 8.0 Hz), 8.96 (1H, s, NH). ¹³C{¹H} NMR (CDCl₃): δ 163.9, 161.8, 147.2, 138.8, 137.4, 135.7, 128.1, 126.6, 123.2, 118.2, 24.4, 21.3. IR (nujol mull, cm⁻¹): ν(C=O) 1664, ν(N-H) 3314. EIMS (70 eV): m/z (%): 240 (25) [M⁺], 120 (100) [M⁺- C₈H₁₀N], 91 (80) [M⁺- C₉H₁₀NO], 77 (38) [M⁺- C₁₀H₁₃NO].

2.4 Synthesis and characterization of palladium complexes

2.4.1 Dichloro[2-(*N*-phenylcarbamoyl)]pyridinepalladium(II) (**1**)

Complex **1** was prepared by adding **L1** (0.15 g, 0.77 mmol) to a solution of PdCl₂(NCCH₃)₂ (0.20 g, 0.77 mmol) in CH₂Cl₂ (40 ml). Upon addition of the reactant, immediate formation of a yellow precipitate was formed. However, to ensure that the reaction goes to completion the reaction mixture was stirred for 6h. The product was then isolated by gravity filtration to give a yellow solid. Yield: 0.16 g (80%). Anal. Calcd for C₁₂H₁₀N₂OPdCl₂·0.5CH₃CN: C, 42.46; H, 3.31; N, 10.60%. Found C, 41.99; H, 2.70; N, 8.18%. ¹H NMR (DMSO): δ 7.12 (1H, t, H⁹, ³J_{HH} = 7.0 Hz), 7.36 (2H, t, H⁸, ³J_{HH} = 7.6 Hz), 7.75-7.69 (3H, m, H⁷ and H⁵), 8.51 (1H, d, H⁶, ³J_{HH} = 7.6 Hz), 8.87 (1H, two d, H³, ³J_{HH} = 5.4 Hz and ³J_{HH} = 5.6 Hz), 9.20 (1H, two s, H⁴), 10.66 (1H, s, NH). ¹³C{¹H} NMR (DMSO): δ 162.0, 155.3, 152.3, 138.7, 138.5, 132.3, 129.0, 125.5, 124.6, 120.7. IR: (nujol mull, cm⁻¹): ν(C=O) 1684, ν(N-H) 3349.



2.4.2 Dichloro[2-(*N*-4-methylphenylcarbamoyl)]pyridinepalladium(II) (**2**)

Complex **2** was prepared in a similar way to **1** by adding **L2** (0.15 g, 0.71 mmol) to a solution of PdCl₂(NCCH₃)₂ (0.18 g, 0.71 mmol) in CH₂Cl₂ (40 ml) to give a light yellow solid. Yield: 0.17 g (61%). Anal. Calcd for C₁₃H₁₂N₂OPdCl₂·0.25CH₂Cl₂: C, 40.93; H, 2.94; N, 6.82%. Found C, 41.39; H, 2.43; N, 7.20%. ¹H NMR (DMSO): δ 2.25 (3H, s, CH₃-phenyl), 7.16 (2H, d, H⁸, ³J_{HH} = 7.4 Hz), 7.40-7.57 (3H, m, H⁷ and H⁵), 8.50 (1H, d, H⁶, ³J_{HH} = 7.0 Hz), 8.85 (1H, two d, H³, ³J_{HH} = 5.4 Hz), 9.17(1H, two s, H⁴), 10.58 (1H, s, NH). ¹³C{¹H} NMR (DMSO): δ 161.7, 155.2, 152.3, 138.6, 136.1, 133.6, 132.3, 129.3, 125.4, 120.7, 20.7. IR (nujol mull, cm⁻¹): ν(C=O) 1681, ν(N-H) 3340.

2.4.3 Dichloro[2-(*N*-(3,5-dimethylphenylcarbamoyl)]pyridinepalladium(II) (3)

Complex **3** was prepared in a similar way to **1** by adding **L3** (0.20 g, 0.88 mmol) to a solution of PdCl₂(NCCH₃)₂ (0.23 g, 0.88 mmol) in CH₂Cl₂ (40 ml) to give a light yellow solid. Yield: 0.32 g (94%). Anal. Calcd. for C₁₄H₁₄N₂OPdCl₂·0.25CH₃CN: C, 45.31; H, 3.33; N, 9.91% Found C, 44.01; H, 3.56; N, 7.13%. ¹H NMR (DMSO): δ 2.23 (6H, s, CH₃-phenyl), 6.76 (1H, s, H⁹), 7.34 (2H, s, H⁷), 7.70 (1H, t, H⁵, ³J_{HH} = 6.0 Hz), 8.47 (1H, d, H⁶, ³J_{HH} = 6.6 Hz), 8.84 (1H, two d, H³, ³J_{HH} = 5.6 Hz), 9.16 (1H, two s, H⁴), 10.50 (1H, s, NH). ¹³C{¹H} NMR (DMSO): δ 161.5, 155.0, 152.0, 138.4, 138.1, 137.7, 132.1, 125.8, 125.1, 118.1, 21.0. IR (nujol mull, cm⁻¹): ν(C=O) 1683, ν(N-H) 3387.

2.4.4 Dichloro[2-(*N*-(3,5-dimethylphenylcarbamoyl)]6-methylpyridinepalladium(II)

(4)

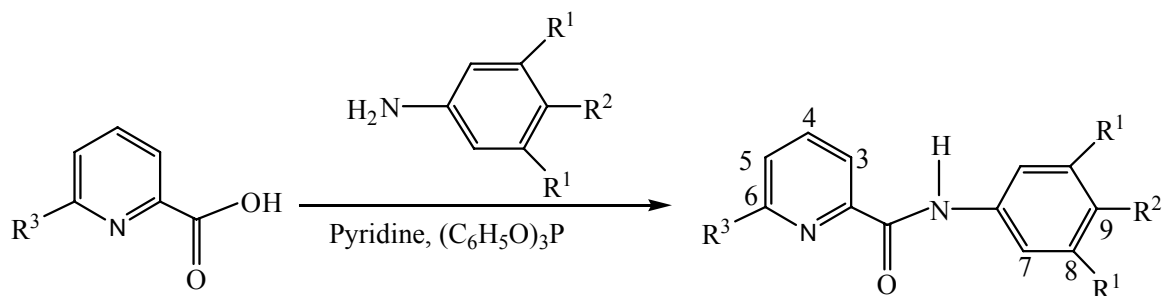
Compound **4** was also prepared in a similar way to **1** by reacting PdCl₂(CH₃CN)₂ (0.22 g, 0.83 mmol) and **L4** (0.22 g, 0.88 mmol) to give a light yellow solid. Yield: 0.22 g (63%). Anal. Calcd. for C₁₅H₁₆N₂OPdCl₂: C, 43.14; H, 3.86; N, 6.71% Found C, 43.03; H, 4.11; N, 6.29%. ¹H NMR (DMSO): δ 2.20 (6H, s, CH₃ aniline), 3.06 (3H, s, CH₃ pyridine), 6.72 (1H, s, H⁹), 7.31 (2H, s, H⁷), 7.65 (1H, d, H³, ³J_{HH} = 8.0 Hz), 8.36 (1H, t, H⁵, ³J_{HH} = 7.6 Hz), 9.16 (1H, s, H⁴), 10.40 (1H, s, NH). ¹³C{¹H} NMR (DMSO): δ 162.5, 161.4, 150.3, 138.2, 138.1, 137.6, 129.4, 126.2, 125.7, 118.3, 25.9, 20.9. IR (nujol mull, cm⁻¹): ν(C=O) 1684, ν(N-H) 3373.

2.5 Results and discussion

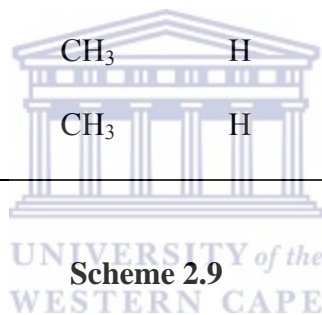
2.5.1 Synthesis and characterization of pyridine carboxamide ligands

Ligands **L1-L4** were synthesized by a triphenylphosphite promoted condensation reaction between pyridine-2-carboxylic acid or 6-methylpyridine carboxylic acid and an equimolar quantity of the appropriate aniline, using pyridine as a solvent (Scheme 2.9). The reactions were refluxed for 4 h after which pale yellow oils were obtained in all the reactions. The reaction mixtures were acidified followed by neutralization with solid sodium bicarbonate to give white precipitates which were filtered, washed several times with distilled water to remove excess aniline and sodium bicarbonate.

To ensure that excess solid sodium bicarbonate was removed, the solids obtained were taken into dichloromethane and then filtered. The dichloromethane filtrates were then evaporated to give white solids, which were recrystallized from dichloromethane and hexane. All the ligands were obtained as white solids in good yields (56-65%) and were also found to be stable in air, which allowed being stored at room temperature for a long period. The difference between **L1-L4** is in the substituents on the phenyl and pyridine rings as shown in Scheme 2.9. The ligands showed high solubility in most polar solvents such as, dichloromethane, diethyl ether, chloroform, dimethylformamide and even in toluene, which is non-polar. However, they were all insoluble in hexane, as such it was easy to recrystallize them in mixtures of the solvents in which they dissolved and hexane.



Ligand	R ¹	R ²	R ³
L 1	H	H	H
L 2	H	CH ₃	H
L 3	CH ₃	H	H
L 4	CH ₃	H	CH ₃



Scheme 2.9

All the compounds were characterized by ¹H and ¹³C NMR, IR, mass spectrometry and by microanalysis. The ¹H NMR spectrum of **L1**, which has unsubstituted rings, showed distinct peaks other than the peak at 2.19 ppm, which is due to acetone. In the aromatic region of the ¹H NMR spectrum of **L1**, seven resonances were found which integrate for nine protons. The singlet at 9.24 ppm is assigned to the NH proton of the amide linkage. The two triplets at 7.21 ppm and 7.40 ppm, and the doublet at 7.69 ppm are assigned to the protons H⁹, H⁸ and H⁷ respectively of the phenyl ring. The doublet of a doublet at 7.52 ppm, the singlet at 8.24 ppm, and the two doublets at 8.31 ppm and 8.78 ppm are

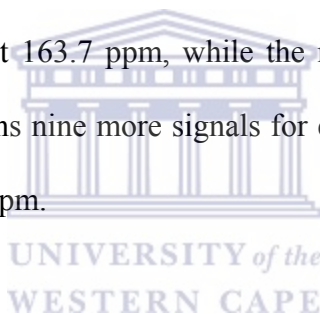
assigned to the pyridine ring H⁵, H⁴, H³ and H⁶ protons respectively. For the broad singlet peak at 8.24 ppm, a doublet of a doublet was expected since the proton assigned to this peak (H⁴) is between the two inequivalents protons (i.e H⁵ and H³). The report by Bhattacharya has no ¹H NMR spectrum of this ligand. The only reported data is for **L2**. Hence a detailed assignment for **L2** is given below in order to compare my data with that reported in the literature.

The ¹H NMR spectrum of **L2** (Figure 2.1) shows an upfield singlet peak at 2.35 ppm that is assigned to the methyl protons attached to the phenyl ring. The singlet at 9.08 ppm is assigned to the NH proton of the amide linkage. The singlet and the two doublets appearing at 7.95 ppm, 8.21 ppm and 8.76 ppm respectively are due to the pyridine ring protons. Due to the introduction of the methyl group at the C-4 of the phenyl ring, H⁸ peak appeared as a doublet as expected at 7.18 ppm, while H⁷ and H⁵ peaks at 7.54-7.40 ppm show an overlap and thus appear as a multiplet. The multiplet is caused by the presence of the methyl group on the phenyl ring, which caused the doublet at H⁷ to shift upfield and then appears almost in the same region as the H⁵ peak. However, no such effect was observed when 3,5-dimethyl substituents were introduced to form **L3**, which also showed distinct peaks similar to **L2** as such I have offered no detailed assignment for **L3**.

Bhattacharya *et al.*²³ reported that in the aromatic region of the ¹H NMR spectrum of **L2**, six resonances were found to integrate for eight protons. However, in the ¹H NMR spectrum we obtained, five resonances were found to integrate for eight protons, which

are in the aromatic region. This is due to the multiplet peaks of H⁵ and H⁷ that were counted as one resonance, while Bhattacharya reported them as separate peaks. Another difference that was observed is the triplet of a doublet for H⁴ that was reported by Bhattacharya. In our case, the peak appeared as a broad singlet, which also shows that there is coupling of the protons. This could be attributed to the low magnetic field of the instrument that was used to analyze our compounds. In terms of the shifts, all our peaks appeared upfield as compared to what they have reported. However, all protons of the ligand were assigned in a similar pattern to theirs.

In the proton decoupled ¹³C NMR spectrum of **L2** (Figure 2.2), the signal due to the C=O of the amide linkage appears at 163.7 ppm, while the methyl carbon signal appears at 20.4 ppm. The spectrum contains nine more signals for eleven aromatic carbon atoms in the region 151.9 ppm to 120.3 ppm.



In **L4**, introduction of a methyl on the pyridine again led to the overlapping of H⁵ and H⁷ peaks. Unlike **L2** and **L3**, which showed one upfield peak due to the methyl groups, **L4** showed two peaks because of the additional methyl group attached to the pyridine ring. Since a methyl group increases the electron density on the ring it is attached to, its presence has a profound effect on the phenyl ring protons, the pyridine ring protons, as well as the NH protons with respect to the chemical shifts. For instance, **L2** peaks shifted upfield by an average of 0.19 ppm as compared to **L1** peaks. The NMR data on the whole identifies the presence of the various fragments in the ligands. These are pyridine, phenyl and NH functional group.

Infrared spectroscopy was used to identify the functional groups C=O and N-H in **L1-L4**. Figure 2.3 represent such infrared spectrum. All the free ligands **L1-L4** exhibited C=O stretching bands from 1654 to 1677 cm^{-1} and N-H stretching bands from 3305 to 3334 cm^{-1} (Table 2.1). These peaks are in the range 1656-1718 cm^{-1} for C=O and 3242-3351 for NH infrared stretching frequencies reported by Woolins *et al.*²⁴ for pyridine carboxamides.

Table 2.1 Selected IR frequencies (cm^{-1}) of the ligands.

Ligand	$\nu_{\text{(C=O)}} \text{ cm}^{-1}$	$\nu_{\text{(N-H)}} \text{ cm}^{-1}$
L1	1654	3334
L2	1677	3309
L3	1658	3305
L4	1664	3314

UNIVERSITY of the
WESTERN CAPE

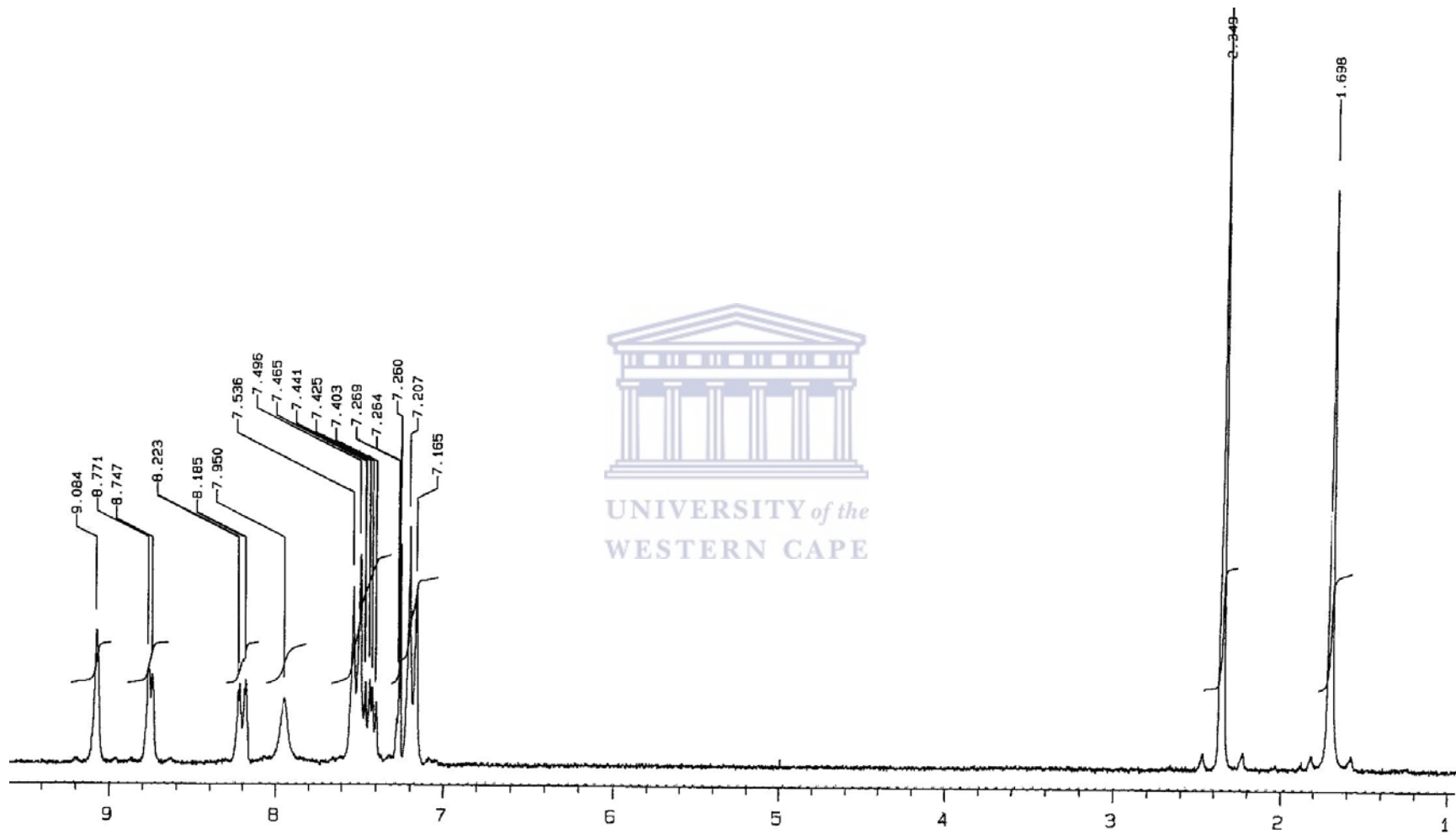


Figure 2.1 ^1H NMR spectrum of 2-[N-(4-methylphenyl)carbamoyl]pyridine (**L2**).

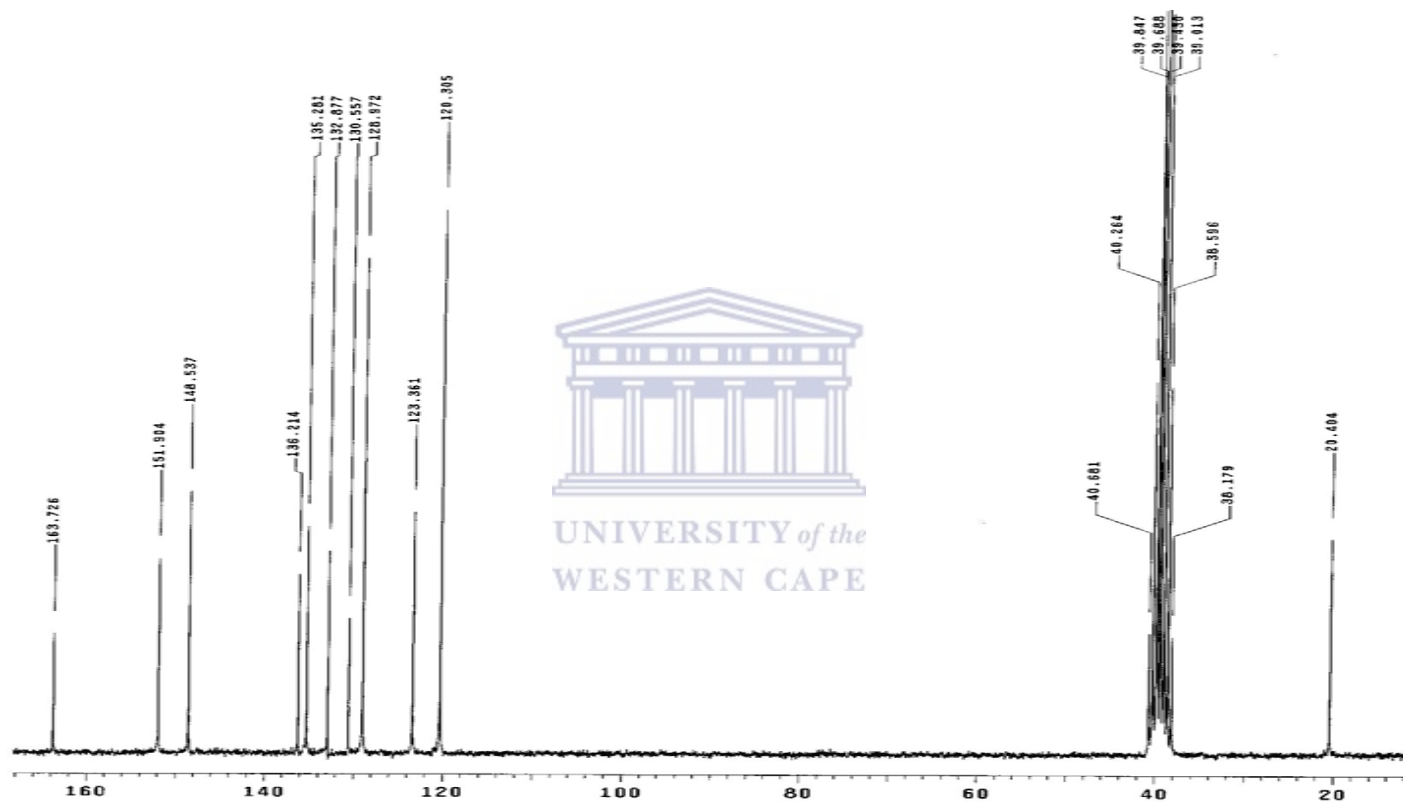


Figure 2.2 $^{13}\text{C}\{^1\text{H}\}$ NMR of 2-[N-(4-methylphenylcarbamoyl)]pyridine (**L2**).

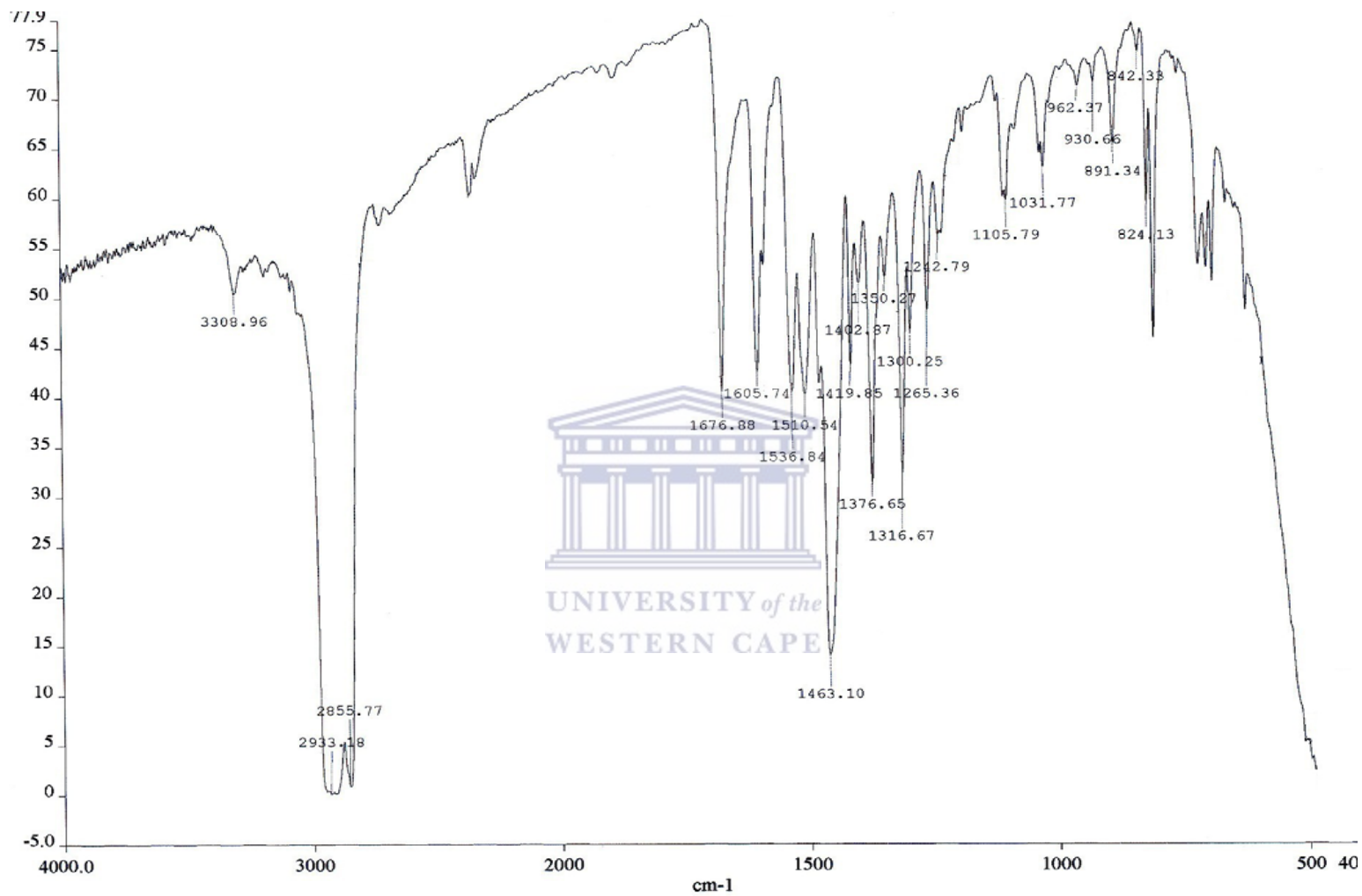
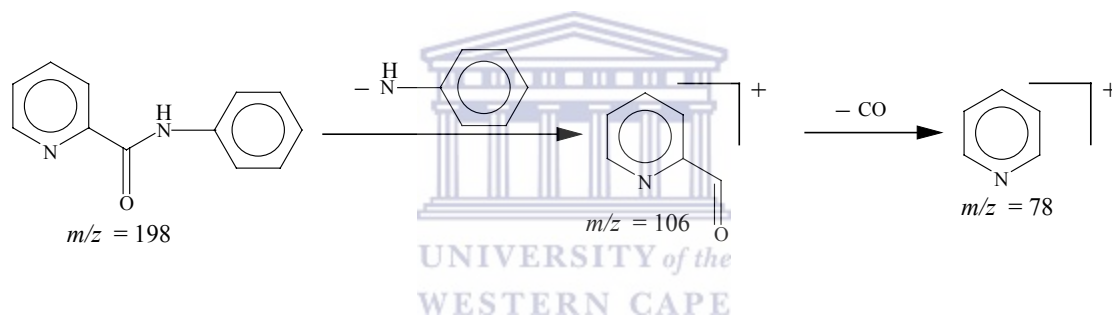


Figure 2.3 Infrared spectrum of 2-[N-(4-methylphenylcarbamoyl)]pyridine (**L2**).

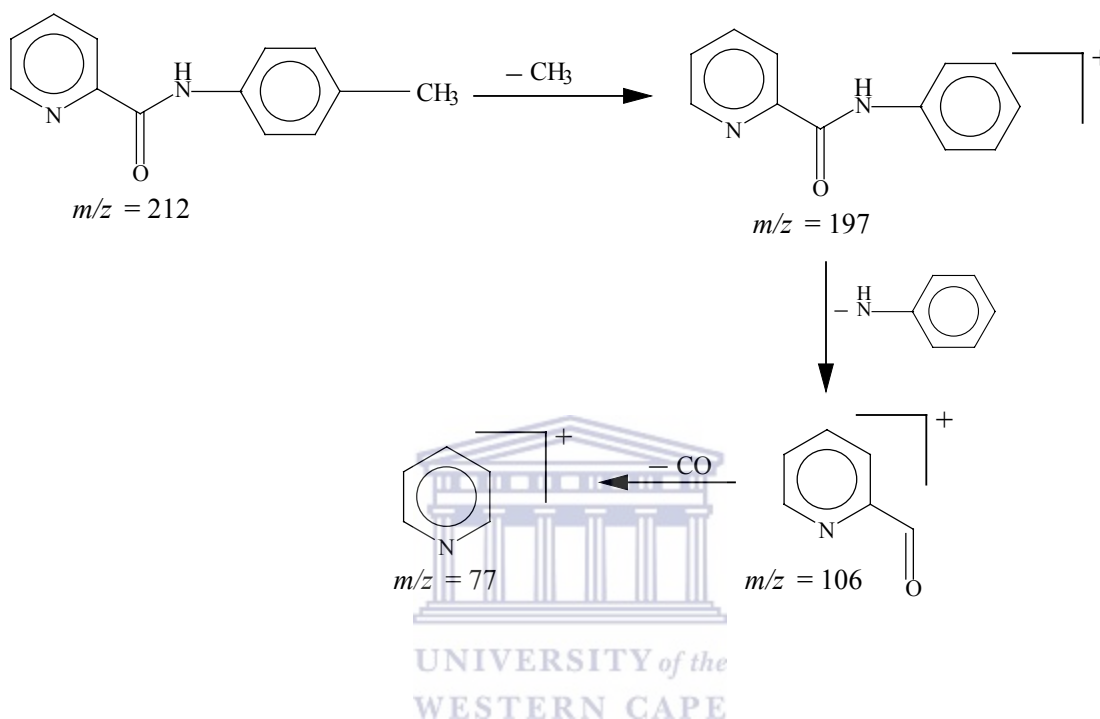
Generally, mass spectrometry is used to derive structural information about a compound by looking at its fragmentation pattern. The mass spectral fragmentation patterns of large molecules are usually complex, and the molecular ion is often not the base peak. In addition, many other fragment ions are observed. It is therefore often difficult to assign definite structures to fragment ions. In most cases the positive charge remains with the fragment that is likely to stabilize it. The molecular ion of **L1**, which does not have a substituent, was found to be $m/z = 198$. Firstly, the ligand breaks at the C-N bond, and is followed by the loss of the carbonyl group as shown in Scheme 2.10.



Scheme 2.10 Fragmentation pattern of 2-[N-(phenylcarbamoyl)]pyridine (**L1**)

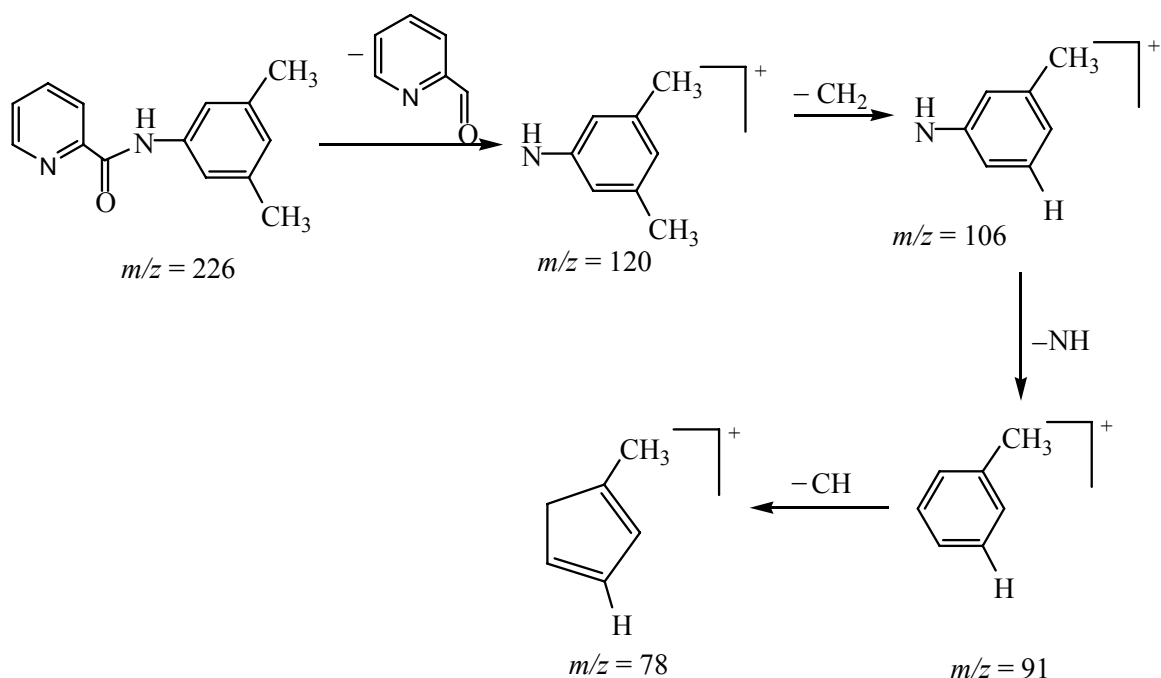
L2, which has a molecular ion of $m/z = 212$ (Figure 2.4), fragments by first losing the methyl group attached to the phenyl ring forming an ion with a molecular mass of 197 (Scheme 2.11). The C-N bond then breaks in a similar way to **L1** to lose C_6H_5N , forming a fragment ion at $m/z = 106$. This is followed by the loss of the carbonyl to give an ion with a molecular weight of 78, which corresponds to a pyridine molecular ion. Fragmentation pattern for **L4** is similar to **L1** and **L2** but that of **L3** is different. The loss of fragments for **L4**, which has the molecular ion of $m/z = 240$, is similar to **L1** except

that **L4** loses a methyl group attached to the pyridine ring before it forms the ion with $m/z = 78$.

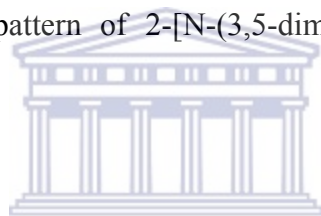


Scheme 2.11 Fragmentation pattern of 2-[N-(4-methylphenylcarbamoyl)]pyridine (**L2**)

Fragmentation pattern for **L3** is different from **L1**, **L2** and **L4** and is represented in Scheme 2.12. This compound has a molecular ion of $m/z = 226$ (Figure 2.5) and the initial fragmentation is the breaking of the C-N bond to lose C_6H_4NO as an ion with $m/z = 120$. It is then followed by the loss of CH_2 to form a fragment ion with $m/z = 106$. The third step is the loss of NH , with the final step being the loss of CH to form a fragment ion at $m/z = 78$ which is a base peak, identified as methylcyclopentadiene.



Scheme 2.12 Fragmentation pattern of 2-[N-(3,5-dimethylphenylcarbamoyl)]pyridine (L3)



By a combination of the NMR, IR and mass spectral data the proposed structures of **L1-L4** were confirmed. Microanalytical data agree well with the empirical formulae of the compounds.

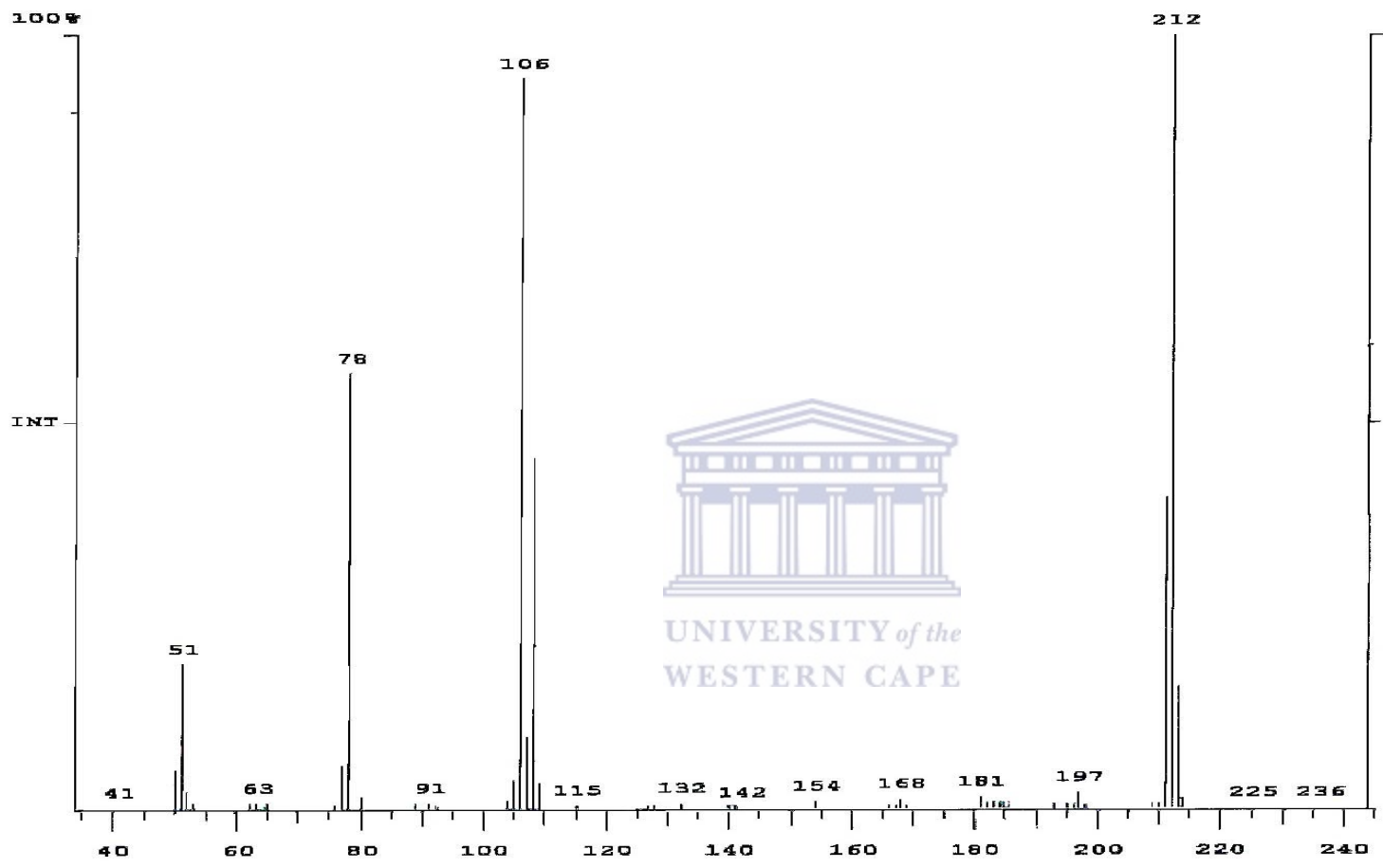


Figure 2.4 Mass spectrum of 2-[N-(4-methylphenyl)carbamoyl]pyridine (**L2**).

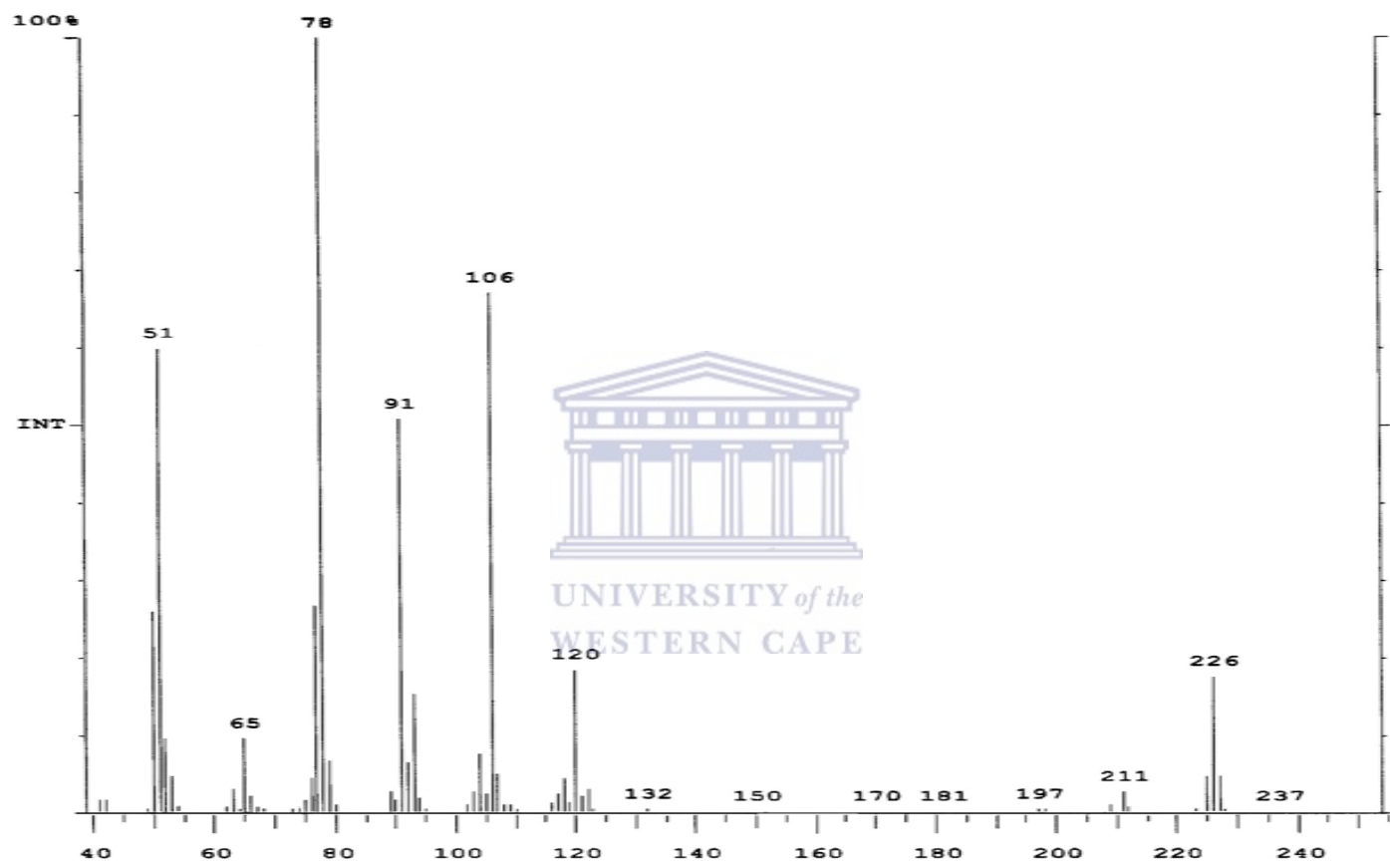
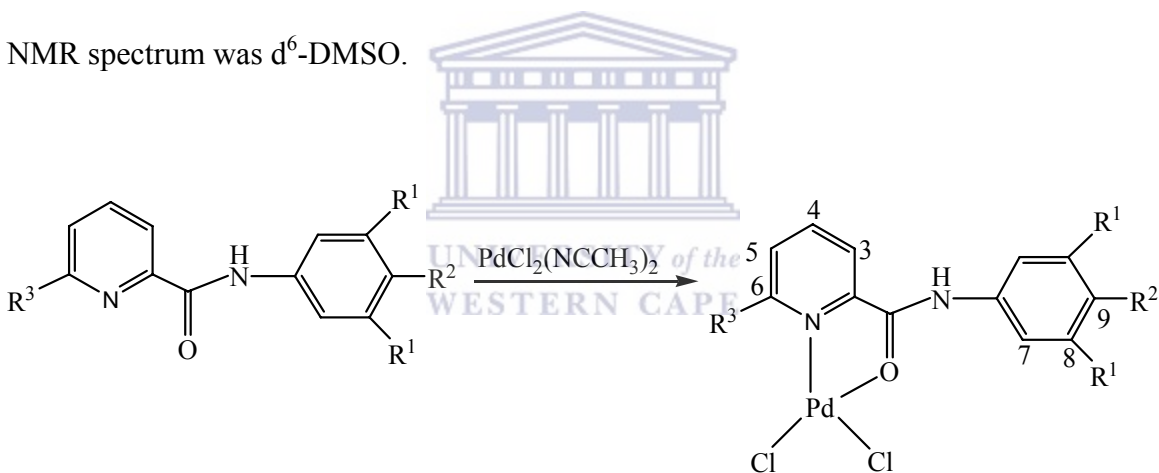


Figure 2.5 Mass spectrum of 2-[N-(3,5-dimethylphenylcarbamoyl)]pyridine (**L3**).

2.5.2 Synthesis and characterization of pyridinecarbamoyl palladium(II) complexes

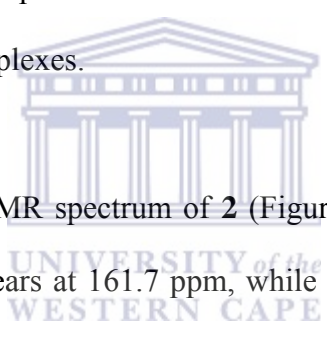
Complexes **1-4** were synthesized according to Scheme 2.13 by reacting $\text{PdCl}_2(\text{NCCH}_3)_2$ with an equimolar quantities of the pyridine carboxamide ligands (**L1-L4**) in dry dichloromethane, to give complexes as pure yellow solids. All the complexes prepared precipitated immediately from solution after addition of reactants, but to ensure complete reaction, the reaction mixtures were stirred for 6 h. The products were isolated by gravity filtration, dried in air and were isolated in high yields (61-94%). They were however found to be insoluble in most organic solvents such as dichloromethane, chloroform and diethyl ether and only dissolved in highly polar solvents such as dimethylsulfoxide (DMSO) and dimethylformamide (DMF). So, unlike the ligands, the solvent used for ^1H -NMR spectrum was d^6 -DMSO.



Complex	R^1	R^2	R^3
1	H	H	H
2	H	CH_3	H
3	CH_3	H	H
4	CH_3	H	CH_3

Scheme 2.13

In the ^1H NMR spectra of the complexes, all the signals due to the ligands protons were retained but some peaks were found to have shifted from their positions when compared to the free ligands. The ^1H NMR spectra also showed some splitting of the peaks. For example, the ^1H NMR spectrum of complex **2** (Figure 2.6) showed two singlet peaks for H^5 and two doublets for H^3 . However, comparison of the free ligands and the complexes in terms of shift of the protons was not considered. This is due to the different solvents that were used to characterize the compounds through ^1H NMR spectroscopy. In all complexes, H^3 and H^4 peaks were observed to have rearranged from their positions and then appeared downfield as compared to H^6 that was downfield in the free ligands. Comparison of H^3 and H^4 also proved to be different from the free ligands, with H^4 appearing downfield in the complexes.



In the proton decoupled ^{13}C NMR spectrum of **2** (Figure 2.7), the signal of the carbon atom of the amide linkage appears at 161.7 ppm, while the signal of the methyl carbon atom appears at 20.7 ppm. The signals due to the aromatic carbon atoms appear in the region 155.2 ppm to 120.7 ppm.

The two singlets for H^5 and two doublets for H^3 that were observed in the ^1H NMR spectra of the complexes could be a sign of an isomer, with the possibility of the palladium metal binding to the pyridyl nitrogen atom and the amide nitrogen or the carbonyl oxygen atom. The proton decoupled ^{13}C NMR spectra of the complexes also showed two additional peaks that appear adjacent to the peaks at 155.2 ppm and 152.3 ppm, which support the argument for linkage isomerism.

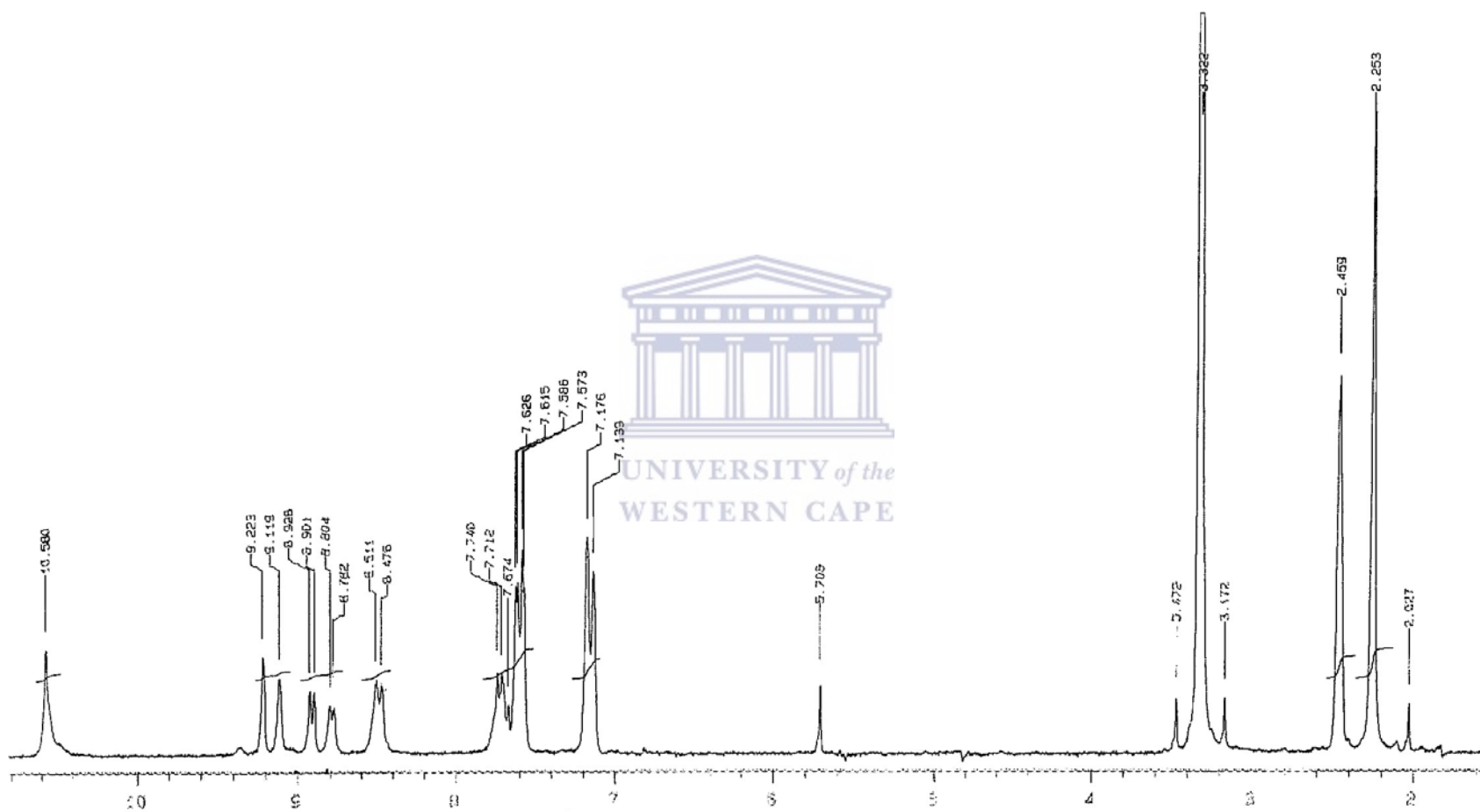


Figure 2.6 ^1H NMR spectrum of dichloro[2-(N-4-methylphenylcarbamoyl)]pyridine palladium(II) (2).

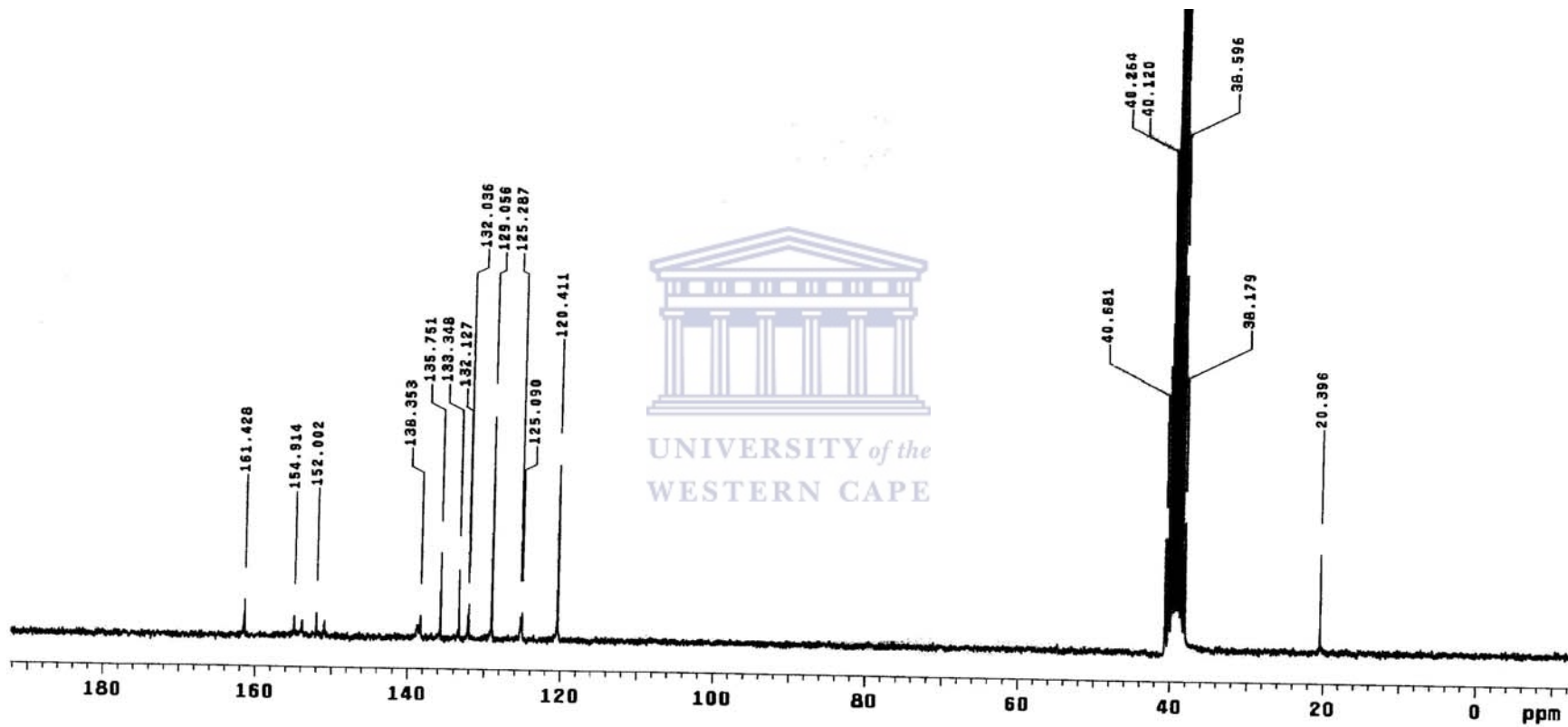


Figure 2.7 $^{13}\text{C}\{^1\text{H}\}$ NMR of dichloro[2-(N-4-methylphenylcarbamoyl)]pyridine palladium(II) (2).

Complexes **1-4** exhibited C=O stretching bands in the range 1679-1684 cm^{-1} and N-H stretching bands in the range 3343-3387 cm^{-1} (Table 2.2). A typical IR spectrum is depicted by the spectrum of complex **2** in Figure 2.8. Comparison of the IR spectra of the free ligands **L1-L4** with that of their complexes, showed a higher frequency shift in the C=O stretching of the amide group. Whereas in free ligands these amide stretching were found at 1654-1677 cm^{-1} , in the complexes they were found at 1679-1684 cm^{-1} . Higher frequency shift of the carbonyl group is due to the coordination of the palladium metal to the ligand. The carbonyl group, which is an electron withdrawal, will pull the electrons from the palladium metal with the chloride atoms attached to the palladium doing the same. As a result the stretching bond will be strong, causing the carbonyl to absorb at higher frequency than the one in the free ligand.

Table 2.2 Selected IR frequencies (cm^{-1}) of the complexes.

Complex	$\nu_{\text{(C=O)}} \text{ cm}^{-1}$	$\nu_{\text{(N-H)}} \text{ cm}^{-1}$
1	1684	3349
2	1679	3343
3	1683	3387
4	1684	3373

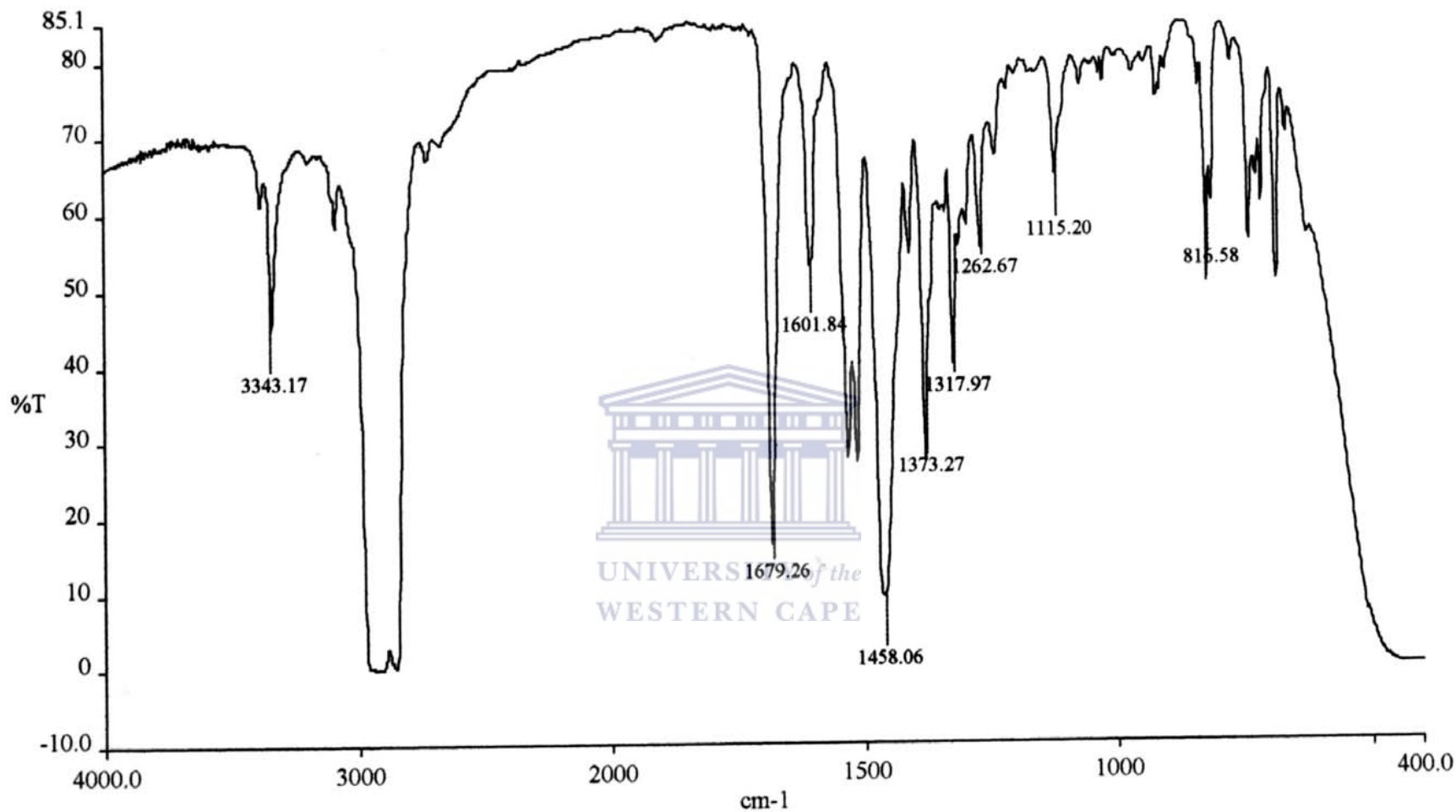


Figure 2.8 Infrared spectrum of dichloro[2-(N-4-methylphenylcarbamoyl)]pyridine palladium(II) (2).

Different results have been reported by Dutta *et al.*²² They found that the C=O stretching frequencies of the coordinated amide ligands appeared at a lower frequency compared to that of the free ligands. In their conclusion, they ascribe the lowering of the C=O stretching frequencies as a characteristic of the amide nitrogen coordination. Chan *et al.*²¹ also reported the similar coordination. Higher C=O stretching frequencies of the complexes compared to the free ligands is a typical of coordination through the oxygen atom of the amide linkage. This is also supported by the presence of $\nu_{(N-H)}$ peak in the IR spectra and the appearance of the amido proton peak in the ^1H NMR spectra of the complexes, which confirm that the ligands had not lost the amido proton.

However, cobalt complexes prepared from pyridine carboxamide ligands by Chan *et al.*²¹ showed the absence of $\nu_{(N-H)}$ peak in the IR spectra, which was also supported by the absence of the amido proton peak in the ^1H NMR spectra. Horn *et al.*²⁵ have also observed the same chemistry with ruthenium complexes. The presence of the NH peak in the IR and ^1H NMR spectra in our compounds assures us that for the palladium complexes the metal is bonded to the pyridyl nitrogen atom and the carbonyl oxygen atom. However, even in our case the possibility of the palladium metal binding to the pyridyl nitrogen and the amide nitrogen cannot be ruled out. This is due to the results obtained from the ^1H NMR and ^{13}C NMR, which showed the appearance of two extra peaks in the spectra of the complexes, which leads to the possibility of isomers as explained before, but it appears the major products are carbonyl bound ligand complexes as proposed in Scheme 2.13.

Based on the above spectroscopic analysis, the structures of complexes **1-4** were proposed as shown in Scheme 2.13. Microanalysis data support this proposed structure, but attempts to grow crystals for X-ray structural analysis were unsuccessful. Nevertheless the four palladium(II) complexes were fairly well characterized and were used as catalyst precursors in the polymerization and oligomerization of phenylacetylene.

2.6 Conclusions

Ligands **L1-L4** were synthesized using the methodology that was reported by Bhattacharya *et al.*²³ and obtained in good yields (56-65%). These compounds were then reacted with Pd(NCCH₃)₂Cl₂ to give the respective palladium(II) complexes as yellow solids in high yields. All the complexes precipitated directly from the solution, which made it difficult for us to grow crystals. Complex **1-4** were found to be soluble in highly polar solvents such as dimethylsulfoxide and dimethylformamide.

The techniques that were used to characterize the compounds are NMR spectroscopy, IR spectroscopy, mass spectrometry and elemental analysis. However, since efforts to grow crystals were unsuccessful, the bonding of the pyridine carboxamide ligands to the palladium metal was deduced from ¹H NMR and IR spectroscopy data. The data obtained showed that all the palladium complexes contained an amide proton, which was absent from the ruthenium complexes that were previously prepared by Horn *et al.*²⁵ using the same ligand system. The ¹H NMR and ¹³C NMR spectra also gave us a sign of the possibility of how the ligand is coordinated to the palladium metal via the pyridyl nitrogen and the amide nitrogen or carbonyl nitrogen. Finally, all the synthesized

complexes reported in this chapter were then used to prepare active catalysts for oligomerization and polymerization of phenylacetylene, the results of which form the subject of chapter 3 of this thesis.

2.7 References

1. Kurosaki, H.; Sharma, R. K.; Aoki, S.; Inoue, T.; Okamoto, Y.; Sugiura, Y.; Doi, M.; Ishida, T.; Otsuka, M.; Goto, M. *J. Chem. Soc. Dalton Trans.* 2001, 441.
2. Leung W, -H.; Ma, J.-X.; Yam, V. W.-W.; Che, C.-M.; Poon, C.-K. *J. Chem. Soc. Dalton Trans.* 1991, 1071.
3. Trost, B. M.; Hachiya, I. *J. Am. Chem. Soc.* 1998, **120**, 1104.
4. (a) Huc, I.; Krische, M. J.; Funeriu, D. P.; Lehn, J. M. *Eur. J. Inorg. Chem.* 1999, 1415; (b) Collinson, S. R.; Gelbrick, T.; Hursthouse, M. B.; Tucker, J. H. R. *Chem. Commun.* 2001, 555.
5. Epperson, J. D.; Ming, L. J.; Baker, G. R.; Newkome, G. R. *J. Am. Chem. Soc.* 2001, **123**, 8583.
6. Redmore, S. M.; Rickard, C. E. F.; Webb, S. J.; Wright, L. J. *Inorg. Chem.* 1997, **36**, 4743.
7. Adolfsson, H.; Moberg, C. *Tetrahedron Asymmetry* 1995, **6**, 2023.
8. (a) Trost, B. M.; Hung, M.-H. *J. Am. Chem. Soc.* 1983, **105**, 7757; (b) Trost, B. M.; Tometzki, G. B.; Hung, M.-H. *J. Am. Chem. Soc.* 1987, **109**, 2176.
9. Aoki, I.; Kawacharay, Y.; Sakaki, T.; Hanada, T.; Shinkai, S. *Bull. Chem. Soc. Jpn.* 1993, **66**, 927.
10. Chang, S. K.; Hamilton, A. D. *J. Am. Chem. Soc.* 1988, **110**, 1318.

11. Collinson, S. R.; Gelbrich, T.; Hursthouse, M. B.; Tucker, J. H. R. *Chem. Commun.* 2001, 555.
12. Deschenaux, R.; Kosztics, I.; Nicolet, B. *J. Mater. Chem.* 1995, **5**, 2291.
13. (a) Zimmerman, S. C.; Murray, T. J. *Tetrahedron Lett.* 1994, **35**, 4077; (b) Jorgensen, W.L.; Prachata, J. *J. Am. Chem. Soc.* 1990, **112**, 2008.
14. Beer, P. D.; Graydon, A. R.; Johnson, A. O. M.; Smith, D. K. *Inorg. Chem.* 1997, **36**, 2112.
15. (a) Zeng, F.; Zimmerman, S. C. *Chem. Rev.* 1997, **97**, 1682; (b) Brady, P. A.; Levy, E. G. *Chem. Ind.* 1995, **1/2**, 18.
16. Bosman, A. W.; Janssen, H. M.; Meijer, E. W. *Chem. Rev.* 1999, **99**, 1665.
17. Newkome, G. R.; Woosley, B. D.; He, E.; Moorefield, C. N.; Guther, R.; Baker, G. H.; Escamillia, J.; Merrill, H.; Luftmann, H. *Chem. Commun.* 1996, 2737.
18. Zhang, J.; Liu, Q.; Duan, C.; Shao, Y.; Ding, J.; Miao, Z.; You, X.-Z.; Guo, Z. *J. Chem. Soc., Dalton Trans.* 2002, 591.
19. Rowland, J. M.; Thornton, M. L.; Olmstead, M. M.; Mascharak, P. K. *Inorg. Chem.* 2001, **40**, 1069.
20. Ray, M.; Mukherjee, R.; Richardson, J. F.; Mashuta, M. S.; Buchanan, R. M. *J. Chem. Soc. Dalton Trans.* 1994, 965.
21. Qi, J.-Y.; Ma, H.-X.; Li, X.-J.; Zhou, Z.-Y.; Choi, M. C. K.; Chan, A. S. C.; Yang, Q.-Y. *Chem. Commun.* 2003, 1294.
22. Dutta, S.; Bhattacharya, P. K.; Tiekink, E. R. T. *Polyhedron.* 2001, **20**, 2027.
23. Dutta, S.; Pal, S.; Bhattacharya, P. K. *Polyhedron* 1999, **18**, 2157.

24. Jain, S. L.; Bhattacharya, P.; Molton, H. L.; Slawin, A. M. Z.; Crayston, J. A.; Woolins, J. D. *Dalton Trans.* 2004, 862.
25. Dutta, S.; Battacharya, P. K.; Horn, E.; Tiekink, E. R. T. *Polyhedron* 2001, **20**, 1815.



CHAPTER 3

POLYMERIZATION OF PHENYLACETYLENE CATALYZED BY NITROGEN DONOR LIGANDS PALLADIUM COMPLEXES

3.1 Introduction

Phenylacetylene is the most often studied monosubstituted acetylene for acetylene polymerization.¹ Conventional radical, cationic, or anionic initiation methods give only low yield of phenylacetylene oligomers.² In 1974, Masuda *et al.*⁴ found that phenylacetylene is effectively polymerized by WCl_6 and $MoCl_5$ catalysts which had been used for the olefin metathesis reactions and metathesis polymerization of cycloolefins. Since then, there have been many studies on the polymerization of phenylacetylene and related acetylene compounds using tungsten and molybdenum-based catalytic systems.⁵ The molecular weight of poly(phenylacetylene) obtained using WCl_6 is about 15 000. $MoCl_5$ is less active than WCl_6 toward this monomer, and the molecular weight of the product with $MoCl_5$ is only about 6 000.⁶

Living and stereospecific polymerization are also attained using molybdenum-based catalysts. These polymerizations are considered to proceed by metathesis polymerization mechanism similar to ring-opening polymerization mechanism of cycloolefins.⁷

Some of the prominent catalysts for the polymerization of substituted acetylenes are based on rhodium metal, and they only polymerize monosubstituted acetylenes via an insertion mechanism.⁸ Rhodium complexes with monodentate phosphines such as $Rh(C\equiv CC_6H_5)(2,5\text{-norbornadiene})[P(C_6H_5)_3]_2$ have also been reported to promote the

living polymerization of phenylacetylene and its substituted derivatives with selective formation of *cis-transoidal* poly(phenylacetylene).⁹

Recently, late transition metal complexes of nitrogen donor ligands have been shown by Brookhart and co-workers to be very active catalysts for α -olefin polymerization. One of the key factors that determine their active catalytic ability is the highly electrophilic metal centre. Thus the active species in the Brookhart type catalysts are $[(N-N)MR]^+$ (M = Ni and Pd, R = CH₃).¹⁰ Since facile coordination of the α -olefin monomer in the polymerization reaction also plays an important role in the activity of the catalyst, it is expected that a more electrophilic complex will be a very active catalyst. A report by Jordan *et al.*¹¹ suggests that weaker σ -donor pyrazole and pyrazolyl late transition metal complexes should fulfill this criterion. A report by Darkwa *et al.*¹² shows that pyrazole palladium(II) complexes catalyze polymerization of ethylene, and that the weaker σ -donor pyrazole plays an important role in the activity of the catalyst. Based on this fact we envisaged that cationic species of the pyrazole palladium compounds could catalyze phenylacetylene polymerization.

Very few studies involving pyrazole or pyrazolyl complexes as catalyst precursors for phenylacetylene polymerization have been reported. Ozawa *et al.*¹³ reported the polymerization of phenylacetylene catalyzed by {hydridotris(pyrazolyl)borate}rhodium(I) complexes with high yields and molecular weights ranging from 1.5×10^4 to 3.2×10^4 with low polydispersity indices.

In this chapter we report on the activity of the pyridine carboxamide and pyrazole palladium(II) catalysts towards phenylacetylene polymerization by investigating parameters such as solvent ratio effect, time effect and the use of different halide abstractors such as silver nitrate and silver triflate. Comparison is also made between pyridine carboxamide palladium(II) catalysts and σ -donor pyrazole palladium(II) catalysts (Scheme 3.1).

3.2 Materials and instrumentation

All manipulations were performed under dry, deoxygenated nitrogen atmosphere using standard Schlenk techniques. Dichloromethane was dried and distilled over P_2O_5 and acetonitrile was dried over P_2O_5 and stored over molecular sieves (A4). Phenylacetylene (98%), silver trifluoromethanesulfonate and silver nitrate were obtained from Aldrich and used as received. Compounds $[Pd(pz)_2Cl_2]$ (**5**), $[Pd(3,5-Me_2pz)_2Cl_2]$ (**6**), $[Pd(3,5-tBu_2pz)_2Cl_2]$ (**7**) and $[Pd(3,5-tBu_2pz)_2ClMe]$ (**9**)¹² were prepared according to literature procedure, but the preparation and characterization of $[Pd\{3,5-(CF_3)_2pz\}_2]$ (**8**) is described since this is a new compound.

NMR spectra were recorded on a Varian Gemini 2000 instrument (1H at 200 MHz, ^{13}C at 50 MHz). The chemical shifts are reported in δ (ppm) and referenced to residual protons and ^{13}C signals of deuterated chloroform as internal standard. IR spectra were recorded using NaCl plates on a PERKIN ELMER, paragon 1000PC FT-IR spectrometer. Polymer molecular weights were determined by gel permeation chromatography on a Waters 600E

instrument with a Waters 410 differential refractometer detector (THF, at 30 °C, rate = 1.0 cc/min) with PL mixed-C column using polystyrene standards.

3.3 Synthesis and characterization of [Pd{3,5-(CF₃)₂pz}₂Cl₂] (8)

To a solution of PdCl₂(NCCH₃)₂ (0.13 g, 0.50 mmol) in CH₂Cl₂ (20 ml) was added a solution of (3,5-CF₃)₂pz (0.21 g, 1.00 mmol) in CH₂Cl₂ (10 ml). The solution was stirred for 3 h. After the reaction time, hexane (10 ml) was added to the solution, which was then refrigerated for two weeks to afford orange crystals suitable for single crystals X-ray analysis. Yield = 0.16 g, 53%. ¹H NMR (DMSO): δ 7.45 (2H, s, 4-pz)

3.3.1 Crystallographic experimental section

Data collection

An orange crystal with approximate dimensions 0.46 x 0.36 x 0.22 mm³ was selected under oil under ambient conditions and attached to the tip of a nylon loop. The crystal was mounted in a stream of cold nitrogen at 100(2) K and centered in the X-ray beam by using a video camera. The crystal evaluation and data collection were performed on a Bruker CCD-1000 diffractometer with Mo K_α (λ = 0.71073 Å) radiation and the diffractometer to crystal distance of 4.9 cm. The initial cell constants were obtained from three series of ω scans at different starting angles. Each series consisted of 20 frames collected at intervals of 0.3° in a 6° range about ω with the exposure time of 10 sec per frame. A total of 81 reflections were obtained. The reflections were successfully indexed by an automated indexing routine built in the SMART program. The final cell constants were calculated from a set of 10709 strong reflections from the actual data collection.

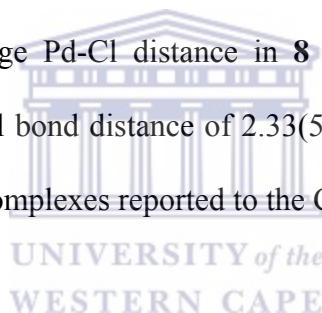
The data were collected by using the full sphere data collection routine to survey the reciprocal space to the extent of a full sphere to a resolution of 0.80 Å. A total of 15027 data were harvested by collecting three sets of frames with 0.25° scans in ω with an exposure time 30 sec per frame. These highly redundant datasets were corrected for Lorentz and polarization effects. The absorption correction was based on fitting a function to the empirical transmission surface as sampled by multiple equivalent measurements.¹⁴

Structure solution and refinement

The systematic absences in the diffraction data were uniquely consistent for the space group $P2_1/n$ that yielded chemically reasonable and computationally stable results of refinement.¹⁴ A successful solution by the direct methods provided most non-hydrogen atoms from the E -map. The remaining non-hydrogen atoms were located in an alternating series of least-squares cycles and difference Fourier maps. All non-hydrogen atoms were refined with anisotropic displacement coefficients. All hydrogen atoms were included in the structure factor calculation at idealized positions and were allowed to ride on the neighboring atoms with relative isotropic displacement coefficients. There is also one molecule of solvate water per palladium complex in the lattice. The final least-squares refinement of 277 parameters against 3807 data resulted in residuals R (based on F^2 for $I \geq 2\sigma$) and wR (based on F^2 for all data) of 0.0202 and 0.0535, respectively. The final difference Fourier map was featureless. The ORTEP diagram is drawn with 50% probability ellipsoids.

3.3.2 X-ray analysis of complex **8**

The Pd{(3,5-CF₃)₂pz}₂Cl₂ complex (**8**) was synthesized following the procedure described by Darkwa *et. al.*,¹² and was obtained in moderate yield (53%). Single crystals of **8** suitable for X-ray analysis were grown by slow diffusion of hexane into a solution of CH₂Cl₂ at -4 °C. Crystallographic data of **8** is represented in Table 3.1, while selected bond lengths and bond angles are shown in Table 3.2. The molecular drawing of **8** is given in Figure 3.1. The palladium complex (**8**) contains the central atom in slightly distorted square planar geometry with the two pyrazole units *trans* to each other. The average Pd-N(pz) bond length of 2.0162(15) Å in **8** agrees well with the average Pd-N(pz) bond length of 2.06(9) Å obtained by averaging Pd-N(pz) bond distances in 229 related compounds. The average Pd-Cl distance in **8** of 2.2876(5) Å is significantly shorter than the averaged Pd-Cl bond distance of 2.33(5) Å obtained by averaging 2055 Pd-Cl bonds in 1268 relevant complexes reported to the CSD.¹⁵



While the Pd-N(pz) bond distances of 2.016(15) Å in **8** is statistically indistinguishable from the corresponding [Pd(3,5-*t*Bu₂pz)₂Cl₂] complex of 2.017(2) Å, the Pd-Cl bond distances of 2.2876(5) Å in **8** as expected, are considerably shorter than those of the [Pd(3,5-*t*Bu₂pz)₂Cl₂] complex 2.5853(7) Å, indicating the effect of the electron withdrawing CF₃ groups of the pyrazole unit.

Table 3.1 Crystal data and structure refinement for 8.

Empirical formula	$C_{10}H_6Cl_2F_{12}N_4OPd$	
Formula weight	603.49	
Temperature	100(2) K	
Wavelength	0.71073 Å	
Crystal system	Monoclinic	
Space group	$P2_1/n$	
Unit cell dimensions	$a = 12.5046(5)$ Å	$\alpha = 90^\circ$.
	$b = 8.1964(3)$ Å	$\beta = 96.4800(10)^\circ$.
	$c = 18.3119(7)$ Å	$\gamma = 90^\circ$.
Volume	$1864.85(12)$ Å ³	
Z	4	
Density (calculated)	2.149 Mg/m ³	
Absorption coefficient	1.408 mm ⁻¹	
F(000)	1160	
Crystal size	$0.46 \times 0.36 \times 0.22$ mm ³	
Theta range for data collection	1.88 to 26.39°.	
Index ranges	$-15 \leq h \leq 15$, $-10 \leq k \leq 10$, $-22 \leq l \leq 22$	
Reflections collected	15027	
Independent reflections	3807 [R(int) = 0.0195]	
Completeness to theta = 26.39°	99.7 %	
Absorption correction	Multi-scan with SADABS	
Max. and min. transmission	0.7470 and 0.5636	
Refinement method	Full-matrix least-squares on F ²	
Data / restraints / parameters	3807 / 3 / 277	
Goodness-of-fit on F ²	1.015	
Final R indices [I > 2σ(I)]	R1 = 0.0202, wR2 = 0.0523	
R indices (all data)	R1 = 0.0218, wR2 = 0.0535	
Largest diff. peak and hole	0.753 and -0.579 e.Å ⁻³	

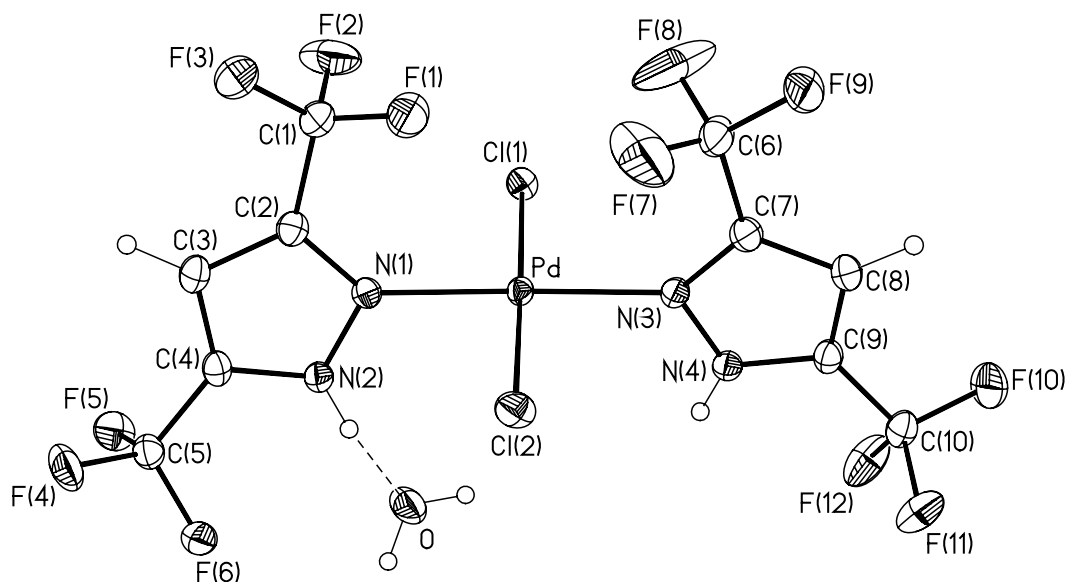


Figure 3.1 Molecular structure of compound **8**

Table 3.2 Selected bond lengths [Å] and bond angles [°] for **8**

Bond lengths [Å]		Bond angles [°]	
Pd-N(1)	2.0108(15)	N(1)-Pd-N(3)	176.99(6)
Pd-N(3)	2.0215(15)	N(1)-Pd-Cl(2)	88.09(5)
Pd-Cl(2)	2.2748(5)	N(3)-Pd-Cl(2)	89.00(5)
Pd-Cl(1)	2.3004(5)	N(1)-Pd-Cl(1)	90.93(5)
F(1)-C(1)	1.332(3)	N(3)-Pd-Cl(1)	91.98(5)
F(2)-C(1)	1.326(3)	Cl(2)-Pd-Cl(1)	179.004(18)

3.4 Polymerization procedures for phenylacetylene

3.4.1 Polymerization of phenylacetylene catalyzed by 1-9 using solvent mixtures of CH₂Cl₂ and CH₃CN at room temperature

In a typical experiment a solution of silver triflate (0.042 g, 0.160 mmol) in 20 ml of CH₂Cl₂/CH₃CN (1:1) was added to [Pd(4-MeC₆H₄)(NH)(CO)(C₅H₄N)Cl₂] (**2**) (0.031 g, 0.080 mmol) in 20 ml of degassed CH₂Cl₂ for a final solvent mixture composition of 3:1. A white precipitate of AgCl appeared immediately. The mixture was stirred for 10 min and filtered afterwards to give a yellow solution. To the yellow solution was added phenylacetylene (0.44 ml, 4.0 mmol, 50 equiv.). The resulting solution was stirred for 3 h, during which the initial yellow solution changed to dark red. The solution was then evaporated to give a dark reddish brown residue, which was left to dry overnight in air and then redissolved in a minimum amount of CH₂Cl₂, followed by addition of a large amount of methanol to precipitate poly(phenylacetylene) as a yellowish-orange powder. The polymer was isolated by filtration, dried and weighed. Yield: 0.35 g (86%). ¹H NMR (CDCl₃): δ 5.84 (s, vinyl), 6.64 (s, ph), 6.95 (s, ph). ¹³C{¹H} NMR (CDCl₃): δ 126.19, 127.06, 127.27, 131.29, 138.86, 142.39. FT-IR (nujol, cm⁻¹): 739, 754, 886, 964, 1026, 1070, 1152, 1299, 1594.

3.4.3 Polymerization of phenylacetylene catalyzed by 9 at -78 °C.

In a typical reaction performed at low temperature (-78 °C), a colourless solution of silver triflate (0.04 g, 0.14 mmol) in 30 ml of CH₂Cl₂/CH₃CN (1:1) was added to a colourless solution of [Pd(3,5-^tBu₂pz)₂ClMe] (**9**) (0.07 g, 0.14 mmol) in 10 ml of degassed CH₂Cl₂ for a final solvent mixture composition of 5:3. The white precipitate of AgCl appeared

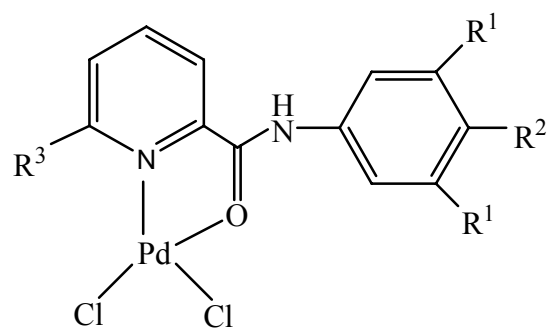
immediately. The mixture was stirred for 10 min and filtered afterwards. The Schlenk tube containing the filtrate was then placed in the Dewar flask and cooled to $-78\text{ }^{\circ}\text{C}$ (dry ice and acetone) over 10 min. Phenylacetylene (0.75 ml, 7.00 mmol, 50 equiv.) was then added via a syringe and the resultant solution was stirred for a further 15 min. The colourless solution changed to reddish yellow immediately. After 15 min, the reddish yellow solution was filtered and the filtrate evaporated to give a reddish yellow residue, which was left to dry overnight. The crude residue was redissolved in a minimum amount of CH_2Cl_2 and a large amount of methanol was added to precipitate a polymer. The polymer was then isolated by filtration, dried in air and weighed. ^1H and ^{13}C NMR spectra, and IR spectrum were similar to the one reported above.

3.5 Results and discussion

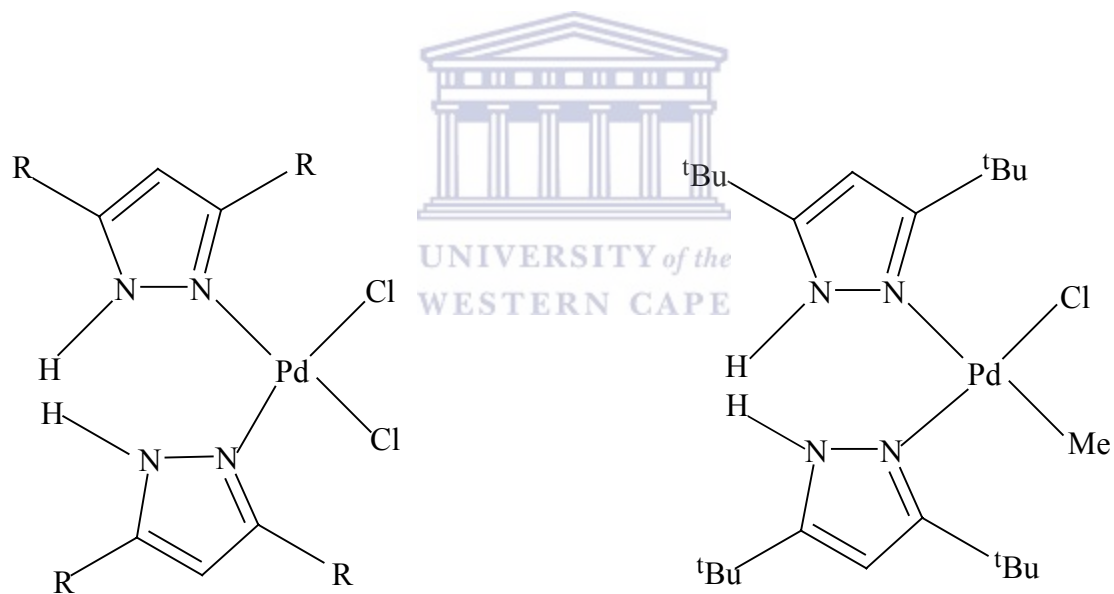
3.5.1 Conversion of catalyst precursors to active catalysts and phenylacetylene polymerization.

The polymerization of phenylacetylene was performed with active catalysts generated from the following metal complexes: $[\text{Pd}(\text{C}_6\text{H}_5)(\text{NH})(\text{CO})(\text{C}_5\text{H}_4\text{N})\text{Cl}_2]$ (**1**), $[\text{Pd}(4\text{-MeC}_6\text{H}_4)(\text{NH})(\text{CO})(\text{C}_5\text{H}_4\text{N})\text{Cl}_2]$ (**2**), $[\text{Pd}(3,5\text{-Me}_2\text{C}_6\text{H}_3)(\text{NH})(\text{CO})(\text{C}_5\text{H}_4\text{N})\text{Cl}_2]$ (**3**), $[\text{Pd}(3,5\text{-Me}_2\text{C}_6\text{H}_3)(\text{NH})(\text{CO})(6\text{-MeC}_5\text{H}_3\text{N})\text{Cl}_2]$ (**4**), $[\text{Pd}(3,5\text{-Rpz})_2\text{Cl}_2]$ (R = H (**5**), Me (**6**), ^tBu (**7**), CF_3 (**8**) and $[\text{Pd}(3,5\text{-}^t\text{Bu}_2\text{pz})_2\text{ClMe}]$ (**9**) in mixtures of $\text{CH}_2\text{Cl}_2/\text{CH}_3\text{CN}$.





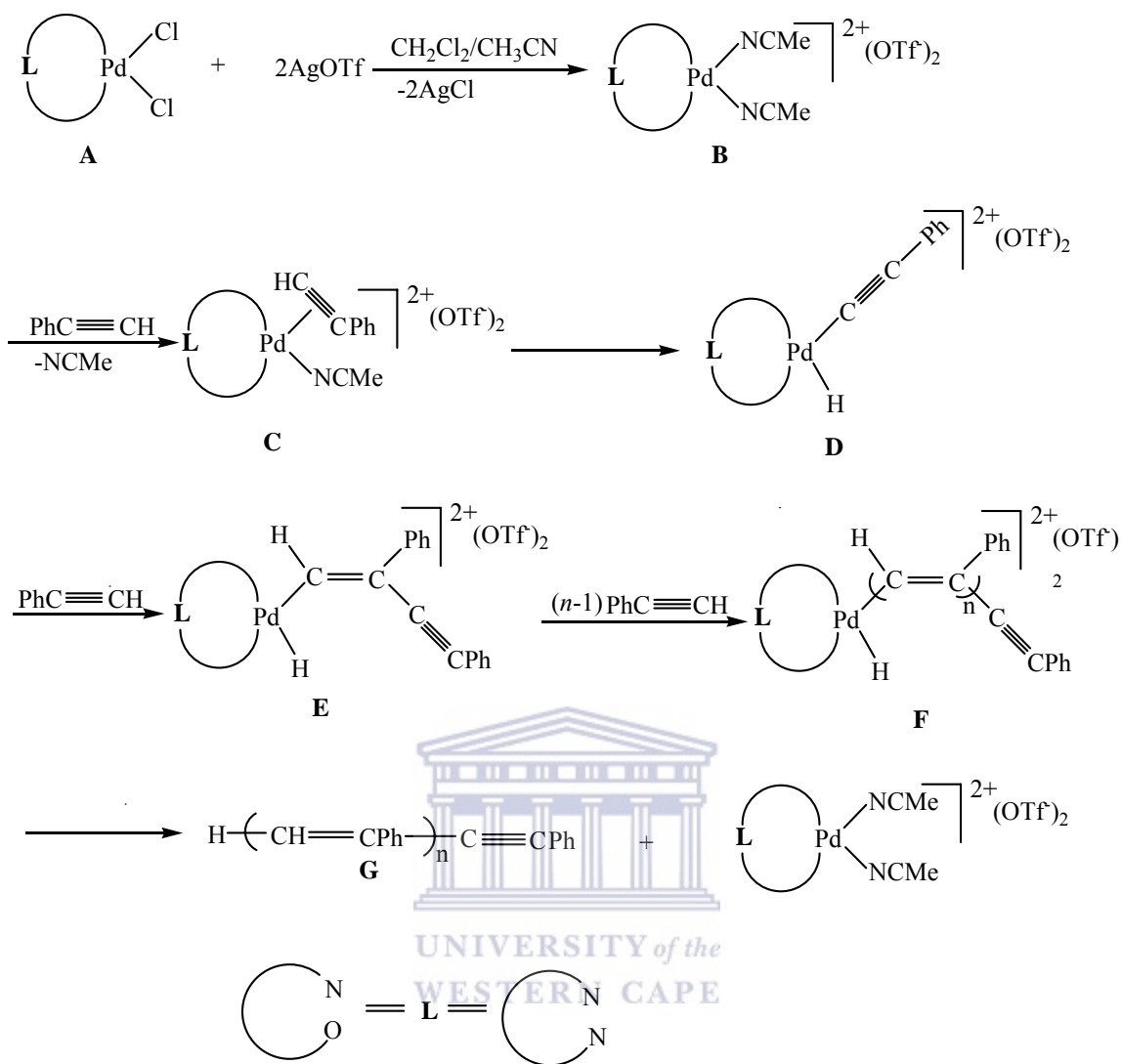
Complex	R ¹	R ²	R ³
1	H	H	H
2	H	CH ₃	H
3	CH ₃	H	H
4	CH ₃	H	CH ₃



(R = H (**5**); Me (**6**); ^tBu (**7**); CF₃ (**8**))

(**9**)

Scheme 3.1 Complexes used as catalysts precursors for generating active phenylacetylene polymerization catalysts.

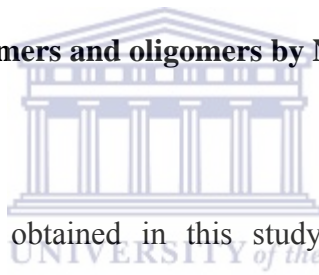


Scheme 3.2 Reaction sequence for palladium-catalyzed polymerization of phenylacetylene.

Scheme 3.2 is the reaction steps in active catalyst generation to where the polymer comes off from the metal centre in the catalyst. The active catalyst is formed when the two chloride atoms of the palladium complex **A** are removed with silver triflate dissolved in a mixture of dichloromethane and acetonitrile. Acetonitrile, which is a weak coordination, then binds to the palladium to form a cationic complex indicated as **B**. The role of the

acetonitrile is to stabilize the active catalyst. The monomer displaces one of the acetonitrile to form **C**, which then undergoes oxidative addition to form **D**. The fourth step involves the insertion of a new monomer into the Pd-C bond to give **E**. This step is repeated (n-1)-times giving **F**, which then undergoes reductive-elimination to form linear polymer **G**. In instances where this termination reaction occurs early in the sequence of steps an oligomer is formed. Generally a polymer was isolated by the addition of methanol to dichloromethane solution to precipitate the polymer. However evaporation of the methanol solution gave dark brown solid, which were identified by both NMR spectroscopy and GPC as oligomers.

3.5.2 Characterization of polymers and oligomers by NMR spectroscopy, IR spectroscopy and GPC



The polymers and oligomers obtained in this study were characterized by NMR spectroscopy, with polymers being further characterized by infrared spectroscopy. The ¹H NMR spectra of all the polymers displayed a sharp singlet due to the vinylic protons in the polymer at 5.84 ppm in addition to a set of broad peaks at 6.65 ppm (2H, *ortho*) and 6.95 ppm (3H, *meta* and *para*) (Figure 3.2a). These spectra are typical of poly(phenylacetylene) that has a *cis-transoidal* structure (Figure 3.3).

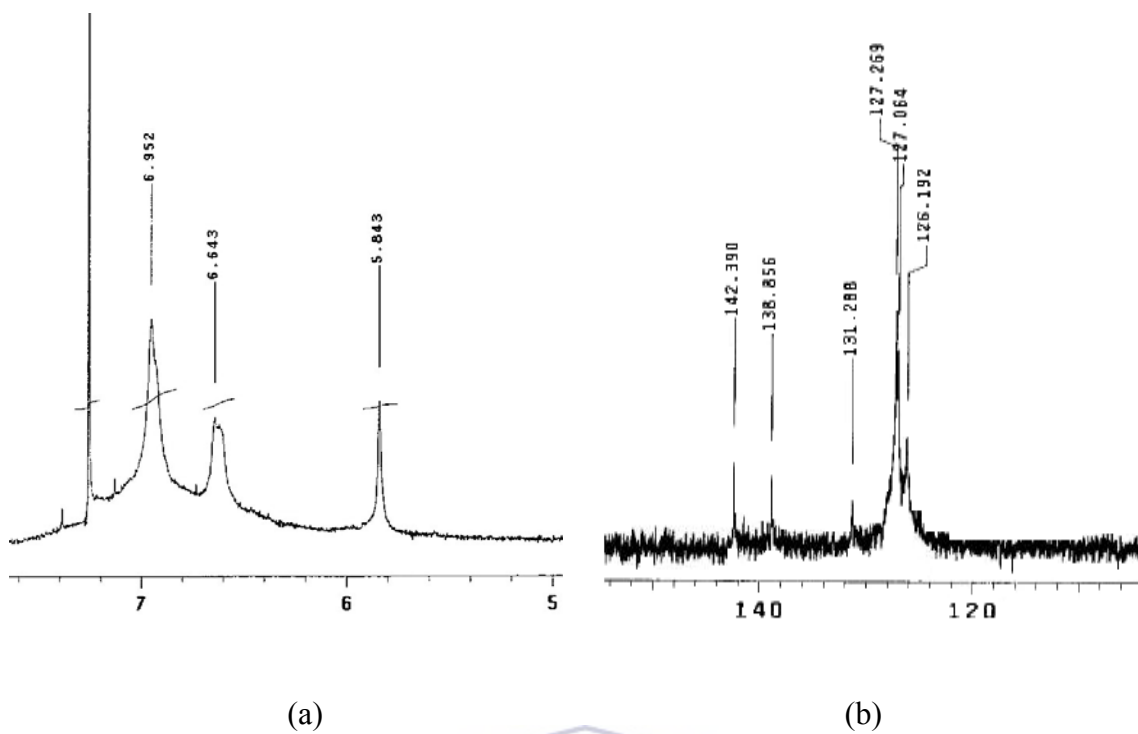


Figure 3.2 (a) ^1H and (b) $^{13}\text{C}\{^1\text{H}\}$ NMR spectra of *cis-transoidal* poly(phenylacetylene) in CDCl_3 at room temperature.

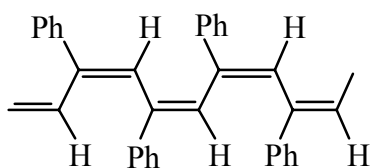
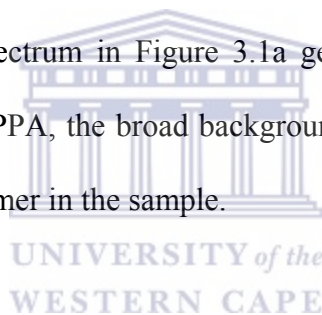


Figure 3.3 Structure of *cis-transoidal* poly(phenylacetylene)

The ^1H NMR spectrum of the polymer (Figure 3.2a) showed no peaks beyond 7.60 ppm. This is a sign of a linear polymer rather than cyclic. Simionescu *et al.*,¹⁶ have reported that the ^1H NMR peaks of the cyclotrimers phenylacetylene appear between 7.6 and 8.2 ppm.

The high stereoregularity of these polymers is supported by ^{13}C NMR spectrum^{9,17} (Figure 3.2b). The set of signals of poly(phenylacetylene) at 142.4 ppm and 138.9 ppm are for quaternary carbons, at 131.3 ppm for vinylic carbon, at 127.3 ppm and 127.1 ppm for *ortho* and *meta* aromatic carbons and at 126.2 ppm for *para* aromatic carbon being observed. A similar assignment was made for *cis-transoidal* poly(phenylacetylene) by Furlani *et al.*¹⁸ Though the spectrum in Figure 3.1a generally shows the predominant stereoisomer as *cis-transoidal* PPA, the broad background of the spectrum is a sign that there is some *trans-cisoidal* isomer in the sample.



Indeed when the polymer that was analyzed by ^1H NMR spectroscopy in Figure 3.2a was left in solution for several hours, there was a gradual formation of more *trans-cisoidal* isomer. ^1H NMR data at 24 h, 48 h, and 72 h show degradation in solution with *cis* content, dropping from 95% to 88% after 24 h, to 84% after 48 h and to 78% after 72 h (Figure 3.4). This decrease in *cis* content of the polymer in solution has also been observed by Mastrorilli *et al.*¹⁹ The *cis* content in *cis-transoidal* polymerization of phenylacetylene was determined by using the area of the peak from 5.84 ppm multiplied by 10^4 , and then divided by the total area of the spectrum which is multiplied by 16.66 as shown on p.83.

Using the formular by Percec *et al.*²⁰ *cis* content can be calculated as follows:

At 0 h

$$\begin{aligned} \% \text{ cis} &= A_{5.84} \times 10^4 / A_{\text{total}} \times 16.66 \\ &= 7.66 \times 104 / 48.28 \times 16.66 \\ &= 95.23 \\ &\approx 95\% \end{aligned}$$

$$\begin{aligned} A_{\text{total}} &= A_{5.84} + A_{6.34} + A_{6.95} \\ &= 7.66 + 16.29 + 34.33 \\ &= 48.28 \end{aligned}$$

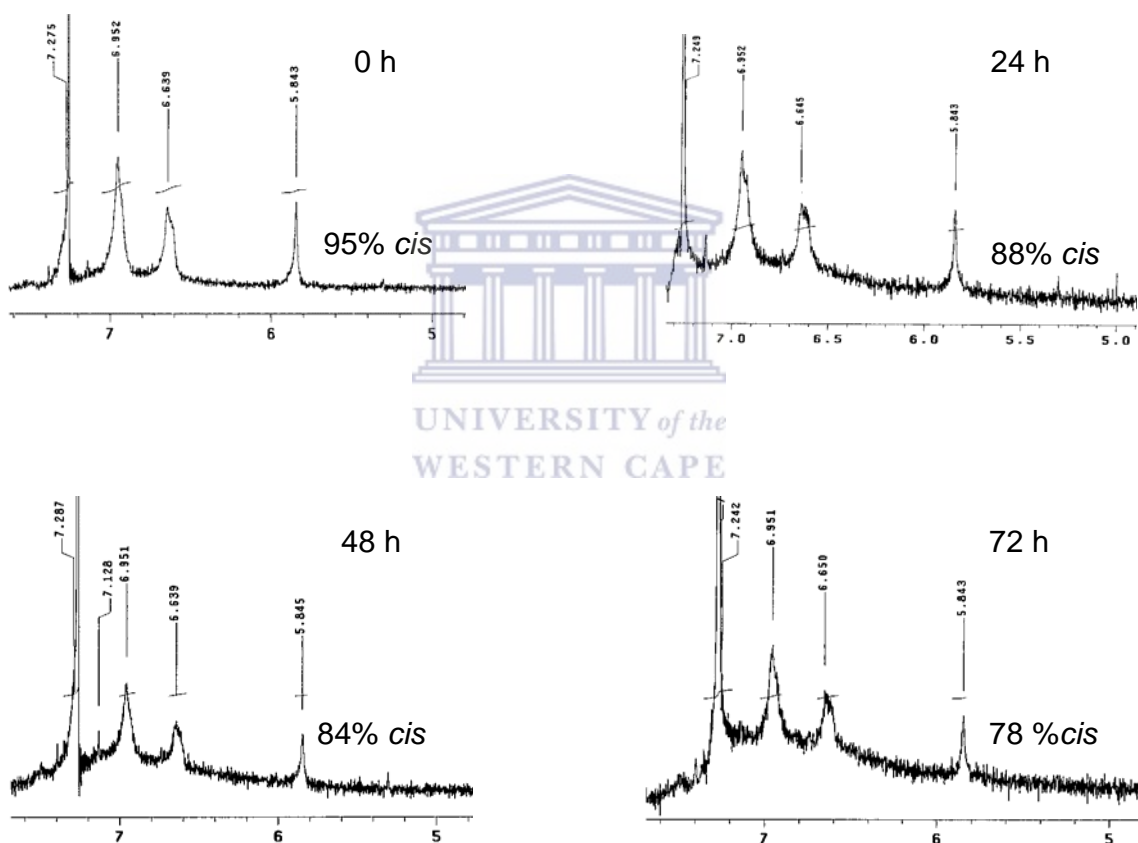


Figure 3.4 ¹H NMR spectra showing poly(phenylacetylene) degradation in chloroform.

After 72 h, the polymer in solution was exposed to air for two weeks. The solvent, which was chloroform, evaporated slowly until it was completely dry. The dry material was re-

dissolved in deuterated chloroform and characterized by ^1H NMR spectroscopy to give a broad singlet peak centred at 7.2 ppm (Figure 3.5). This peak is typical of *trans-cisoidal* poly(phenylacetylene) (Figure 3.6).

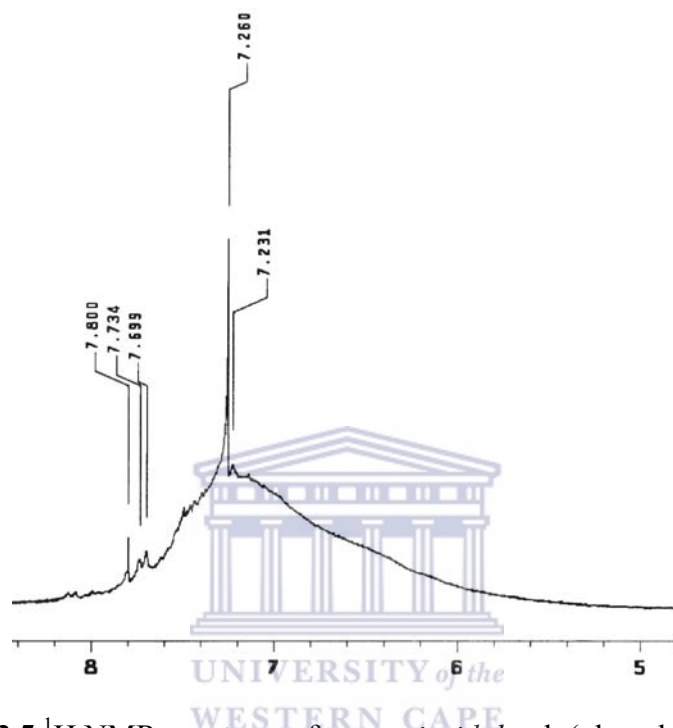


Figure 3.5 ^1H NMR spectrum of *trans-cisoidal* poly(phenylacetylene)

The ^1H NMR spectra of the oligomers (Figure 3.7) are similar to those of *trans-cisoidal* poly(phenylacetylene), but were identified as oligomers mainly from the GPC data.

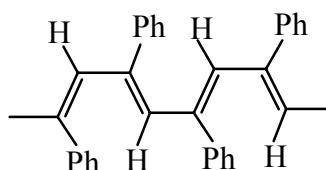


Figure 3.6 Structure of *trans-cisoidal* poly(phenylacetylene)

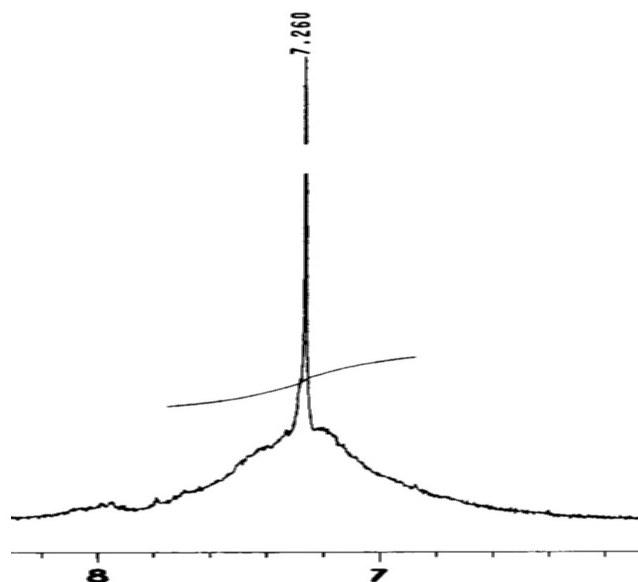


Figure 3.7 ^1H NMR spectrum of a *trans-cisoidal* oligomer

A typical infrared spectrum of a polymer isolated from these catalysts show two sharp absorptions at 754 and 739 cm^{-1} and a broad peak at 886 cm^{-1} (Figure 3.8), which are characteristic of *cis*- poly(phenylacetylene).²⁰

Generally, data from NMR and IR spectroscopy give enough information about the stereoisomers of materials formed, but whether they are polymeric or oligomeric are only confirmed from molecular weight measurements obtained from GPC as will be shown later. The following sections describe how different catalysts and experimental conditions produced oligomers and /or polymers.

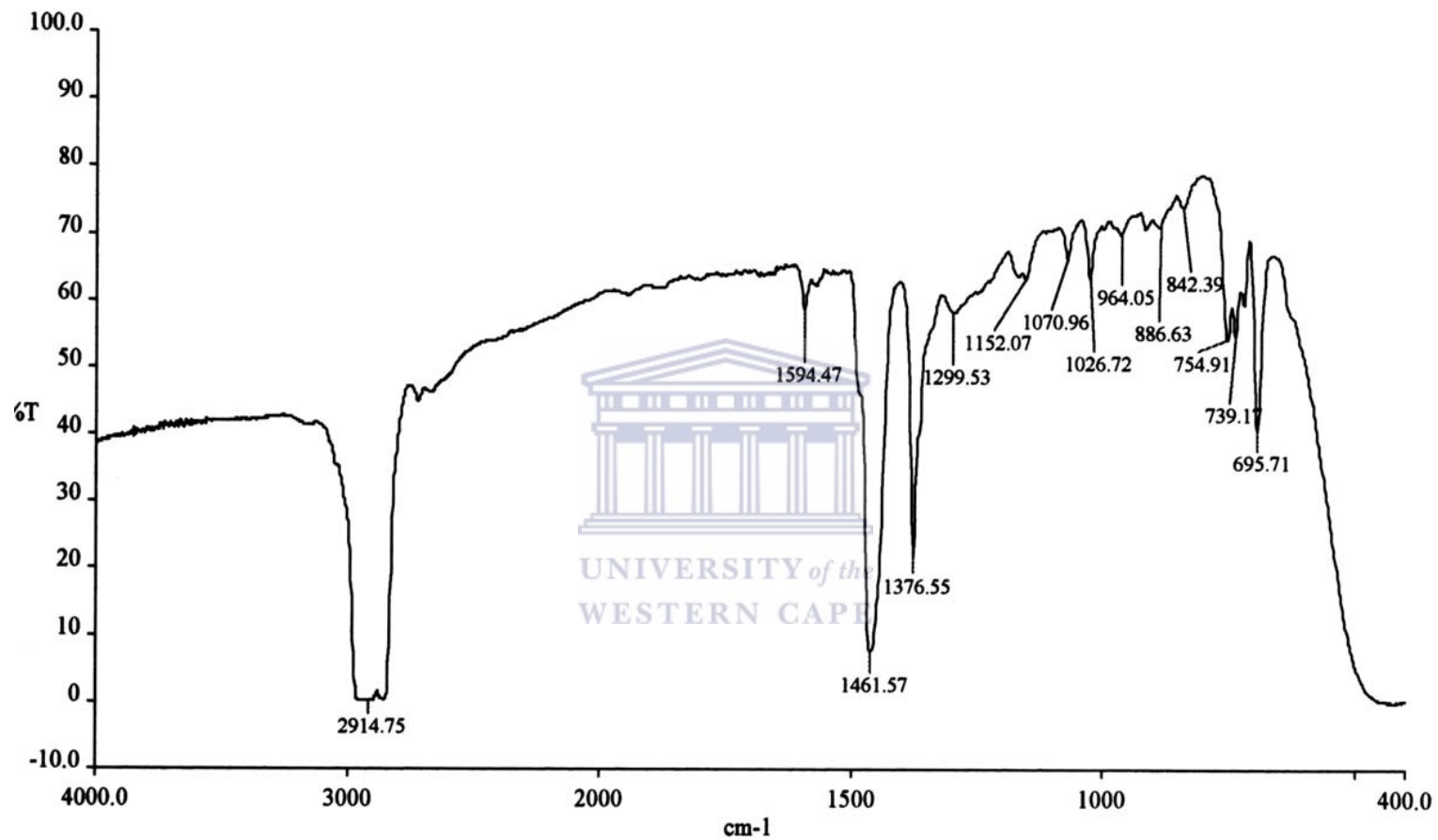


Figure 3.8 Infrared spectrum of a polymer isolated from a reaction run in a mixture of $\text{CH}_2\text{Cl}_2:\text{CH}_3\text{CN}$

3.5.3 Polymerization of phenylacetylene catalyzed by 1-4

This section describes polymerization performed with pyridine carboxamide palladium catalysts. All the reactions in Table 3.3 were performed with a 1:50 molar ratio of the catalyst and the monomer in a mixture of dichloromethane and acetonitrile at 25 °C for 3 hours. When the polymerization proceeded, the initially yellow solution gradually turned dark red. After the solution was evaporated, the dark red solid obtained was recorded as the combined yield of the polymers and oligomers. The crude material was then taken into a minimum amount of dichloromethane, and a large amount of methanol was added to give yellowish orange powders, which were identified as the polymers. Evaporation of the methanol filtrates produced dark brown solids, which were identified as oligomers. The yellowish-orange polymers are soluble in common solvents such as dichloromethane, chloroform, toluene, tetrahydrofuran (THF), dimethyl sulfoxide (DMSO) and dimethylformamide (DMF) but insoluble in methanol, hexane, diethyl ether and acetone while the oligomers are also soluble in common organic solvents including methanol.

Due to the similarity of the ^1H NMR spectra of the methanol soluble products, which contain mainly oligomers, and methanol insoluble products, which contain only polymers, molecular weight measurements were used to distinguish between them. Poly(phenylacetylene) polymers are generally believed to have molecular weights of more than 1 000 Da and the oligomers have molecular weights of less than 1 000 Da. For example, Keller *et al.*²¹ have reported the molecular weights of 800 Da for material obtained from the reaction of phenylacetylene catalyzed by $\text{W}(\text{NO})_2(\text{O}_2\text{CEH})_2$ (EH = -

CH(C₂H₅)(CH₂)₃CH₃) with SiCl₄ as the Lewis acid catalyst, while Douglas *et al.*²² have reported the molecular weights of around 460 Da for reaction of phenylacetylene catalyzed by nickelocene.

Table 3.3 Polymerization of phenylacetylene catalyzed by 1-4

Entry	Cat.	Solvent	% Conv.	<i>M_w</i> ^b	<i>M_n</i> ^b	<i>M_w/M_n</i> ^b
1	1	(1:1)	64	15 726	6 919	2.27
2	1	(5:3)	82	15 033	7 148	2.10
3	1	(3:1)	66	15 440	6 837	2.26
4	1	(7:1)	43	13 553	5 767	2.35
5	2	(1:1)	73	15 535	7 259	2.14
6	2	(5:3)	55	17 959	6 591	2.72
7	2	(3:1)	86	14 988	7 273	2.06
8	2	(7:1)	64	14 188	5 324	2.66
9	3	(1:1)	66	16 748	7 262	2.31
10	3	(5:3)	71	14 022	6 856	2.04
11	3	(3:1)	61	14 715	4 834	3.04
12	3	(7:1)	64	9 908	4 875	2.03
13	4	(1:1)	67	12 579	7 007	1.80
14	4	(5:3)	60	9 573	5 233	1.83
15	4	(3:1)	73	8 426	4 436	1.90
16	4	(7:1)	58	10 961	6 769	1.62

^aAll reactions were run for 3 h in mixtures of CH₂Cl₂:CH₃CN; [Pd] = 2.0 x 10⁻³ mol/L; Pd:PA = 1:50; temperature = 25 °C. ^bDetermined by GPC in THF based on polystyrene standards.

However, there are cases where some authors reported oligomers with molecular weights as high as 3 000 Da. Such examples are by Kishimoto *et al.* who reported molecular weight of an oligomer as 3 400 Da for reaction of phenylacetylene catalyzed by [Rh(OCH₃)(nbd)]₂.²³ In the first two mentioned cases the oligomers translate roughly to 8

and 5 repeating units of the monomer while for the latter case the oligomers translate to 34 repeating units. Clearly there is a huge discrepancy between these two assumptions.

The materials obtained from our reactions are stable in air. Their stability is due to the tri-substituted C=C bonds, which are less reactive than their disubstituted analogues.²⁴

Higashimura *et al.*²⁵ have reported that polymer stability increases with increasing bulkiness of substituents.

Generally, our data shows that catalyst **2** (entry 5-8) is the most active. It gives the highest percentage conversion of 86% relative to other catalysts under similar conditions.

The molecular weights of the polymers prepared from catalyst **2** generally decrease as the CH₂Cl₂/CH₃CN ratio increases from 1:1 to 7:1, with the exception of entry 6 where (5:3) ratio was used. Coincidentally the same trend is observed for catalysts **1** and **3** with the polymers obtained from 5:3 showing the same discrepancy. It is yet unclear what causes this discrepancy. Catalyst **1** gives % conversion as low as 43% (entry 4). The relationship between catalysts **3** and **4** is that they both show average % conversion ranging between 58 and 73. However, in catalyst **4** the trend of the molecular weights is observed even when the 5:3 ratio was used, with the exception of entry 16 (7:1) instead of 15 (5:3) as was seen with the other catalysts.

In summary, catalysts **1-4** showed high activity toward phenylacetylene polymerization with % conversion ranging from 55 to 86% (Table 3.3). Molecular weights of polymers obtained ranges from 8 426 to 17 959 Da and with polydispersity indices ranging from 1.62 to 3.04. The highest molecular weights were obtained when equal amounts of

dichloromethane and acetonitrile were used for catalysts **1**, **3** and **4** (entries 1, 9 and 13). However, in the case of catalyst **2**, the highest molecular weight was obtained when the solvent ratio was 5:3. The molecular weights decrease as the CH₂Cl₂:CH₃CN ratio increases.

However, in terms of the % conversion, no trend was found in all catalysts. This data shows that molecular weights increased when the proportion of acetonitrile increased with the exception of some few entries (2, 6, 10 and 16). It can thus be concluded that when minimum amount of acetonitrile is used, it only stabilizes the catalyst, whereas in cases where large amount of acetonitrile, it stabilizes the catalyst and also promote polymerization.



3.5.4 Polymerization of phenylacetylene catalyzed by 5-9

This section describes polymerization performed with pyrazole palladium catalysts. Catalysts **5-8** were also generated by the removal of two chloride atoms with silver triflate or silver nitrate in a mixture of dichloromethane and acetonitrile (Scheme 3.2). Polymerization reactions from catalysts **5-8** initially turned yellow after the addition of the solution of AgOTf or AgNO₃, and then turned dark red in 2 min after the addition of phenylacetylene. However, catalyst **9** was different. Unlike catalysts **5-8** that were generated by the removal of two chloride atoms, catalyst **9** was generated by the removal of one chloride atom. This is due to the presence of methyl group that is bonded to the palladium metal of the catalyst. Polymerization reactions turned colourless upon the addition of the solution of AgOTf or AgNO₃, and then immediately turned dark red upon

the addition of phenylacetylene. After the solution was evaporated, the dark red solid obtained was recorded as the combined yield of the polymers and oligomers, which was taken into a minimum amount of dichloromethane and a large amount of methanol to give a reddish yellow powder.

3.5.4.1 Effect of solvent ratio on polymerization catalyzed by **5**.

The results of polymerization reactions using catalyst precursor **5** are listed in Table 3.4 (entry 1-3). All reactions were run under the same conditions except the solvent ratio. Molecular weights of polymers decrease as the CH₂Cl₂:CH₃CN ratio decreases from 3:1 to 1:1.

3.4 Polymerization of phenylacetylene catalyzed by **5-9**

Entry	Cat	Solvent ratio	% Conversion	TON (kg/mol.h)	<i>M_w</i> ^b	<i>M_w/M_n</i> ^b
1	5	1:1	12	2.35	2 402	1.75
2	5	3:1	17	3.53	15 860	1.50
3	5	5:3	22	4.41	2 527	1.92
4	6	5:3	27	5.59	1 483	1.10
5	7	5:3	32	6.47	16 354	1.47
6	8	5:3	45	9.12	23 345	1.19
7	9	5:3	39	7.94	22 579	1.64
8 ^c	5	5:3	30	6.18	13 475	2.67
9 ^c	6	5:3	35	7.06	16 822	2.56
10 ^c	7	5:3	38	7.65	15 407	3.06
11 ^c	8	5:3	56	11.47	*	*
12 ^c	9	5:3	46	9.41	23 237	2.16

^aAll reactions were run for 15 min in mixtures of CH₂Cl₂:CH₃CN (40 ml); Pd:PA = 1:50; temperature = 25 °C; [Pd] = 3.5 x 10⁻³ mol/L; activator = AgNO₃; ^bdetermined by GPC;

^cactivator = AgOTf; *GPC data not available.

Although acetonitrile helps in solubilizing the activators used, its main purpose is to stabilize the cationic active catalyst. However, in this case, excess amount of the coordinating solvent lead to a decrease in molecular weights. According to Li *et al.*,²⁶ excess coordinating solvent could lead to the rate of monomer π -complex formation to be insufficient for polymerization to proceed at a reasonable rate. Low polydispersity indices were obtained for all reactions. The essence of performing these experiments was to determine the best solvent ratio for σ -donor pyrazole palladium(II) catalysts (**5-9**).

A bar graph (Figure 3.9) shows the effect of solvent ratio on percentage conversion. The graph shows that high percentage conversion is found when the $\text{CH}_2\text{Cl}_2:\text{CH}_3\text{CN}$ ratio is 5:3. Thus this ratio was used for all other pyrazole complexes used here as catalysts.

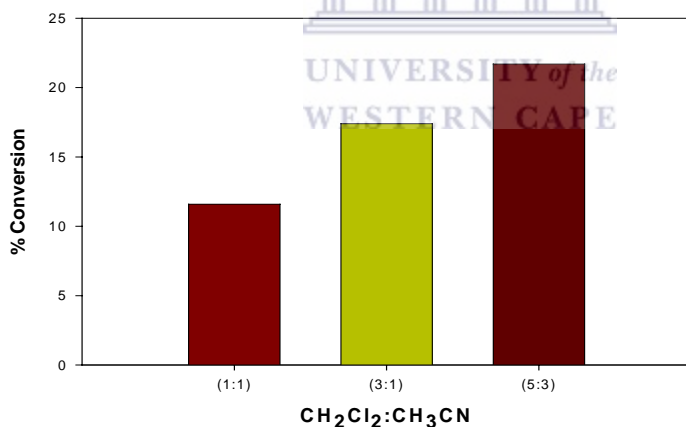


Figure 3.9 Effect of solvent ratio on % conversion using catalyst **5**

3.5.4.2 Polymerization of phenylacetylene catalyzed by 5-9 at constant time

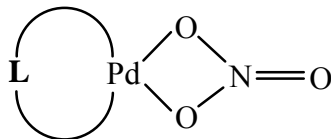
Catalysts **5**, **6**, **7** and **9** showed low % conversions at room temperature (25 °C). Table 3.4 (entry 3-12) show the polymerization results obtained using the above catalysts. The catalytic activity of **8** is higher as compared to the other catalysts. This is because catalyst

8 with trifluoromethyl substituents is more bulky than **5**, **6**, **7** and **9**. In fact, the steric bulk of trifluoromethyl substituents in **8** will facilitate chain growth in reactions in which catalyst **8** was used. Ozawa *et al.*¹³ observed lower yields for less bulky substituents on pyrazolyl catalysts when Rh(I) tris(pyrazolyl)borate complexes were used for phenylacetylene polymerization. They reported that the steric bulkiness of substituents on the ligands is one of the most important factors to control the catalytic activity. Thus, the catalytic reaction proceeds more rapidly as the substituents became sterically more demanding.

However, in case of catalysts **7** and **9**, which have comparable bulkiness, it was found that catalyst **9** is more active than **7**. This is mainly because the catalytic activity of **9** is enhanced due to the Pd-CH₃ group as opposed to two Pd-Cl bonds, the former which facilitates phenylacetylene polymerization. The existence of this Pd-C bond in **9** prompted us to investigate its activity under different conditions.

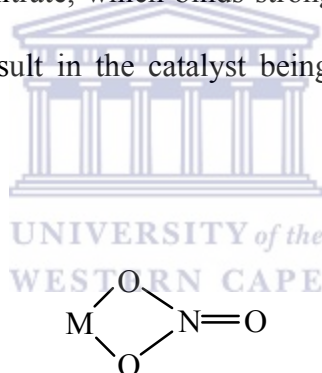
3.5.4.3 Polymerization of phenylacetylene catalyzed by 5-9 using different activators

Two different activators, AgOTf and AgNO₃ were used for comparison. Both of them showed the same trend as indicated in Figure 3.10 and Figure 3.11, which show the influence of catalysts on percentage conversion. Figure 3.10 and Figure 3.11 show that the best catalyst is **8**, and similar trend is observed in both cases. Thus, percentage conversion increases in the order **5** < **6** < **7** < **9** < **8**. However, low yields were obtained for catalysts **5-9** when AgNO₃ was used. This is because the nitrate has the ability to bind to the vacant sites of the metal instead of the acetonitrile as shown in Scheme 3.3.



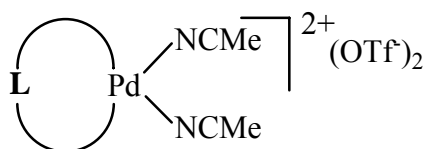
Scheme 3.3

The binding mode of the nitrate ligand to a metal was confirmed by Addison *et al.*,²⁷ who reported that the nitrate group is a versatile ligand and numerous modes of coordination have been found in nitrato complexes. However, the most common mode of coordination is the symmetric bidentate mode shown in Scheme 3.4 where M can be any metal, for example Cu, Co, Ni, Pd. The nitrate, which binds strongly, will end up competing with the monomer, and that will result in the catalyst being less stable which will lead to decomposition of the catalyst.



Scheme 3.4

However, in the case of the triflate ion, though it might bind to the vacant sites, the same cannot be experienced. This is because triflate ion is a weak coordination and therefore can easily be displaced which will cause triflate ion to act as a counter ion as shown in Scheme 3.5.



Scheme 3.5

The yields increased by 6-13% when silver triflate was used as an activator. Low molecular weights were obtained for catalysts **5** (2 527 Da) and **6** (1 483 Da) when AgNO_3 was used; whilst tertiarybutyl (**7** and **9**) and trifluoromethyl (**8**) substituted catalysts gave high molecular weights, 16 354, 22 579 and 23 345 Da respectively. However, in cases where AgOTf was used, high molecular weights ranging from 13 000 to 23 000 Da, were obtained for all catalysts with the exception of catalyst **8** (entry 11^c).

The low molecular weights that were obtained as reported above, correspond to the molecular weights of the oligomers reported by Kishimoto *et al.*²³ Overall the data shows that for AgNO_3 to be considered as an activator, catalysts with bulkier ligands must be employed.

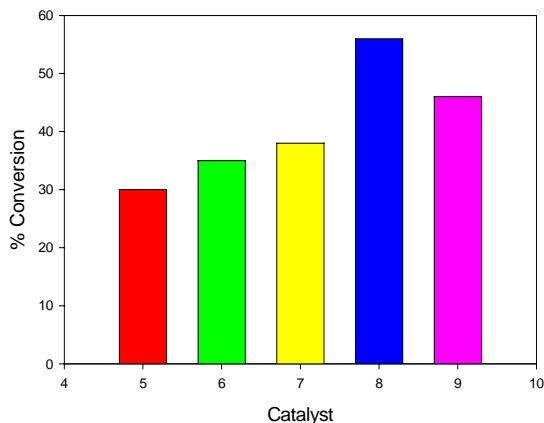


Figure 3.10 Influence of catalyst on % conversion using AgOTf as an activator

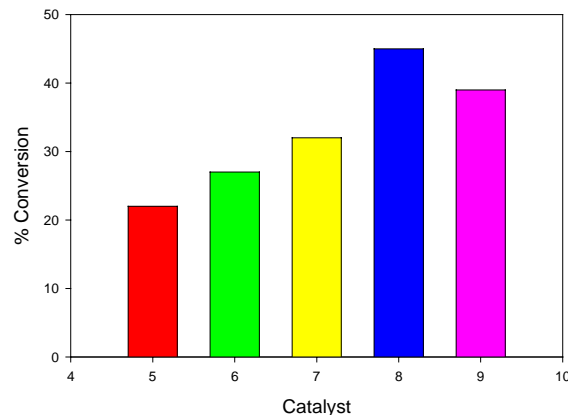


Figure 3.11 Influence of catalyst on % conversion using AgNO₃ as an activator

3.5.4.4 Effect of time on polymerization catalyzed by **9**

Table 3.5 shows the results of polymerization carried out using catalyst precursor **9**, with AgNO₃ as the activator (entries 1-5) and AgOTf (entries 6-13). Figure 3.12 shows the graph of the effect of time on TON. Generally, reaction time is known to have a huge effect on the activity of the catalyst, which is due to the stability of the active catalyst species in solution. In these experiments, we investigated the effect of time on phenylacetylene polymerization activity using catalyst **9**. TON was used as a measure of activity for these catalysts. TON, which is turnover number, is the mass of the product obtained per mole of the catalyst per hour. The graph shows that when time increases, TON decreases. This is true since TON is time dependent. These times related experiments gave molecular weights as high as more than 10 000 Da (with the exception of entries 4 and 13) with low polydispersity indices as shown from the table.

Table 3.5 Polymerization of phenylacetylene catalyzed by 9

Entry	Cat.	Time (min)	% Conv.	TON (kg/mol.h)	M_w^b	M_w/M_n^b
1 ^c	9	2	26	41.67	16 715	1.43
2 ^c	9	5	36	23.98	21 363	1.37
3 ^c	9	15	39	7.94	22 579	1.64
4 ^c	9	30	42	4.26	2 219	1.81
5 ^c	9	60	50	2.28	12 593	1.36
6	9	2	38	63.73	26 541	2.52
7	9	5	41	25.74	27 084	2.34
8	9	15	46	9.41	23 237	2.16
9	9	30	51	5.15	22 343	2.84
10	9	60	54	2.72	24 212	2.09
11	9	120	58	1.47	26 000	2.19
12	9	360	97	0.82	*	*
13	9	1440	99	0.21	6 458	1.81
14 ^d	9	15	74	14.41	*	*
15 ^d	9	30	80	7.65	*	*
16 ^d	9	60	90	4.12	*	*
17 ^d	9	120	97	2.35	*	*

^aAll reactions were run in 40 ml solvents; CH₂Cl₂:CH₃CN = 5:3; Pd:PA = 1:50; temperature = 25 °C; [Pd] = 3.5 x 10⁻³ mol/L; activator = AgOTf; ^bdetermined by GPC; ^cactivator = AgNO₃; ^dreactions run at -78 °C; *GPC data not available.

Figure 3.13 shows the effect of time on percentage conversion. The graph shows that percentage conversion increases as time increases. From 2 min (38%) to 120 min (58%), a slow increase in % conversion was observed indicating a slow conversion of the monomer with time. However, the graph then drastically increased to a maximum when the polymerization reaction was run for 6 h, and then remained constant after 24 h. Almost 100 % of the product was obtained in 6 h. The yields reported for 6 h and 24 h differ by 1.6%. Conversion increases slowly initially during the first 6 h and then levels off afterwards. Similar results have already been reported before.²⁸ This phenomenon corresponds to a slow deactivation process. The point that yields increase with time is

supported by Ozawa *et al.*,¹³ who have reported polymerization of phenylacetylene by rhodium catalyst. For example, they reported that polymerization of phenylacetylene by $\text{Tp}^{\text{Me}_2}\text{Rh}(\text{cod})$ gave a yield of 5% after 3 h, which then increased to 91% after 24 h.

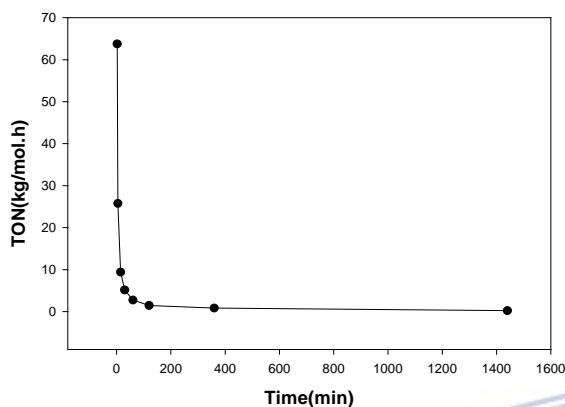


Fig 3.12 Effect of time on TON using catalyst **9**

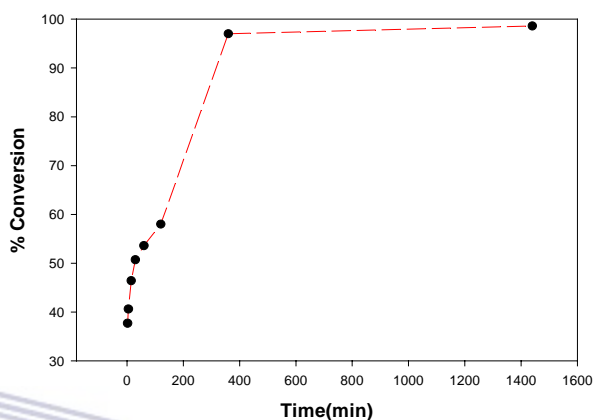


Fig 3.13 Effect of time on % conversion using catalyst **9**

3.5.4.5 Effect of time on polymerization catalyzed by **9** at -78 °C

In order to improve the yields, we then decided to run reactions at lower temperatures. Table 3.5 (entries 14-17) shows the results of polymerization reactions carried out with catalyst precursor **9** at low temperature. When the temperature was dropped from 25 °C to -78 °C, the yields of the PPA obtained were almost quantitative. All the reactions gave high yields as compared to those at room temperature as seen in Table 3.5 (entries 8-11), which show that the catalytic activity towards phenylacetylene polymerization is high at lower temperatures than room temperatures. In conclusion, low temperatures allow monomer insertion into growing polymer chain and chain termination is reduced.

According to Percec, an increase in reaction temperature facilitates the termination reactions of poly(phenylacetylene).²⁹

3.6 Conclusions

Complexes **1-4** showed high % conversions toward polymerization of phenylacetylene while complexes **5-9** showed low low % conversions toward the same transformation. In all reactions, the ratio of the monomer to catalyst was kept at 50:1 and the solvent used being a mixture of dichloromethane and acetonitrile.

Comparison of catalysts **5-9** proved that complexes with bulky substituents are better catalysts than those with less bulky substituents. The catalytic activity of these complexes decreases in the order **8 > 9 > 7 > 6 > 5**. Catalysts **7-9** gave high molecular weights with low polydispersity indices irrespective of the activator used, whilst low molecular weights were obtained for catalysts **5** and **6** when the activator was silver nitrate. Although catalyst **2** proved to be the most active catalyst, the catalytic activity of complexes **1-4** is almost the same and high molecular weights were obtained in all catalysts. In general, catalysts **1-4** are more electrophilic due to the electron- withdrawing group, which is the carbonyl group while catalysts **5-9** are less electrophilic. Characterization of all the polymers obtained gave a *cis-transoidal* structure.

3.7 References

1. Chauser, M. G.; Rodionov, Yu. M.; Misin, V. M.; Cherkashin, M. I. *Russ. Chem. Rev.* 1976, **45**, 348.

2. Amdur, S.; Cheng, A. T. Y.; Wong, C. J.; Ehrlich, P.; Allendoerfer, R. D. *J. Polym. Sci., Polym. Chem. Ed.* 1978, **16**, 407.
3. Masuda, T.; Hasegawa, K.-I.; Higashimura, T. *Macromolecules* 1974, **7**, 728.
4. (a) Gibson, V. C. *Adv. Mater.* 1994, **6**, 37. (b) Ivin, K. J. *Olefin Metathesis*; Academic Press: London, 1983.
5. Masuda, T.; Higashimura, T. *Acc. Chem. Res.* 1984, **17**, 51.
6. Masuda, T.; Higashimura, T. *Adv. Polym. Sci.* 1987, **81**, 121.
7. Ivin, K. J. *Olefin Metathesis and Metathesis Polymerization*. Academic Press: London, 199.
8. Tabata, M.; Yang, W.; Yokota, K. *Polym. J.* 1990, **22**, 1105.
9. Kishimoto, Y.; Eckerle, P.; Miyatake, T.; Ikariya, T.; Noyori, R. *J. Am. Chem. Soc.* 1994, **116**, 12131.
10. Johnson, L. k.; Killian, C. M.; Brookhart, M. *J. Am. Chem. Soc.* 1995, **117**, 6414.
11. Tsuji, S.; Swenson, D. C.; Jordan, R. F. *Organometallics* 1999, **18**, 4758.
12. Li, K.; Darkwa, J.; Guzei, I. A.; Mapolie, S. F. *J. Organomet. Chem.* 2002, **660**, 108.
13. Katayama, H.; Yamamura, K.; Miyaki, Y.; Ozawa, F. *Organometallics* 1997, **16**, 4497.
14. Bruker-AXS. (2000-2003) SADABS V.2.05, SAINT V.6.22, SHELXTL V.6.10 & SMART 5.622 Software Reference Manuals. Bruker-AXS, Madison, Wisconsin, USA.
15. Allen, F. H. *Acta Crystallogr. Sect. B*, 2002, **B58**, 380.
16. Simionescu, C. I.; Percec, V. *J. Polym. Sci., Polym. Chem. Ed.* 1980, **18**, 147.

17. Percec, V.; Rinaldi, P. L. *Polym. Bull.* 1983, **9**, 548.
18. Furlani, A.; Napoletan, C.; Russo, M. V.; Feast, W. J. *Polym. Bull. (Berlin)* 1986, **16**, 311.
19. Matrorilli, P.; Nobile, C. F.; Rizzuti, A.; Suranna, G. P.; Acierno, D.; Amendola, E. *J. Mol. Catal. A: Chem.* 2002, **178**, 35.
20. Simionescu, C. I.; Percec, V.; Dumitrescu, S. *J. Polym. Sci., Polym. Chem. Ed.* 1997, **15**, 2497.
21. Matusiak, R.; Keller, A. *Polym. Bull.* 1999, **43**, 199.
22. Douglas, W. E.; Overend, A. S. *J. Organomet. Chem.* 1993, **444**, C62.
23. Kishimoto, Y.; Miyatake, T.; Ikariya, T.; Noyori, R. *Macromolecules* 1996, **29**, 5054.
24. Gruber, A. S.; Boiteux, G.; de Souza, R. F.; de Souza, M. O. *Polym. Bull.* 2002, **47**, 529.
25. Masuda, T.; Tang, B.-Z.; Higashimura, T. *Macromolecules* 1985, **18**, 2369.
26. Li, K.; Wei, G.; Darkwa, J.; Pollack, S. K. *Macromolecules* 2002, **35**, 4573.
27. Addison, C. C.; Logan, N.; Wallwork, S. C.; Garner, C. D. *Structural aspects of Coordinated nitrate groups, Q. Rev.* 1971, **25**, 289.
28. (a) Shen, Z.; Faron, M. F. *J. Polym. Sci., Chem.* 1984, **22**, 1009; (b) Masuda, T.; Sasaki, N.; Higashimura, T. *Macromolecules* 1975, **8**, 717.
29. Percec, V.; Rinaldi, P. L. *Polym. Bull.* 1983, **9**, 548.



CHAPTER 4

4.1 Summary

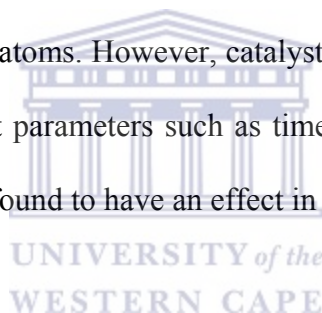
Four pyridine carboxamide ligands, two known (**L1** and **L2**) and two new (**L3** and **L4**), were prepared following the procedure reported by Bhattacharya *et. al.* However, the yields obtained were lower when compared to those reported by Bhattacharya *et. al.* All the ligands were found to be soluble in most polar solvents and were analyzed by ^1H and ^{13}C NMR spectroscopy, IR spectroscopy, mass spectrometry and elemental analysis.

The complexes dichloro{2-(N-phenylcarbamoyl)}pyridinepalladium(II) (**1**), dichloro{2-(N-4-methylphenylcarbamoyl)}pyridinepalladium(II) (**2**), dichloro{2-(N-3,5-dimethylphenylcarbamoyl)}pyridinepalladium(II) (**3**) and dichloro{2-(N-3,5-dimethylphenylcarbamoyl)}6-methylpyridinepalladium(II) (**4**) were prepared by reacting $\text{PdCl}_2(\text{NCCH}_3)_2$ with the appropriate pyridine carboxamide ligands, and were isolated in high yields. All the complexes were found to be insoluble in most organic solvents and only soluble in high polar solvents. Similar techniques that were used to characterize the ligands were also used for the complexes i.e NMR spectroscopy, IR spectroscopy and elemental analysis. Due to the poor solubility of the complexes, crystal structure elucidation was not possible. However, data from the IR spectroscopy was pivotal in determining the bonding mode in the complexes.

Complexes **1-4** were successfully used as catalyst precursors in the polymerization of phenylacetylene. However, because of their poor solubility as mentioned above, the

complexes were first converted into their cationic precursors to enhance their solubility. These cationic precursors were found to catalyse polymerization of phenylacetylene.

Other catalysts that were successfully tested for comparison purposes for polymerization and oligomerization of phenylacetylene are $[\text{Pd}(3,5\text{-Rpz})_2\text{Cl}_2]$ ($\text{R} = \text{H}$ (**5**), Me (**6**), $t\text{Bu}$ (**7**), CF_3 (**8**) and $[\text{Pd}(3,5\text{-}t\text{Bu}_2\text{pz})_2\text{ClMe}]$ (**9**). The synthesis of complexes **5**, **6**, **7** and **9** was not reported in this thesis since it is known from literature. However, the same procedure was used in synthesizing complex **8**. The X-ray structure of complex **8** shows the two pyrazole distorted square planar geometry around the palladium center with the two pyrazole ligands *trans* to each other. Like catalysts **1-4**, catalysts **5-8** were also generated by the removal of two chloride atoms. However, catalyst **9** was generated by the removal of one chloride atom. Different parameters such as time and temperature were used for this mode of catalyst and were found to have an effect in polymerization reactions.



Comparison between pyridine carboxamide palladium(II) catalysts (**1-4**) and σ -donor pyrazole palladium(II) catalysts (**5-9**) was made. Catalysts **1-4** were found to give high percentage conversions than catalysts **5-9**. However, polymerization reactions performed at low temperature ($-78\text{ }^\circ\text{C}$) using pyrazole catalyst (**9**) can give percentage conversions as high as those obtained with pyridine carboxamide palladium catalysts (**1-4**).

The stereoregularity of poly(phenylacetylene) was determined by the use of NMR and IR spectroscopy. The polymers obtained have *cis-transoidal* structure, whilst the polymer that was exposed to air in solution and the oligomers gave a *trans-cisoidal* structure. High

cis content (95%) was obtained when the polymer was characterized at 0 h, but was found to show degradation when left in solution for several hours.

